Reducible Dehn Surgeries, Ribbon Concordance and Satellite Knots

by

Holt W. Bodish

A dissertation accepted and approved in partial fulfillment of the
requirements for the degree of
Doctor of Philosophy
in Mathematics

Dissertation Committee:
Robert Lipshitz, Chair
Boris Botvinnik, Core Member
Jon Brundan, Core Member
Dan Dugger, Core Member
Jiabin Wu, Institutional Representative

University of Oregon
Spring 2024

DISSERTATION ABSTRACT

Holt W. Bodish

Doctor of Philosophy in Mathematics

Title: Reducible Dehn Surgeries, Ribbon Concordance and Satellite Knots

In this thesis we investigate knots and surfaces in 3- and 4-manifolds from the perspective of Heegaard Floer homology, knot Floer homology and Khovanov homology. We first investigate the *Cabling Conjecture*, which states that the only knots that admit reducible Dehn surgeries are cabled knots. We study this question and related conjectures in Chapter 2 and develop a lower bound on the slice genus of knots that admit reducible surgeries in terms of the surgery parameters and study when a slope on an almost L-space knot is a reducing slope. In particular, we show that when $g(K)$ is odd and > 3, the only possible reducing slope on an almost L-space knot is $g(K)$ and in that case the complement of an almost L-space knot does not contain any punctured projective planes. In Chapter 3 we investigate the effect of satellite operations on knot Floer homology using techniques from bordered Floer homology [LOT18] and the immersed curve reformulation [HRW22; Che19; CH23]. In particular we study the functions $n \mapsto g(P_n(K)), \epsilon(P_n(K))$ and $\tau(P_n(K))$ for some families of $(1,1)$ patterns P from the immersed curve perspective. We also consider the function $n \mapsto \dim(\widehat{\mathrm{HFK}}(S^3, P_n(K), g(P_n(K)))$, and use this together with the fibered detection property of knot Floer homology [Ni07] to determine, for a given pattern P, for which $n \in \mathbb{Z}$ the twisted pattern P_n is fibered in the solid torus. In Chapter 4 we answer positively a question posed by Lipshitz and Sarkar about the existence of Steenrod operations on the Khovanov homology of prime knots [LS18, Question 3]. The proof relies on a construction of a particular type of surface, called a ribbon concordance in $S^3 \times I$, interpolating between any given knot and a prime knot together with the fact that the maps induced on Khovanov homology by ribbon concordances are split injections [Wil12; LZ19].

This thesis contains previously published material and unpublished coauthored material.

ACKNOWLEDGMENTS

I want to first thank my advisor Robert Lipshitz for his care, invaluable guidance, support and encouragement over the last six years. I want to thank my committee: Boris Botvinnik, Daniel Dugger, Jon Brundan and Jiabin Wu. I am grateful for all my low-dimensional topologist friends at the University of Oregon, especially the One Flew Over the Sutured Nest group (Gary, Siavash, Jesse and Champ) for the weekly zoom meetings over the pandemic and for teaching each other cool math. I am grateful to my coauthor Robert DeYeso III and collaborator Subhankar Dey for many interesting discussions. I also want to acknowledge the mathematicians from Montana for their advice and support early in my career: David Ayala, Ryan Grady, Charles Katerba and Eric Chesebro. I would not know about math research and especially about knots and tangles if it were not for Eric inviting me to participate in an undergraduate research group after he taught my Calculus II class.

I am forever grateful to my family and friends, especially my parents for their encouragement and support and my brother Elijah for introducing me to the wild world of mathematics and his friendship throughout my life. Finally I want to express my immense and everlasting gratitude and love to my spouse Masha Korchagina for their devotion, love, and support throughout my time in graduate school and beyond. I could not have done it without them.

DEDICATION

For Masha

TABLE OF CONTENTS

Chapter Page

LIST OF FIGURES

Figure Page

CHAPTER 1

INTRODUCTION

1.1 Background

In this section we will introduce some background and notation that we will use throughout the arguments in this thesis.

Genus, Fiberedness, and Concordance

A knot K is a smooth embedding $K : S^1 \to S^3$ considered up to ambient isotopy. We will also write K for the image of the embedding. In this thesis we are interested in properties of surfaces embedded in S^3 or B^4 bounded by the knot. Any knot K bounds an orientable surface Σ in S^3, called a Seifert surface. We define the 3-genus, $g(K)$, of a knot as

$$g(K) = \min\{g(\Sigma) : \Sigma \subset S^3, \text{and } \partial\Sigma = K\}$$

As such, the genus is difficult to compute. It is however a powerful knot invariant. For example it detects the unknot: $g(K) = 0$ if and only if K is isotopic to the unknot.

Similarly, any surface in $S^3 = \partial B^4$ can be pushed into B^4 so that $\partial\Sigma = \Sigma \cap S^3 = K$. Then, we can define the 4-genus, $g_4(K)$, of a knot K as

$$g_4(K) = \min\{g(\Sigma) : \Sigma \subset B^4, \partial\Sigma = \Sigma \cap S^3 = K\}$$

Given a Seifert surface Σ for a knot K, the embedding of Σ into S^3 gives rise to a pairing on $H_1(\Sigma)$ which gives bounds on the 3- and 4-dimensional genus of K. The pairing S, called the Seifert pairing, is defined as follows. Given a curve a representing a class $[a] \in H_1(\Sigma)$, let a^+ denote the result of pushing the curve a off the surface in the positive normal direction of Σ. Let $S(a, b) = lk(a, b^+)$. Moreover, given a basis for $H_1(\Sigma)$ the Seifert pairing is represented by a matrix, called the Seifert matrix.

Two important knot invariants that are defined in terms of the Seifert matrix are the knot signature, $\sigma(K)$, and the Alexander polynomial, $\Delta_K(t)$.

The matrix $S + S^T$ is symmetric, so it can be diagonalized over $\mathbb{Q}$. The knot signtaure, $\sigma(K)$, is defined to be the signature of this symmetric matrix, namely the number of positive eigenvalues minus the number of negative eigenvalues. The Alexander polynomial is defined as $\Delta_K(t) = \det(t^{1/2}S - t^{1/2}S^T)$ and it turns out that $\Delta_K(t)$ is a Laurent polynomial in t that satisfies $\Delta_K(1) = 1$ and $\Delta_K(t) = \Delta_K(t^{-1})$. The breadth of the Laurent polynomial $\Delta_K(t)$, defined as the difference of the largest and smallest exponents that occur, is a lower bound for $g(K)$:

$$\text{breadth}(\Delta_K(t)) \leqslant 2g(K).$$

Further, the signature gives a lower bound for the slice genus:

$$|\sigma(K)| \leqslant g_4(K)$$

A knot is called *slice* if $g_4(K) = 0$ and so the signature vanishes on the set of slice knots. We call two knots K and K' *(smoothly) concordant* if there is a smoothly embedded annulus $S^1 \times I \to S^3 \times I$ so that $S^1 \times \{0\} = K$ and $S^1 \times \{1\} = K'$. For example it is easy to see that a knot K is concordant to the unknot U if and only if K is slice. The set of knots considered up to concordance has a group structure given by connected sum. Let us denote this group by $\mathcal{C}$. Then the signature actually gives a homomorphism $\sigma : \mathcal{C} \to \mathbb{Z}$.

In Chapter 2 and 3 we study knot invariants coming from Heegaard Floer and knot Floer homology that in some sense generalize the above invariants. Knot Floer homology, introduced by Ozsváth and Szabó [OS04b] and independently by Rasmussen [Ras03a], is a bigraded Abelian group $\widehat{\text{HFK}}(S^3, K) \cong \bigoplus_{m,A} \widehat{\text{HFK}}_m(S^3, K, A)$ and the graded Euler characteristic is the Alexander polynomial:

$$\Delta_K(t) = \sum_{m,A} (-1)^m \dim(\widehat{\text{HFK}}_m(S^3, K, A))t^A.$$

The A-grading is called the Alexander grading and the m-grading is the homological or Maslov grading. An important property that we use repeat-

edly in our arguments in Chapter 3 is the genus detection property of knot Floer homology [OS04a, Theorem 1.2]:

$$g(K) = \max\{A : \widehat{\mathrm{HFK}}(S^3, K, A) \neq 0\}.$$

This shows that knot Floer homology is a strictly stronger invariant than the Alexander polynomial, for which there are non-trivial knots such that $\Delta_K(t) = 1$. In particular, since the knot genus detects the unknot, knot Floer homology detects the unknot.

Knot Floer homology is the homology of the associated graded of a $\mathbb{Z}$-filtered $\mathbb{Z}$-graded chain complex defined in terms of a Heegaard diagram for the pair (S^3, K). See Section 1.2. From the definition, there is a spectral sequence with E_2 page $\widehat{\mathrm{HFK}}(S^3, K)$ and E_∞ page $\widehat{\mathrm{HF}}(S^3) \cong \mathbb{F}$ [OS03b]. Then, there is a numerical invariant $\tau(K)$, which is defined to be the minimal Alexander grading of any cycle homologous to a generator of $\widehat{\mathrm{HF}}(S^3)$. The invariant $\tau(K)$ is a lower bound for the slice genus, $|\tau(K)| \leqslant g_4(K)$ [OS03b, Corollary 1.3]. Similarly to the knot signature, τ also gives a homomorphism $\tau : \mathcal{C} \to \mathbb{Z}$. Although in general $\tau(K)$ is different from $\sigma(K)$, it agrees with $\sigma(K)$ up to a factor for a few classes of knots, for example alternating knots [Pet13]. The invariant $\tau(K)$ has also proved fruitful in the discovery of many subgroups of infinite rank in the smooth knot concordance group [Lev16; Hom14; Hed07].

In addition to the complexity of the surface Σ in S^3 or B^4 measured in terms of the genus, we are also interested in the complement of Σ in S^3. In particular, we are interested in when this complement is a product. We call a knot K fibered with fiber Σ if there is a locally trivial fiber bundle $S^3 - \nu(K) \to S^1$ with fiber Σ. It is easy to see that K is fibered if and only if $S^3 - \nu(\Sigma) \cong \Sigma \times I$. It is worth pointing out that while it is possible for a knot to have two or more minimal genus Seifert surfaces that are non-isotopic, fibered knots have a unique minimal genus Seifert surface up to isotopy. As with the genus, there is an obstruction coming from the Alexander polynomial of fibered knots, namely if K is fibered then the Alexander polynomial is monic.

In Chapter 3 we will repeatedly use the fact that knot Floer homology detects when a knot is fibered in S^3 [Ni07; Juh08b]: K is fibered in S^3 if and only if $\dim(\widehat{\mathrm{HFK}}(S^3, K, g(K))) = 1$. Since the trefoil knot and the figure eight knot are the only genus 1 fibered knots in S^3, it follows that knot Floer homology detects these knots as well as the unknot.

Computing knot Floer homology directly from the definition is extremely difficult. Although there are combinatorial models, for example the grid homology of [OSS15] and the nice diagrams of [OSS12] that do not require any of the analysis that originally goes into the construction, the number of generators in this construction also makes computations impractical. In the following, we make use of bordered Floer homology and the bordered pairing theorem to compute knot Floer homology of satellite knots in Chapter 3, where we apply the genus and fiberedness detection results to some families of satellite knots and compute τ for these same families, thus giving smooth slice genus bounds, as well as independence results and constructions of satellite operators that do not acts surjectively on the smooth concordance group. See Section 1.3 and Chapter 3 for more details.

Dehn Surgery

A link in S^3 is an embedding $L : \bigsqcup S^1 \to S^3$ up to ambient isotopy. A fundamental theorem in knot theory and low-dimensional topology says that any closed, connected orientable 3-manifold can be obtained from S^3 by cutting out a neighborhood of a link L and re-gluing. This cutting out and re-gluing operation is called Dehn surgery. We will study this operation in Chapter 2, so we give a brief overview of it here.

Given a knot K in S^3, we can thicken K to a tubular neighborhood, $\nu(K)$, which is diffeomorphic to a solid torus. Cutting S^3 along the boundary $\partial\nu(K)$, we get two 3-manifolds-with-boundary: the complement of the knot in S^3, $S^3 - \nu(K)$, and the tubular neighborhood of K, $\nu(K) \cong D^2 \times S^1$. We can then use any homeomorphism $h : \partial D^2 \times S^1 \to \partial(S^3 - \nu(K))$ to reglue

the solid torus and obtain a potentially new 3-manifold

$$(S^3 - \nu(K)) \cup_h (D^2 \times S^1).$$

It turns out that the diffeomorphism class of the 3-manifold obtained in this way only depends on the image of the meridian $h(\partial D^2 \times \{pt\})$. In fact, $H_1(S^3 - \nu(K))$ is generated by a meridian μ of K, and there is a unique homology class of curve on the boundary $\partial(S^3 - \nu(K))$ that is null-homologous in $S^3 - \nu(K)$ (the boundary of the Seifert surface from the previous section). We call this curve a preferred longitude λ. Then μ and λ form a basis for $H_1(\partial(S^3 - \nu(K)))$ and any simple closed curve (e.g. $h(\partial D^2 \times \{pt\})$) is isotopic to a curve of the form $p\mu + q\lambda$, with $gcd(p, q) = 1$. This sets up a bijection between the set of simple closed curves on $\partial(S^3 - \nu(K))$ and the set of reduced fractions p/q together with $\infty = 1/0$ (∞ corresponds to gluing back along the meridian, so ∞ surgery on any knot K in S^3 gives back S^3). Since the diffeomorphism type of the manifold only depends on the isotopy class of the attaching curve, we will write $S^3_{p/q}(K)$ to denote the 3-manifold

$$(S^3 - \nu(K)) \cup_h (D^2 \times S^1)$$

where $h(\partial D^2 \times \{pt\}) = p\mu + q\lambda$, and we will call it the result of $\frac{p}{q}$-Dehn surgery on K, and call $\frac{p}{q}$ a slope. If L is a link with multiple components, Dehn surgery on L is Dehn surgery on each component of L. We say the surgery is integral if all the slopes are integral (i.e. $q = 1$).

Theorem 1.1.1. *[Lic62; Wal60] Every closed orientable 3-manifold can be obtained from S^3 by performing an integral Dehn surgery on a link $L \subset S^3$.*

As we will discuss in Chapter 2 the question of which 3-manifolds can be obtained from Dehn surgery (rational or integral) on a knot in S^3 is still far from resolved. However, recently techniques have been developed that allowed for the construction or recognition of 3-manifolds that are not Dehn surgery on a knot.

In Chapter 2 we study the question of when a Dehn surgery on a knot can produce a non-trivial connected sum of two 3-manifolds, called an *reducible* 3-manifold, from the perspective of Heegaard Floer homology. As such, we want to understand the Heegaard Floer homology of 3-manifolds that are Dehn surgery along a knot: $\mathrm{HF}^\circ(S^3_{p/q}(K))$. We give a brief discussion of the definition of Heegaard Floer homology here, and postpone discussing the computation of Heegaard Floer homology of Dehn surgeries using the mapping cone formula of [OS11] until Chapter 2.

Let Y be a closed, connected, oriented 3-manifold and let $\mathcal{H} = (\Sigma, \alpha, \beta, z)$ be a pointed Heegaard diagram for Y. Here $\Sigma \subset Y$ is a closed, connected, orientable surface of genus g, $Y - \Sigma$ consists of two handlebodies H_0 and H_1, $\alpha = \{\alpha_1, \ldots, \alpha_g\}$ is a collection of non-intersecting simple closed curves that form a set of compressing disks for H_0 (we'll refer to this as the α-handlebody) and $\beta = \{\beta_1, \ldots, \beta_g\}$ is a collection of non-intersecting simple closed curves that form a set of compressing disks for H_1 (we'll refer to this as the β-handlebody). We also require that α and β intersect transversely and that z is contained in $\Sigma - (\alpha \cup \beta)$. From this data we construct two Lagrangian submanifolds of the symmetric product $Sym^g(\Sigma) = \Sigma^{\times g}/S_g$, where S_g is the symmetric group acting on the coordinates of $\Sigma^{\times g}$, for an appropriate choice of symplectic form on $Sym^g(\Sigma)$. The Lagrangian submanifolds are the tori determine by the α and β curves

$$\mathbb{T}_\alpha = \alpha_1 \times \cdots \times \alpha_g$$

and similarly for $\mathbb{T}_\beta$. The Heegaard Floer chain complex $\mathrm{CF}^\infty(\mathcal{H})$ is freely generated over $\mathbb{F}_2$ by pairs $[x, i]$ where $x \in \mathbb{T}_\alpha \cap \mathbb{T}_\beta$ and $i \in \mathbb{Z}$. The differential is given by

$$\partial^\infty[x, i] = \sum_{\{y \in \mathbb{T}_\alpha \cap \mathbb{T}_\beta\}} \sum_{\{\phi \in \pi_2(x,y) | \mu(\phi) = 1\}} \#\widehat{\mathcal{M}}(\phi)[y, i - n_z(\phi)]$$

Here $\pi_2(x, y)$ denotes the set of homotopy classes of Whitney disks from

x to y, $\mu(\phi)$ denotes the Maslov index of ϕ, $\widehat{\mathcal{M}}(\phi)$ is the moduli space space of J-holomorphic disks in the class of ϕ, and $n_z(\phi) = \#(\phi \cap (\{z\} \times Sym^{g-1}(\Sigma)))$. Moreover, if we let $\mathrm{Spin}^c(Y)$ denote the set of Spin^c structures on Y (an affine copy of $H^2(Y;\mathbb{Z})$), there is a map $s_z : \mathbb{T}_\alpha \cap \mathbb{T}_\beta \to \mathrm{Spin}^c(Y)$ so that x and y are connected by a Whitney disk if and only if $s_z(x) = s_z(y)$. Therefore $\mathrm{CF}^\infty(\mathcal{H})$ naturally splits over Spin^c structures on Y: $\mathrm{CF}^\infty(\mathcal{H}) = \bigoplus_{s \in \mathrm{Spin}^c(Y)} \mathrm{CF}^\infty(\mathcal{H}, s)$. There is also an action by $\mathbb{F}_2[U, U^{-1}]$ on $\mathrm{CF}^\infty(\mathcal{H}, s)$ given by $U[x, i] = [x, i-1]$ and the U action decreases the grading by 2. There are other flavors of the Heegaard Floer chain complex for a pointed Heegaard diagram, $\widehat{\mathrm{CF}}(\mathcal{H}, s), \mathrm{CF}^-(\mathcal{H}, s)$ and $\mathrm{CF}^+(\mathcal{H}, s)$, which are generated by elements $[x, i]$ with $s_z(x) = s$ and $i = 0$, $i < 0$, or $i \geqslant 0$ respectively. We will write $\mathrm{CF}^\circ(\mathcal{H}, s)$ for any of these flavors of the Heegaard Floer chain complex, and $\mathrm{HF}^\circ(\mathcal{H}, s)$ for the homology of this chain complex. In this notation we have the following theorem

Theorem 1.1.2. *[OS04d] The isomorphism class of* $\mathrm{HF}^\circ(\mathcal{H}, s)$ *as a* $\mathbb{F}_2[U]$ *module is an invariant of the* 3*-manifold* Y*.*

Given this theorem, we will write $\mathrm{HF}^\circ(Y, s)$ instead of $\mathrm{HF}^\circ(\mathcal{H}, s)$. In Chapter 2 we will recall how to compute $\mathrm{HF}^\circ(S^3_{p/q}(K))$ from data associated to the knot Floer chain complex using the mapping cone formula of [OS11]. In our work in Chapter 2 we are mostly interested in $\widehat{\mathrm{HF}}(S^3_p(K), s)$ and $\mathrm{HF}^+(S^3_p(K), s)$. Importantly, if Y is a rational homology 3-sphere, and $s \in \mathrm{Spin}^c(Y)$, we have the following structure theorem for $\mathrm{HF}^+(Y, s)$: $\mathrm{HF}^+(Y, s) \cong \mathcal{T}^+ \oplus \mathrm{HF}_{red}(Y, s)$ [OS04c, Theorem 10.1] where $\mathrm{HF}_{red}(Y, s)$ is a finite dimensional U-torsion module (called the reduced Heegaard Floer homology) and $\mathcal{T}^+ \cong \mathbb{F}[U, U^{-1}]/UF[U]$ (called the tower summand). An important numerical invariant of rational homology 3-spheres derived from this is the grading of the element $1 \in \mathcal{T}^+$, which we denote $d(Y, s)$. It turns out that $d(Y, s) \in \mathbb{Q}$ and if Y and Y' are Spin^c-homology cobordant, that is if they cobound a Spin^c 4-manifold W with $H_*(W;\mathbb{Z}) \cong H_*(Y_i;\mathbb{Z})$, then $d(Y, s) = d(Y', s')$ where s and s' are restrictions of the same Spin^c structure t on W. In our

work in Chapter 2 we will investigate the behaviour of the d-invariant for reducible manifolds.

Khovanov Homology

Khovanov homology is a bi-graded Abelian group, denoted $\mathrm{Kh}^{i,j}(K)$, that categorifies the Jones polynomial in the sense that the graded Euler characteristic recovers the Jones polynomial $V(K)$ up to a factor of $(q+q^{-1})$ [Kho99]:

$$(q+q^{-1})V(K) = \sum_{i,j}(-1)^i \dim(\mathrm{Kh}^{i,j}(K))q^j$$

Khovanov homology is an invariant of the isotopy class of a knot or link in S^3 that is combinatorially defined from a diagram of the knot or link. Khovanov homology is most strikingly useful in its functoriality under knot cobordisms. Namely given an oriented cobordism $\Sigma : K_0 \to K_1$ there is an induce map $Kh(\Sigma) : Kh(K_0) \to Kh(K_1)$.

Ribbon Concordance

Let us consider the concordance $S^1 \times I$ sitting inside of $S^3 \times I$ so that the projection map $S^3 \times I \to I$ restricts to a Morse function of $S^1 \times I$. Then a concordance is called *ribbon* if there are only index 0 and 1 critical points for this Morse function, that is the concordance annulus can be built with only births and band attachments, no deaths. A fundamental open problem in knot theory is the *Slice-Ribbon conjecture* which asserts that a knot is slice if and only if the knot is ribbon.

Recently progress has been made relating ribbon concordanes between knots to properties on the induced maps on Khovanov and knot Floer homology. Work of Zemke in [Zem19] and Levine and Zemke in [LZ19] showed that ribbon concordance of knots induce injective maps on knot Floer homology and Khovanov homology, respectively. Classical work of Kirby and Lickorish [KL79] shows that any knot K is ribbon concordant to a prime

knot, which implies that the Khovanov homology of any knot K is a summand of the Khovanov homology of a prime knot; see Chapter 4. This observation allows for the propagation of Steenrod squares from the Khovanov homology of composite knots to the Khovanov homology of prime knots.

1.2 Chapter 2: Reducible Surgeries on Slice and Almost L-Space Knots

This chapter contains unpublished co-authored material with Robert DeYeso III. Recall that Heegaard Floer homology is the homology of a graded chain complex $\mathrm{CF}^\circ(Y)$ where $\circ \in \{\hat{}, +, -, \infty\}$, where $\mathrm{CF}^\circ(Y)$ is either a $\mathbb{Z}$-graded $\mathbb{F}_2$-vector space, a $\mathbb{F}[U]$-module or a $\mathbb{F}[U, U^{-1}]$-module for $\circ \in \{\hat{}, +, -, \infty\}$. The chain homotopy type of any flavor of the chain complex is a smooth 3-manifold invariant. The definition of knot Floer homology is similar to the definition for Heegaard Floer homology. One starts with a doubly-pointed Heegaard diagram for the pair (S^3, K) which is the data of a tuple $(\Sigma, \alpha, \beta, z, w)$ so that w and z are in the complement of the α and β curves and $(\Sigma, \alpha, \beta, z)$ is a pointed Heegaard diagram for S^3. The knot K is the union of two arcs: an arc a in $\Sigma - \alpha$ connecting w to z and pushed into the α-handlebody and and arc b in $\Sigma - \beta$ connecting z to w and pushed into the β-handlebody. The chain complex $\mathrm{CFK}^-(S^3, K)$ is generated over $\mathbb{F}[U]$ by the intersections between the α and β tori, and the differential is defined as

$$\partial^- x = \sum_{y} \sum_{\substack{\phi \in \pi_2(x,y) \\ ind(\phi)=1}} \#\widehat{\mathcal{M}}(\phi) U^{n_w(\phi)} y$$

The chain complex $\mathrm{CFK}^-(S^3, K)$ has a $\mathbb{Z}$-grading, called the homological or Maslov grading, denoted m, and a $\mathbb{Z}$-filtration called the Alexander filtration, denoted A. The differential decreases the Maslov grading by one and respects the Alexander filtration. For generators x and y the relative Maslov and Alexander gradings are defined as

$$M(x) - M(y) = ind(\phi) - 2n_w(\phi) \quad \text{and} \quad A(x) - A(y) = n_z(\phi) - n_w(\phi)$$

Furthermore, $M(Ux) = M(x) - 2$ and $A(Ux) = A(x) - 1$. Moreover, setting $U = 0$ we obtain the filtered complex $\widehat{\mathrm{CFK}}(S^3, K)$. The homology of the associated graded is denoted by $\widehat{\mathrm{HFK}}(S^3, K)$ and the filtration induces a spectral sequence with E_∞-page $\widehat{\mathrm{HF}}(S^3)$. We lift the Maslov grading to an absolute grading by setting the Maslov grading of this generator to be zero.

There is a related complex, that governs the mapping cone formula and specializes to the hat and minus complexes above. Define the complex $\mathrm{CFK}^\infty(S^3, K) := \mathrm{CFK}^-(S^3, K) \otimes \mathbb{F}[U, U^{-1}]$. This is a $\mathbb{Z} \oplus \mathbb{Z}$-filtered $\mathbb{Z}$-graded chain complex. We view this complex in the (i, j)-plane where a generator $U^n x$ is plotted at the coordinates $(-n, A(x) - n)$. Then, given a subset $S \subset \mathbb{Z} \oplus \mathbb{Z}$ such that $(i, j) \in S$ implies $(i', j') \in S$ for all $(i', j') \leqslant (i, j)$, we can form a subcomples $C\{S\}$, the set of all generators of $\mathrm{CFK}^\infty(S^3, K)$ with (i, j) coordinates in S. Note that in this language $CFK^-(S^3, K) = C\{i \leqslant 0\}$ and $\widehat{\mathrm{CFK}}(S^3, K) = C\{i \leqslant 0\}/C\{i < 0\}$. In these terms we can define $\tau(K)$ as follows [OS03b]

$$\tau(K) = \min\{s \,|\, \iota : C\{i = 0, j \leqslant s\} \to C\{i = 0\} \text{ induces a non-trival map on homology}\}$$

An important computational tool in the theory of Heegaard Floer homology is the mapping cone formula which relates information about the knot Floer complex to the Heegaard Floer homology of the 3-manifold obtained by Dehn surgery on K [OS11]. Using the mapping cone formula one can both compute the Heegaard Floer homology of many 3-manifolds that are surgery on knots and one can also hope to obstruct certain 3-manifolds from being realized as Dehn surgery on a knot (or a knot of a particular type) in S^3.

An easy obstruction to a 3-manifold being Dehn surgery on a knot is that the first homology of the 3-manifold must be $\mathbb{Z}$ or $\mathbb{Z}/n\mathbb{Z}$. Therefore, many 3-manifolds, e.g. T^3 and $(S^1 \times S^2)\#(S^1 \times S^2)$, cannot be obtained by Dehn surgery on a knot in S^3. Similarly, it is easy to see from the Wirtinger presentation for $\pi_1(S^3 - \nu(K))$ that a 3-manifold obtained by Dehn surgery on a knot must also have weight-one fundamental group, that is the fundamental group is normally generated by a single element. If we restrict atten-

tion to integer homology 3 spheres (3-manifolds with the same integral homology as S^3) there are examples of irreducible integer homology 3-spheres that do not arise as Dehn surgery on a knot. The first example was discovered by David Auckly [Auc97], using gauge theory and Donaldson's Diagonalization theorem. Auckly's construction is sufficiently complicated that he was not able to verify if the fundamental group was weight one.

More recently, the mapping cone formula and Heegaard Floer homology has proved useful in studying this question. For example, Hom-Karakurt-Lidman in [HKL16] showed that many irreducible integer homology spheres are not surgery along a knot in S^3 (see also [HL16]). Their proof involves in a non-trivial way both the mapping cone formula of [OS11] and the computation of Heegaard Floer homology of some small Seifert fibered spaces. In particular they find a relation between the d-invariant of an integer homology 3-sphere Y and the module structure on $\mathrm{HF}_{red}(Y)$ when Y is Dehn surgery on a knot K in S^3, and show that this relation does not hold for a family of Seifert fibered spaces, namely the Seifert fibered spaces $\Sigma(p, 2p-1, 2p+1)$. Furthermore, because their examples are relatively small 3-manifolds, they were able to verify that they have weight one fundamental group.

In a similar direction, one might ask when Dehn surgery on a knot produces a non-trivial connected sum of two or more 3-manifolds, called a *reducible* 3-manifold. Perhaps surprisingly, there are numerous examples of such knots. In [Mos71], Moser showed that $S^3_{pq}(T_{p,q}) \cong L(p,q)\#L(q,p)$ where $T_{p,q}$ denotes the (p,q) torus knot, and by a similar argument one can show that $S^3_{pq}(K_{p,q}) \cong L(p,q)\#S^3_{q/p}(K)$, where $K_{p,q}$ denotes the (p,q)-cable of the knot K. In [GS86], the authors propose the following conjecture, called the *Cabling Conjecture*, which is still open:

Conjecture 1.2.1. *If K is a knot that admits a reducible surgery with slope p, then $K = J_{r,s}$ for some knot J and $p = rs$.*

Note that this question is asking when does Dehn surgery on a knot contain an essential separating 2-sphere. This conjecture has been verified in many cases, and many properties of the resulting reducible manifold are

known. See Chapter 2 for a more comprehensive survey. We only mention a few important results here. If Dehn surgery on a knot is a reducible 3-manifold, then there must be a non-trivial lens space summand (and so the surgery slope has to be > 1) and the slope is integral [GL87]. In particular there are no reducible integer homology spheres that can be obtained from S^3 by Dehn surgery on a knot. Additionally, the *Cabling Conjecture* is known for torus and satellite knots [Mos71; Sch90] so it remains to study integral surgeries on hyperbolic knots. Moreover for hyperbolic knots the reducing slopes satisfy the restrictive bound $1 < |p| \leqslant 2g(K) - 1$ [MS03]. Two other related conjectures that we explore are the *Two-Summands Conjecture* and the *Multiple Reducing Slopes Conjecture*. The two-summands conjecture asserts that at most two summands can result from Dehn surgery along a knot in S^3 and the multiple reducing slope conjecture asserts that any knot has at most one reducing slope. If we consider slopes as curves on the boundary of the knot complement, we can compute their geometric intersection in T^2. A theorem of Gordon and Luecke [GL96, Theorem 1.2] shows that if there are multiple reducing slopes for a given knot, then they have geometric intersection 1, and since they are integral slopes this implies they are consecutive integers. Furthermore, no more than three summands can occur in a Dehn surgery along a knot in S^3 [Val99; How02], and if three summands occur one is an integer homology sphere and the other two are non-trivial lens spaces.

Recently, Heegaard Floer homology has proved useful in studying the Cabling, Multiple Reducing Slopes and Two Summand Conjecture, as well as the general question of when a 3-manifold is surgery along a knot. Since there is a non-trivial lens space summand in any reducible surgery on a knot in S^3, which has the simplest possible Floer homology in each Spin^c structure, and Heegaard Floer homology satisfies a Künneth formula for connected sums [OS04c, Theorem 1.5], we have the following

Theorem 1.2.2 ([HLZ15] Lemma 2.6)**.** *Suppose K satisfies $S^3_p(K) \cong L(a,s)\#R$ where $p = ar$ and $|H_1(R;\mathbb{Z})| = r$. Then for any $t \in \mathrm{Spin}^c(S^3_p(K))$ and any $\alpha \in H^2(S^3_p(K))$ we have $\mathrm{HF}^+(S^3_p(K),[t]) \cong \mathrm{HF}^+(S^3_p(K),[t+\alpha r])$ as relatively*

graded $\mathbb{F}[U]$ *modules.*

In [HLZ15], the authors use the above observation to show that if an L-space knot K has a reducible surgery, then the reducing slope is $2g(K) - 1$ [HLZ15, Theorem 1.3]. So in particular, L-space knots do not have multiple reducing slopes and do not have properly embedded punctured projective planes in their complements, since the surgery slope is odd [HLZ15, Corollary 1.5]. Moreover, they show using the mapping cone formula that for knots of genus 1 and 2, there are not multiple reducing slopes. Greene, in [Gre15], verified the Cabling Conjecture when the resulting manifold is a connected sum of two lens spaces, and in [Mei17] Meier shows that a slice knot satisfies the two-summands conjecture by comparing the d-invariants of $S^3_p(K)$ when K is slice (which are equal to the d invariant of $L(p, 1)$ by [NW15, Proposition 1.6]) to $L(r, a)\#L(s, b)\#Y$, where $p = rs$ and Y is an integer homology sphere and showing that these are never equal, using the computation of d-invariants of lens space provided in [OS03a].

In Chapter 2, we use the mapping cone formula and d-invariants to study reducible Dehn surgeries on slice and almost L-space knots in S^3 and determine obstructions to general knots admitting reducible surgeries. Recall that if a knot K is slice, then so is the $(p, 1)$-cable of K, $K_{p,1}$. Then as above, $S^3_p(K_{p,1}) \cong L(p, 1)\#S^3_{1/p}(K)$. In particular, in a reducible surgery on a cable of a slice knot there are two summands, one a lens space that carries all the homology and the other an integer homology 3-sphere. Using the formula for the d-invariant of surgery along a knot established in [NW15, Proposition 1.6], it also follows that $d(S^3_{1/p}(K)) = 0$. We show that this holds in a general reducible surgery on a slice knot

Theorem 1.2.3. *For a slice knot K and a reducing slope p, $S^3_p(K) \cong L(p, 1)\#Y$, where Y is an integer homology 3-sphere with $d(Y) = 0$.*

The above theorem, when combined with [GS86, Proposition 1.4], gives the following Corollary, which further restricts the possible reducing slopes on fibered hyperbolic slice knots. Recall that if K is a hyperbolic knot with reducing slope r, then $1 < |r| \leqslant 2g(K) - 1$. We show

Corollary 1.2.4. *If K is a fibered, hyperbolic slice knot of genus g and r is a reducing slope, then $|r| \leqslant g$.*

For a general knot K with a reducing slope $r = pq$, we prove the following slice genus bound:

Theorem 1.2.5. *If $S^3_{pq}(K) \cong Y_p \# Y_q$, then $g_4(K) \geqslant \dfrac{(p-1)(q-1)}{2} = g_4(T_{p,q})$.*

This generalizes a result of [GS86] (See also [Eis22]) that says that the 3-genus of a knot K with reducing slope pq is bounded below by $g(T_{p,q}) = \dfrac{(p-1)(q-1)}{2}$

We also study the question of when a knot can admit multiple reducing slopes and show that if a hyperbolic slice knot K admits multiple reducing slopes r and $r+1$ then $r+1 \leqslant g(K)$. In the following Theorem we make reference to the invariant $\nu(K)$. The map $\hat{\upsilon}_s : \widehat{A}_s \to \widehat{B}_s$ is the map from the mapping cone formula of [OS11] (see also Chapter 2).

Definition 1.2.6. *[OS11, Definition 9.1] For a knot $K \subset S^3$, let $\nu(K) := \min\{s \mid (\hat{\upsilon}_s)_* \neq 0\}$.*

Theorem 1.2.7. *Suppose K is a hyperbolic knot in S^3 with $\nu(K) < g(K)$ that admits consecutive reducing slopes r and $r+1$. Further, suppose that both r and $r+1$ surgery split off an integer homology sphere summand. Then $r+1 \leqslant g(K)$.*

In joint work with Robert DeYeso III, we also study the question of when $2g(K)-1$ surgery on an L-space knot can be reducible and prove the following. This theorem, combined with the work of [DeY21], shows that thin knots satisfy the Cabling Conjecture.

Theorem 1.2.8. *Thin hyperbolic L-space knots do not admit reducible surgeries.*

In a similar direction, building on work of [HLZ15] we show that only certain slopes on almost L-space knots can produce reducible 3-manifolds, see Chapter 2, Section 2.3.

An *L-space* is a rational homology 3-sphere Y so that $\dim(\widehat{\mathrm{HF}}(Y)) = |H_1(Y;\mathbb{Z})|$. A knot K is called an *L-space knot* if $S^3_n(K)$ is an L-space for all $n \geqslant 2g(K) - 1$. In [BS22] the authors define a generalization of an L-space, called an *almost L-space*, which is a rational homology 3-sphere Y so that $\dim(\widehat{\mathrm{HF}}(Y)) = |H_1(Y;\mathbb{Z})| + 2$ (the next to smallest possible dimension). Exactly as above we call a knot K an *almost L-space knot* if $S^3_n(K)$ is an almost L-space for all $n \geqslant 2g(K) - 1$. It turns out that the full knot Floer complex of almost L-space knots can be determined, similarly to the case of L-space knot, see [Bin23]. We use these results to prove the following theorems.

Theorem 1.2.9. *For an almost L-space knot K, the only possible reducing slopes are $g(K)$ (or $\pm g(K)$ if $g(K) = 3$), ± 2, or $(2g(K) - 2)$ (and the latter two only in the case $g(K)$ is even)*

Corollary 1.2.10. *If K is an almost L-space knot with odd genus $g(K)$ and $g(K) > 3$, then $g(K)$ is the only reducing slope.*

Corollary 1.2.11. *If K is an almost L-space knot with odd genus $g(K)$, then the complement of K does not contain any properly embedded punctured projective planes.*

Proof. Suppose that the complement of K contained a properly embedded punctured projective plane P. Then ∂P gives a slope p so that filling along that slope gives an embedded $\mathbb{R}P^2$, $\widehat{P}$. Consider a tubular neighborhood of $\widehat{P}$ in $S^3_p(K)$. If $S^3_p(K) - \widehat{P}$ were a 3-ball, then $S^3_p(K)$ would be homeomorphic to $\mathbb{R}P^3$. By the $\mathbb{R}P^3$ theorem, [Kro+07, Theorem 1.1], this is impossible since K is non-trivial. Therefore $S^3_p(K) \cong \mathbb{R}P^3 \# Y$ for some 3-manifold Y with $p = 2|H_1(Y;\mathbb{Z})|$. However, p is even and is also a reducing slope for an almost L-space knot with odd genus. This contradicts Theorem 1.2.9. □

Corollary 1.2.12. *Almost L-space knots of genus $g(K) \geqslant 2$ do not admit multiple reducing slopes.*

1.3 Chapter 3: Knot Floer Homology, Immersed Curves and Twisted Satellites

In this chapter we study the behavior of certain invariants, coming from classical 3-manifold topology and Heegaard Floer homology, under the operation of taking the n-twisted satellite. Given a knot K in S^3 and a knot P in $S^1 \times D^2$, we can form a new knot in S^3, called the *n-twisted satellite knot* with pattern P and companion K, denoted $P_n(K)$, as follows:

$$(S^3, P_n(K)) = (S^3 - \nu(K)) \cup_\phi (S^1 \times D^2, P),$$

where the map ϕ takes the meridian of the solid torus, $\partial D^2 \times \{pt\}$, to the meridian of K and the longitude of the solid torus, $S^1 \times \{pt\}$, to $n\mu + \lambda$, where μ and λ are a meridian and longitude for the knot.

In general, computing the knot Floer homology of satellite knots from the definition is extremely difficult. Our approach to studying the question of how knot Floer homology behaves under satellite operations uses the bordered Floer homology of [LOT18] and the reformulation of the bordered invariants and the bordered pairing theorem for manifolds with torus boundary in terms of immersed curves [HRW17; HRW22; Che19; CH23].

Bordered Algebra

In this section we describe the algebraic preliminaries to understand the bordered pairing theorem. In what follows we will focus on bordered 3-manifolds with torus boundary. Let $\mathcal{A} = \mathcal{A}(T^2)$. The algebra $\mathcal{A}$ is defined as follows. Over $\mathbb{F}$ it has a basis consisting of two mutually orthogonal idempotents ι_0 and ι_1 and six other nontrivial elements $\rho_1, \rho_2, \rho_3, \rho_{12}, \rho_{23}, \rho_{123}$. The non-zero products in the algebra are given as follows:

$$\rho_1\rho_2 = \rho_{12} \quad \rho_2\rho_3 = \rho_{23} \quad \rho_1\rho_{23} = \rho_{12}\rho_3 = \rho_{123}$$

$$\rho_1 = \iota_0\rho_1\iota_1 \qquad \rho_2 = \iota_1\rho_2\iota_0 \qquad \rho_3 = \iota_0\rho_3\iota_1$$
$$\rho_{12} = \iota_0\rho_{12}\iota_0 \qquad \rho_{23} = \iota_1\rho_{23}\iota_1 \qquad \rho_{123} = \iota_0\rho_{123}\iota_1$$

If we let $\mathcal{I} = \langle\iota_0\rangle \oplus \langle\iota_1\rangle$, then a type D structure over $\mathcal{A}$ is a unital left $\mathcal{I}$ module N together with an $\mathcal{I}$ linear map $\delta : N \to \mathcal{A} \otimes_{\mathcal{I}} N$ such that

$$(\mu \otimes \mathbb{I}) \circ (\mathbb{I} \otimes \delta) \circ \delta = 0$$

A type A structure is a right unital $\mathcal{I}$ module M with a collection of maps $m_{i+1} : M \otimes \mathcal{A}^i \to M$, for $i \geqslant 0$, such that $M = M\iota_0 \oplus M\iota_1$ and

$$0 = \sum_{i=1}^{n} m_{n-i}(m_i(x \otimes a_1 \otimes \cdots \otimes a_{i-1}) \otimes \cdots \otimes a_{n-1}) + \sum_{i=1}^{n-2} m_{n-1}(x \otimes \cdots \otimes a_i a_{i+1} \otimes \cdots \otimes a_n) \tag{1.1}$$

and so that for $x \in M$ and $a_i \in \mathcal{A}$

$$m_2(x, 1) = x$$
$$m_i(x, \cdots, 1, \cdots) = 0$$

Given a type A structure M and a type D structure N, we can form a chain complex, called their box tensor product and denoted $M \boxtimes N$. The underlying vector space is the tensor product $M \otimes_{\mathcal{I}} N$, and the differential is defined by

$$\partial^{\boxtimes}(x \otimes y) = \sum_{i=0}^{\infty} (m_{i+1} \otimes \mathbb{I})(x \otimes \delta_i(y)), \tag{1.2}$$

In the case that the type D structure is bounded, as defined in [LOT18, Section 2], then the above sum is finite and the box tensor complex is well defined.

Bordered 3-manifolds and the Pairing Theorem

Given a closed three manifold Y and a surface F embedded in Y so that $[F] = 0 \in H_2(Y)$, we can cut Y along F to produce two 3-manifolds-with-boundary Y_1 and Y_2 so that $\partial Y_1 \cong -\partial Y_2 \cong F$. Such a 3-manifold-with-boundary together with a diffeomorphism $\phi : F \to \partial Y$ is called a *bordered 3-manifold*. To such a surface, [LOT18] associate a differential graded algebra, $\mathcal{A}(F)$, and to Y_1 and Y_2 as above they associate a right Type A structure $\widehat{\mathrm{CFA}}(Y_1)$ and a left type D structure $\widehat{\mathrm{CFD}}(Y_2)$. Furthermore, given a doubly-pointed bordered Heegaard diagram $\mathcal{H} = (\Sigma, \alpha^a, \beta, z, w)$ for a knot K in Y_1 which becomes null-homologous in Y, we can associate a right type A structure over $\mathcal{A}(F)$ with coefficients in $\mathbb{F}[U]$ denoted $\mathrm{CFA}^-(\mathcal{H})$, or a filtered type A structure $\widehat{\mathrm{CFA}}(\mathcal{H})$. Then the work in [LOT18, Theorem 1.3, 11.21] shows that there are homotopy equivalences

$$\widehat{\mathrm{CF}}(Y) \simeq \widehat{\mathrm{CFA}}(Y_1) \boxtimes \widehat{\mathrm{CFD}}(Y_2)$$
$$\widehat{\mathrm{CFK}}(Y, K) \simeq \widehat{\mathrm{CFA}}(\mathcal{H}) \boxtimes \widehat{\mathrm{CFD}}(Y_2)$$
$$g\mathrm{CFK}^-(Y, K) \simeq \mathrm{CFA}^-(\mathcal{H}) \boxtimes \widehat{\mathrm{CFD}}(Y_2)$$

Warning: $\mathrm{CFA}^-(\mathcal{H})$ depends on the choice of Heegaard diagram for the pair (Y_1, K), but the result of pairing with $\widehat{\mathrm{CFD}}(S^3 \backslash \nu(K))$ does not. We will abuse notation by writing $\mathrm{CFA}^-(Y_1, K)$ when it's clear we have fixed a Heegaard diagram for (Y_1, K).

Bordered Floer and Satellites Knots

In the satellite knot construction, we have two 3-manifolds with torus boundary, $S^3 - \nu(K)$ and $(S^1 \times D^2, P)$ and the latter is a 3-manifold with boundary together with a knot P that becomes null homologous in the glued up manifold. Note that in the n-twisted satellite construction we can either directly add n twists to the pattern knot P, or we can change the framing of the knot complement. The bordered pairing theorem implies that $g\mathrm{CFK}^-(S^3, P_n(K)) \cong \mathrm{CFA}^-(S^1 \times D^2, P) \boxtimes \widehat{\mathrm{CFD}}(S^3 - \nu(K), n)$, where

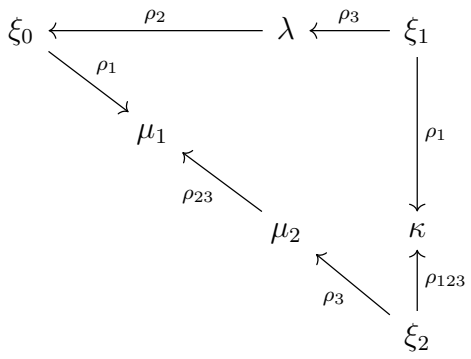

Figure 1.1. Type D structure for 0-framed right handed trefoil complement

$\widehat{\mathrm{CFD}}(S^3 - \nu(K), n)$ denotes the type D structure associated to the n-framed knot complement. So one way to compute the knot Floer homology of n-twisted satellite knots is to understand $\widehat{\mathrm{CFD}}(S^3 - \nu(K), n)$ and $\mathrm{CFA}^-(S^1 \times D^2, P)$.

In the case of a knot in S^3, [LOT18, Theorem 11.26] shows that the type D structure for the n-framed knot complement is algorithmically obtainable from the knot Floer complex $\mathrm{CFK}^-(S^3, K)$. Indeed, they show that given a horizontally and vertically simplified basis for the knot Floer complex $\mathrm{CFK}^-(K)$ and a choice of framing n, one can easily write down the bordered type D structure associated to the n-framed knot complement. See Figure 1.1 for an example of $\widehat{\mathrm{CFD}}(S^3 - \nu(T_{2,3}), 0)$. In fact, we can feed in partial information about $\mathrm{CFK}^-(K)$, and still extract some information about the type D structure. In particular, we will see in Chapter 3, Lemma 3.2.2 that this algorithm allows us to understand a piece of the type D structure $\widehat{\mathrm{CFD}}(S^3 - \nu(K), n)$ only knowing the triple $(\tau(K), \epsilon(K), n)$, and this piece of the type D structure ends up carrying a lot of the information in the pairing with $\widehat{\mathrm{CFA}}(S^1 \times D^2, P)$.

More recently [HRW22] showed that the bordered invariants for manifolds with torus boundary are equivalent to the data of an immersed multicurve in the once-punctured torus $T^2 - \{z\}$. Therefore for the case of type D structures associated to n framed knot complements, $\widehat{\mathrm{CFD}}(S^3 - \nu(K), n)$

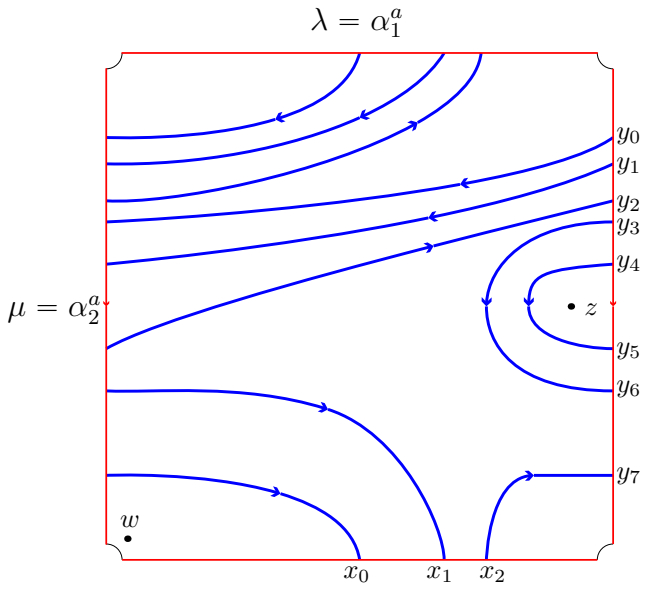

Figure 1.2. A genus-1 doubly-pointed Heegaard diagram. The blue curve is the β curve

gives rise to an immersed multi-curve, which we will denote $\alpha(K, n)$, in the punctured torus $T^2 - \{z\}$. In Chapter 3, Lemmas 3.2.2, 3.8.2 and 3.8.3, we recall how this correspondence works. The work of [LOT18] discussed in the previous paragraph gives a partial structure theorem for one special component of the immersed curve in terms of the triple $(\tau(K), \epsilon(K), n)$, and we use that to give a partial structure theorem for $\alpha(K, n)$ in terms of the triple $(\tau(K), \epsilon(K), n)$.

The other ingredient in the bordered pairing theorem are the Type A structures associated to pattern knots in $S^1 \times D^2$. In general, these are difficult to compute since the definition of the type A structure involves counting holomorphic disks with prescribed boundary conditions in some symplectic manifold associated to a bordered Heegaard diagram for the pair $(S^1 \times D^2, P)$.

A $(1, 1)$-pattern knot is a knot in $S^1 \times D^2$ that has a genus-1 doubly-pointed bordered Heegaard diagrams. A genus-1 doubly pointed bordered

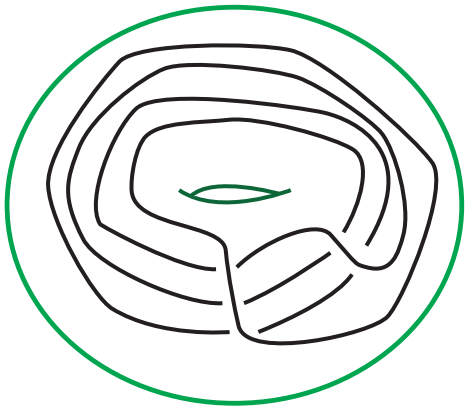

Figure 1.3. The pattern in the solid torus determined by the doubly pointed Heegaard diagram in figure 1.2 by the procedure described in the text

Heegaard diagram is a tuple $(T^2, \alpha^a, \beta(P), z, w)$, where $\alpha^a = \{\mu, \lambda\}$ is a preferred framing of the boundary and $\beta(P)$ is a curve in T^2 that is isotopic to the meridian after forgetting the z basepoint, so when we attach a two-handle to $\beta(P)$ we obtain the 3-manifold-with-boundary $S^1 \times D^2$. The knot P is specified by joining z to w and w to z in the complement of the α^a andv $\beta(P)$ respectively. See figures 1.2 and 1.3 for an example.

For $(1,1)$-patterns P and arbitrary companions K [Che19] showed that the bordered pairing theorem for computing $\widehat{\mathrm{CFK}}(S^3, P_n(K))$ can be reformulated as the intersection Floer homology of two curves in the twice-punctured torus: namely the immersed multi-curve $\alpha(K,n)$ and the β curve from the $(1,1)$ diagram associated to P, $\beta(P)$. See Figure 1.4 for an example of this pairing in $T^2 - \{z, w\}$ where $\alpha(K,n) = \alpha(T_{2,3}, 0)$ and $\beta(P)$ is the β curve from the genus-1 doubly pointed bordered Heegaard diagram in figure 1.2. We review this work in Section 3.2 and use it to prove the main results of Chapter 3, namely a computation of the Heegaard Floer concordance in-

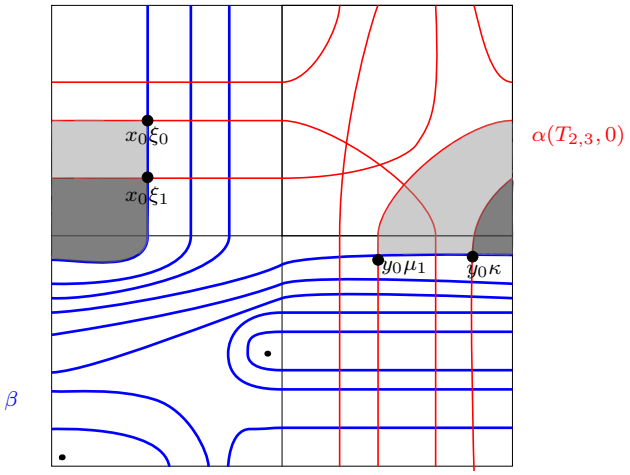

Figure 1.4. Executive summary of the pairing theorem for satellites with $(1,1)$ patterns. Intersection points in the second and fourth quadrant correspond to generators of the knot Floer chain complex of the satellite and Whitney disks as shown connecting two generators and not containing either basepoint are differentials

variants $\tau(P_n(K))$ and $\epsilon(P_n(K))$ for satellite knots with patterns from two novel families of $(1,1)$-patterns. The first family, denoted $P^{(p,1)}$ is a family of patters so that $P^{(p,1)}(U) \sim T_{2,3}$ (called *trefoil patterns*) with winding number $p+1$. See figure 1.3 for a picutre of $P^{(3,1)}$. As discussed in Chapter 3 these trefoil patterns are related to the $(p,1)$ cabling patterns by a finger move applied to the curve $\beta(p,1)$. The second family is a family of pattern knots denoted $Q^{i,j}_n$, shown in figure 3.24, so that $Q^{i,j}_0(U) \sim U$ and the winding number of $Q^{i,j}_n$ is j. The family of patterns $Q^{i,j}$ generalizes both the Whitehead doubling pattern and the Mazur pattern, both of which have been used to probe the structure of the smooth, topological and PL structure of knot concordance and homology cobordism [Hed07], [Lev16].

On top of understanding the behaviour of the concordance invariants $\tau(Q^{i,j}_n(K))$ and $\epsilon(Q^{i,j}_n(K))$ as functions of n, we also study the three genus

and fiberedness of these families of satellite knots via bordered Floer homology. In [HMS08] the authors give a criterion for when a satellite knot fibers in S^3: the n-twisted satellite knot $P_n(K)$ is fibered if and only if both K is fibered in S^3 and P_n is fibered in $S^1 \times D^2$. This result can be read as a way to detect if a pattern knot P_n is fibered in the solid torus, all that is required is to determine whether or not the satellite knot $P_n(T_{2,3})$ is fibered. Since knot Floer homology detects fiberedness of knots in S^3, to show that $P_n(T_{2,3})$ is fibered it is enough to compute the rank of the knot Floer homology of the satellite knot $P_n(T_{2,3})$ in the top Alexander grading. As we will see in Chapter 3 this computation is relatively simple for $(1,1)$-patterns as the type D structure associated to the complement of the right-handed trefoil is relatively simple. Using this, we determine for which triples (i,j,n) the pattern knot $Q^{i,j}_n$ is fibered in the solid torus:

Theorem 1.3.1. *The pattern knots $Q^{i,j}_n \subset S^1 \times D^2$ are fibered if and only if $i = 0$ and either $j \geqslant 2$ and $n \neq 0$ or $j = 1$ and $n \neq 0, -1$.*

It is interesting to compare the above result with the following theorem which classifies fibered unknot patterns.

Theorem 1.3.2. *[HMS08, Theorem 5.1] If P is a pattern so that $P(U) \simeq U$, then P is fibered if and only if it is braided.*

In particular $Q^{i,j}_0$ is never fibered. However, it is interesting that this is in some sense the only bad slope in that for basically all the other values of n and j, the pattern $Q^{0,j}_n$ is fibered and for no values of n is the pattern $Q^{i,j}_n$ fibered when $i > 0$. This raises the interesting question: which (non-braided) unknot patterns admit infinitely many twist parameters so that the resulting pattern (no longer of unknot type in S^3) is fibered.

Another 3 dimensional invariant of knots is their genus, the minimal genus of a surface that the knot bounds. A classical result of Schubert [Sch53] shows that the genus of a satellite with non-trivial companion knot K can be expressed in terms of the genus of the companion, the winding number of the pattern, and the genus of the pattern as follows:

$$g(P(K)) = |w(P)|g(K) + g(P).$$

In particular, since the above equality works for any non-trivial knot K, we might as well take $K = T_{2,3}$. Then the genus of the pattern is $g(P) = g(P(T_{2,3})) - |w(P)|$. Since knot Floer homology detects the genus of knots in S^3, we see that in some sense the bordered invariant $\widehat{\mathrm{CFA}}(S^1 \times D^2, P)$ detects the genus of the pattern knots P_n, by pairing with the type D structure associated to the n-framed trefoil complement $\widehat{\mathrm{CFD}}(S^3 - \nu(T_{2,3}), n)$, finding the genus of the resulting satellite and then using Schubert's formula [Sch53]. We perform this computation for the family of patterns $Q_n^{i,j}$ and find:

Theorem 1.3.3. *For K non trivial, we have*

$$g(Q_n^{i,j}(K)) = jg(K) + \frac{j(j+1)}{2}|n| + \begin{cases} 1 & n \geqslant 0 \\ 1-j & n < 0 \end{cases}$$

We can use the same techniques to determine $g(Q_n^{i,j}(U))$

Theorem 1.3.4. *For $K = U$,*

$$g(Q_n^{i,j}(U)) = \begin{cases} \dfrac{j(j+1)}{2}n + 1 & n > 0 \\ 0 & n = 0 \\ \dfrac{j(j+1)}{2}|n| + 1 - j & n < 0 \end{cases}$$

This shows that the genus of these twisted patterns depends quadratically on j (the winding number) and linearly on the number of meridional twists n added to the pattern. This generalizes work of [PW21], where the study the genus of the n-twisted Mazur pattern $Q^{0,1}$. The question of how the genus of knots that are related by adding full twists grows is also explored in [BM19].

The question of how satellite knots behave with respect to concordance is especially interesting, as there are many open questions that are easily

stated. For example, if W denotes the Whitehead double pattern, it is unknown if $W(T_{-2,3})$ is smoothly slice (it has Alexander polynomial 1, so is topologically slice by work of Freedman). However, in the last 20 years, many invariants have been developed that obstruct certain families of satellite knots from being slice. Two of the more successful invariants are $\tau(K)$ and $\epsilon(K)$ coming from knot Floer homology. Recall that, by construction, the knot Floer homology $\widehat{\mathrm{HFK}}(S^3, K)$ admits a spectral sequence to $\widehat{\mathrm{HF}}(S^3)$ and the invariant $\tau(K)$ is the Alexander grading of the generator that survives this spectral sequence. In fact there are two spectral sequences to $\widehat{\mathrm{HF}}(S^3)$, by symmetry of the knot Floer homology, and the invariant ϵ measures how the above generator interacts with the other spectral sequence. In our work, we also compute τ and ϵ of the two families of satellites with arbitrary companion knots and patterns $P^{(p,1)}$ and $Q^{i,j}_n$. In particular, we show that for the patterns $Q^{i,j}_n$ as above, we have

Theorem 1.3.5. *If K is a knot in S^3 with $\epsilon(K) = -1$, then*

$$\tau(Q^{i,j}_n(K)) = j(\tau(K) + 1) + \frac{j(j-1)}{2}n.$$

If K is a knot in S^3 with $\epsilon(K) = 1$, then

$$\tau(Q^{i,j}_n(K)) = \begin{cases} j\tau(K) + \dfrac{j(j-1)}{2}n + 1 & n < 2\tau(K) \\ j\tau(K) + \dfrac{j(j-1)}{2}n & n \geqslant 2\tau(K) \end{cases}.$$

If K is a knot in S^3 with $\epsilon(K) = 0$, then

$$\tau(Q^{i,j}_n(K)) = \begin{cases} \dfrac{j(j-1)}{2}n & n \geqslant 0 \\ \dfrac{j(j-1)}{2}n + j & n < 0 \end{cases}$$

Corollary 1.3.6. *For $M = Q^{0,1}$ the Mazur pattern, the value of $\tau(Q^{0,1}_n(K))$ does not depend on n, only on n relative to $2\tau(K)$.*

Theorem 1.3.7. *For any knot K, $\epsilon(Q^{i,j}_n(K)) \neq -1$.*

A consequence of the above theorem is that these patterns do not act surjectively as operators on the smooth or rational homology concordance group, since for any knot K, $Q_n^{i,j}(K)$ is never concordant to a knot L with $\epsilon(L) = -1$. This shows that there are infinitely many patterns of arbitrarily large winding number with this property, and shows that this property is preserved by adding twists in the clasp region, and adding full meridional twists to these patterns. Consequently, following a construction of Levine in [Lev16], the patterns $Q_n^{i,1}$ can be used to construct infinitely many knots not concordant to any knot in S^3.

1.4 Chapter 4: Non-trivial Steenrod Squares on the Khovanov Homology of Prime Knots

This chapter contains previously published material. In 2014, Lipshitz and Sarkar introduced a stable homotopy refinement of Khovanov homology [LS14a]. For each knot K and fixed j it takes the form of a suspension spectrum $\mathcal{X}^j(K)$. The cohomology $H^*(\mathcal{X}^j K))$ of this spectrum is isomorphic to the Khovanov homology $\mathrm{Kh}^{*,j}(K)$. In subsequent work (e.g. [LS14c]) they used this refinement to define stable cohomology operations on Khovanov homology. This lead to a refinement of Rasmussen's s-invariant [Ras03b] for each nontrivial cohomology operation, and in particular for the Steenrod squares [LS14c]. In Chapter 4 we positively answer a question posed in Lipshitz-Sarkar [LS18, Question 3]: Are there prime knots with arbitrarily high Steenrod squares on their Khovanov homology? Explicitly, we prove the following theorem:

Theorem 1.4.1. *Given any n, there exists a prime knot P_n so that the operation*

$$\mathrm{Sq}^n : \widetilde{\mathrm{Kh}}^{i,j}(P_n) \to \widetilde{\mathrm{Kh}}^{i+n,j}(P_n)$$

is nontrivial for some (i, j). Here $\widetilde{\mathrm{Kh}}$ denotes reduced Khovanov homology.

We construct these knots explicitly by ribbon concordances. The main results we use are a classical result of Kirby and Lickorish that any knot K is

ribbon concordanct to a prime knot [KL79], a result of Levine-Zemke [LZ19] (see also [Wil12]) that if $\Sigma : K \to K'$ is a ribbon concordance between knots K and K' then the map induce on Khovanov homology $\mathrm{Kh}(\Sigma) : \mathrm{Kh}(K) \to \mathrm{Kh}(K')$ is injective and the fact that there are composite knots with arbitrarily large Steenrod operations on their Khovanov homology [LLS15, Proof of Corollary 1.4, Page 67]. We are also able to use a result of Livingston which shows that any knot is ribbon concordant to a prime satellite knot [Liv81] to show that there are prime satellite knots with arbitrarily large Steenrod squares on their Khovanov homology. Further, using work of [Kaw89], we also note that since any knot K has an invertible concordance to a hyperbolic knot, we can propagate Steenrod squares from composite knots to prime hyperbolic knots as well, without the use of the injectivity result of Levine-Zemke [LZ19].

CHAPTER 2

REDUCIBLE SURGERIES

2.1 Overview

In this chapter we study obstructions to knots admitting reducible surgeries. This chapter draws on unpublished co-authored material joint with Robert DeYeso III, though the included material is all the author's own.

Introduction

In the following section, we will be making use of the relationship between knot Floer homology and the Heegaard Floer homology of 3-manifolds obtained from Dehn surgery along a knot in S^3. This relationship was first worked out by Oszvath and Szabo in [OS11] and we recall their notation and results here. In the first section we are mostly interested in the d-invariants of Dehn surgery, which are the gradings of some distinguished generators in the Heegaard Floer homology. In later sections, we make use of the full mapping cone to study reducible surgeries on almost L-space knots and multiple reducing slopes on general knots.

Let K be a knot in S^3, and denote the result of $\frac{p}{q}$-Dehn surgery on K as $S^3_{p/q}(K)$. This is the operation of removing a tubular neighborhood of K, $\nu(K) \cong S^1 \times D^2$, in S^3 and replacing it with a solid torus $S^1 \times D^2$ so that $\{pt\} \times \partial D^2$ maps to a slope p/q curve on $\partial(\nu(K))$ in terms of a basis $[\mu]$ and $[\lambda]$ $H_1(\partial(\nu(K)); \mathbb{Z})$. Here $[\mu]$ is a curve that bounds a disk in $\nu(K)$ and $[\lambda]$ is a curve on $\partial(\nu(K))$ that intersects μ in a single point and provides the Seifert framing of K (so it is nullhomologous in $S^3 \backslash K$). We are interested in Dehn surgeries that produce essential 2-spheres. A 2-sphere in a 3-manifold is essential if it is not the boundary of an embedded 3-ball B^3, and we say that M is reducible if it contains an essential 2-sphere. The solution of the Property-R conjecture in [Gab87] allows us to assume that $\frac{p}{q} \neq 0$ and that the surgery decomposes as a connected sum. All known examples of reducible surgeries on knots in S^3 are given by pq-surgery on the (p, q)-cable of

a knot K. Letting $C_{p,q}(K)$ denote the (p,q)-cable of K, we have

$$S^3_{pq}(C_{p,q}(K)) \cong L(p,q)\#S^3_{q/p}(K). \tag{2.1}$$

The Cabling Conjecture of Gonzáles-Acuña and Short asserts that these are the only examples.

Conjecture 2.1.1 (Cabling Conjecture - [GS86])**.** *If K is a knot in S^3 which has a reducible surgery, then K is a cabled knot and the reducing slope is given by the cabling annulus.*

The Cabling Conjecture is known to be true for many families of knots: satellite knots [Sch90], alternating knots [MT92], torus knots [Mos71], genus 1 knots [BZ96], and for knots with symmetries and low bridge number (for a survey of known results and techniques see [Boy02].) In particular, it remains to study reducible surgeries on hyperbolic knots with genus larger than one. We will make this assumption throughout the rest of this chapter.

Much is known about reducible surgeries on general knots. Observe that in the case of cabled knots, the reducing slope is integral and one of the connected summands is a non-trivial lens space. Gordon and Luecke [GL87] show that this is the case for any reducing slope. In particular, any reducing slope r satisfies $1 < |r|$ since a reducible surgery contains a non-trivial lens space summand. Due to the theorem of Gordon and Luecke [GL96] that the geometric intersection number of any two reducing slopes is 1, we see that a knot admits at most two reducing slopes, which would necessarily be consecutive integers. Further work in [MS03] shows that for non-cabled knots, the reducing slope r satisfies the restrictive bound

$$1 < |r| \leqslant 2g(K) - 1. \tag{2.2}$$

It is also known that in a reducible surgery, no more than one of the summands is an integer homology sphere, and at most two of the summands are lens spaces [How02; Val99]. It is conjectured that three summands never arise from Dehn surgery on a knot in S^3.

Another bound on the reducing slopes, this time for fibered knots with reducible surgeries with integer homology sphere summands, is proved in [GS86, Proposition 1.4]. We state it here for convenience, rephrased from the original source and using the Poincaré Conjecture.

Theorem 2.1.2 ([GS86])**.** *Suppose K is a fibered knot in S^3 of genus g. If $S^3_r(K) \cong L(r,a)\#Y$ for Y a homology sphere, then $r \leqslant g$.*

More recently, progress has been made on the Cabling Conjecture using tools from Heegaard Floer homology. Hom, Lidman, and Zufelt show in [HLZ15] that L-space knots admit at most one reducing slope $r = 2g(K) - 1$. In [Gre15], Greene shows that the Cabling Conjecture is true for knots that have surgeries to connected sums of lens spaces. Meier shows in [Mei17] that reducible surgeries on slice knots (or more generally knots with $V_i(K) = 0$ for all $i \geqslant 0$) only have two summands. In [DeY21], it is shown that hyperbolic thin knots do not admit reducible surgeries, except possibly when such a knot is also an L-space knot.

In this chapter, we show that slice knots only admit reducible surgeries of a particular type, and more generally we can bound the slice genus of a knot in terms of the reducing slope parameters. The form of the reducible surgery on a slice knot allows us to restrict the possible slopes on fibered, hyperbolic slice knots, as well as restrictions on multiple reducing slopes on slice knots. Our techniques mostly involve studying differences of the d-invariants of a reducible surgery, which are largely affected by the order of second cohomology of the connected summands. To that end, let Y_p denote a manifold with $|H^2(Y_p;\mathbb{Z})| = p$.

Theorem 2.1.3. *Suppose $K \subset S^3$ is a hyperbolic slice knot and p, q are relatively prime integers. If pq is a reducing slope for K and $S^3_{pq}(K) \cong L(p,a)\#Y_q$, then $q = 1$, $a = 1$, and $d(Y) = 0$.*

For fibered, hyperbolic slice knots, Theorem 2.1.3 together with Theorem 2.1.2 implies the following, which when compared with Equation 2.2

shows that we cut down the possible reducing slopes on fibered, hyperbolic slice knots by half.

Corollary 2.1.4. *If K is a fibered, hyperbolic slice knot of genus g and r is a reducing slope, then $r \leqslant g$.*

The proof of Theorem 2.1.3 also gives the following slice genus bounds.

Corollary 2.1.5. *Suppose K admits a reducible surgery of the form $S^3_{pq}(K) \cong Y_p \# Y_q$ with $p > q > 1$ and relatively prime. Then $g_s(K) \geqslant \frac{(p-1)(q-1)}{2} > 0$.*

Remark 1: Note that by [GS86, Theorem 2.2] and [Eis22, Theorem 8], the Alexander polynomial of the (p, q) torus knot divides the Alexander polynomial of any knot K which admits a reducible surgery of the form $Y_p \# Y_q$. This implies that $g_3(K) \geqslant g_3(T_{p.q}) = (p-1)(q-1)/2$. Corollary 2.1.5 above shows that the slice genus satisfies the same bound.

Remark 2: It is not known if more than two summands can occur in a reducible surgery on a slice knot. By [Val99] we know that there are at most three summands, and if three summands occur in a reducible Dehn surgery, then two of them are lens spaces and one is an irreducible integer homology three-sphere. Work in [Mei17] shows that slice knots admit only two summands in any reducible surgery. Corollary 2.1.5 implies that if a slice genus 1 knot K has a reducible surgery with two summands carrying non-trivial homology, then the reducing slope is 6. This implies that the two summands conjecture is true for all reducing slopes on slice genus 1 knots except for the possibility that $S^3_6(K) \cong L(2,1) \# L(3,2) \# Y$ for Y an irreducible homology sphere with $d(Y) = 0$. Similarly the only possible reducing slopes for slice genus 2 knots that could produce more than two summands are $r = 6$ and $r = 10$. As far as we know, Heegaard Floer theoretic invariants cannot obstruct three summands from appearing in these surgeries.

Next, we investigate how Theorem 2.1.3 may be applied to the problem of multiple reducing slopes for slice knots. This theorem and its proof are inspired by [HLZ15, Theorem 1.6]. For the definition of ν, see Definition 2.1.12.

Theorem 2.1.6. *Suppose K is a hyperbolic knot in S^3 with $\nu(K) < g(K)$ that admits consecutive reducing slopes r and $r+1$. Further, suppose that both r and $r+1$ surgery split off an integer homology sphere summand. Then $r+1 \leqslant g(k)$.*

Corollary 2.1.7. *Suppose that r and $r+1$ are simultaneous reducing slopes for a hyperbolic slice knot K in S^3. Then $r+1 \leqslant g(K)$.*

Spin^c *Structures*

Let $\mathrm{Spin}^c(Y)$ denote the set of Spin^c structures on Y, and recall that $\mathrm{Spin}^c(Y)$ is an affine copy of $H^2(Y;\mathbb{Z})$. Given a choice of Spin^c structure s_0 on Y, every other Spin^c structure satisfies $s = s_0 + a$ for some $a \in H^2(Y;\mathbb{Z})$. Furthermore we have an identification $\mathrm{Spin}^c(Y_1 \# Y_2) = \mathrm{Spin}^c(Y_1) \times \mathrm{Spin}^c(Y_2)$ and the projection maps onto each factor, π_{Y_1} and π_{Y_2}, intertwine the conjugation actions. Therefore, for $s \in \mathrm{Spin}^c(Y_1 \# Y_2)$ a self-conjugate Spin^c structure, both $\pi_{Y_1}(s)$ and $\pi_{Y_2}(s)$ are self-conjugate Spin^c structures on Y_1 and Y_2 respectively. Next, observe that if $p = |H_1(Y_1;\mathbb{Z})|$, then $\pi_{Y_1}(s+p) = \pi_{Y_1}(s)$ for any $s \in \mathrm{Spin}^c(Y_1 \# Y_2)$. This gives a relation among the d-invariants of reducible three-manifolds that arise as Dehn surgery along a knot in S^3.

For surgeries on knots in S^3, we fix an identification of $\mathrm{Spin}^c(S^3_{p/q}(K))$ with $\mathbb{Z}/p\mathbb{Z}$, given by $\sigma : \mathbb{Z}/p\mathbb{Z} \to \mathrm{Spin}^c(S^3_{p/q}(K))$ which sends $[i] \to \sigma([i])$ and satisfies $\sigma([i+1]) - \sigma([i]) = [K'] \in H_1(S^3_{p/q}(K)) \cong \mathrm{Spin}^c(S^3_{p/q}(K))$, where $[K']$ is the homology class of the dual knot. For more details on this assignment, see [OS03a, Section 4.1]. We will often abuse notation and write i or $[i]$ for the image of $[i]$ under the map σ, and will take $[i]$ to be notation for $i \pmod p$ unless otherwise stated.

Heegaard Floer Homology

Heegaard Floer homology is an invariant of closed, oriented three manifolds that was introduced by Oszváth and Szabó in [OS04d]. We will assume familiarity with all flavors of Heegaard Floer homology, as well as the

$\mathbb{Z} \oplus \mathbb{Z}$-filtered knot Floer complex $CFK^\infty(K)$ for knots K in S^3 defined in [OS04d] and [Ras03b]. For the readers convenience, we give a brief review of the structure of $HF^+(Y, \mathfrak{s})$, the properties of the d invariants, and the mapping cone formula, since they will be used in our main arguments in the next section.

Given a rational homology three-sphere, consider the invariants $\widehat{HF}(Y)$, $HF^+(Y)$, and $HF^\infty(Y)$. These are a finite dimensional $\mathbb{F}$-vector space, an $\mathbb{F}[U]$-module, and an $\mathbb{F}[U, U^{-1}]$-module respectively. Further, we have $HF^\circ(Y) \cong \bigoplus_{\mathfrak{s} \in \mathrm{Spin}^c(Y)} HF^\circ(Y, \mathfrak{s})$ for $\circ \in \{\widehat{\ }, +, \infty\}$.

For any rational homology three-sphere Y with Spin^c structure $\mathfrak{s}$, we have $HF^\infty(Y, \mathfrak{s}) \cong \mathbb{F}[U, U^{-1}]$. Also, $HF^+(Y, \mathfrak{s})$ decomposes non-canonically into two pieces. The first is the image of $HF^\infty(Y, \mathfrak{s})$ in $HF^+(Y, \mathfrak{s})$. This summand is isomorphic to $\mathbb{F}[U, U^{-1}]/U\mathbb{F}[U]$, which is called the *tower* and is denoted $\mathcal{T}^+$. The grading of $1 \in \mathcal{T}^+$ is an invariant of the pair $(Y, \mathfrak{s})$ and is denoted $d(Y, \mathfrak{s})$. The rational number $d(Y, \mathfrak{s})$ is called the correction term or d invariant. The second summand in $HF^+(Y, \mathfrak{s})$ is the quotient by the image of $HF^\infty(Y, \mathfrak{s})$ and is denoted $HF_{red}(Y, \mathfrak{s})$. It is a finite dimensional $\mathbb{F}$ vector space annihilated by a high enough power of U.

The d-invariant has many useful properties [OS03a, Section 4]:

- Suppose $\overline{\mathfrak{s}}$ is the image of $\mathfrak{s}$ under conjugation. Then $d(Y, \overline{\mathfrak{s}}) = d(Y, \mathfrak{s})$.
- For pairs $(Y_1, \mathfrak{s}_1)$ and $(Y_2, \mathfrak{s}_2)$,
$$d(Y_1 \# Y_2, \mathfrak{s}_1 \# \mathfrak{s}_2) = d(Y_1, \mathfrak{s}_1) + d(Y_2, \mathfrak{s}_2) \tag{2.3}$$
- d is a homology cobordism invariant: If $W : Y \to Y'$ is a $\mathbb{Z}$ homology cobordism and there is a Spin^c structure on W that restricts to $\mathfrak{s}$ on Y and $\mathfrak{s}'$ on Y', then $d(Y, \mathfrak{s}) = d(Y', \mathfrak{s}')$.

By work in [OS11], the d-invariants of (p/q)-surgery along a knot are related to the d-invariants of $L(p, q)$. The latter are determined in [OS03a, Proposition 4.8], where they show

$$d(L(p, q), [i]) = \frac{(2[i] + 1 - p - q)^2 - pq}{4pq} - d(L(q, r), [j]), \tag{2.4}$$

with r and j the reductions of p and i modulo q, respectively. We also use the notation $[i]$ to denote the residue class of i mod p. This formula together $d(S^3) = 0$ allows one to determine the d-invariants of a lens space recursively.

The work of [LL08, Proposition 5.3] also shows that the d-invariants of $L(p,a)$ satisfy the relation

$$d(L(p,a),[i]) - d(L(p,a),[a+i]) = \frac{p-1-2[i]}{p}. \tag{2.5}$$

The Mapping Cone Formula and the ν^+ Invariant

In this section, we establish some terminology and notation for the mapping cone formula and the ν^+ invariant. For more details, see [HW16] and [Gai17]. Material from this section will be used to establish the claimed slice genus bounds and the bound on multiple reducing slopes.

As above, we write HF° to mean either the plus or hat version of Floer homology. Let $C = CFK^\infty(S^3,K)$ denote the knot Floer complex associated to K. This is a $\mathbb{Z}\oplus\mathbb{Z}$-filtered $\mathbb{Z}$-graded chain complex over $\mathbb{F}[U,U^{-1}]$, where the U action lowers the filtration degree by one and the Z grading by 2. Associated to C are the following quotient and sub-quotient complexes useful for computing the plus and hat versions of Floer homology of manifolds arising as Dehn surgery along a knot K. To this end, define:

$$A_k^+ := C\{\max\{i, j-k\} \geqslant 0\} \quad \text{and} \quad \widehat{A}_k := C\{\max\{i,j-k\} = 0\}$$

as well as

$$B^+ := C\{i \geqslant 0\} \quad \text{and} \quad \widehat{B} := C\{i = 0\}$$

where i and j refer to the two filtration degrees. From the definition of $CFK^\infty(S^3,K)$ the complex B° is isomorphic to $CF^\circ(S^3)$.

There is an obvious map $v_k^+ : A_k^+ \to B^+$ defined by projection. Similarly, there is a map $h_k^+ : A_k^+ \to B^+$ which projects to $C\{j \geqslant k\}$, shifts to $C\{j \geqslant 0\}$ via multiplication by U^k, and then applies a chain homotopy equivalence between $C\{i \geqslant 0\}$ and $C\{j \geqslant 0\}$ (both of which compute

$CF^+(S^3)$, so by general theory are chain homotopic). There are similar maps for the hat versions.

Just as $HF^+(Y,\mathfrak{s})$ decomposes as a tower and a reduced part, the homology of the quotient complexes $A_k^+(K)$ decompose non-canonically as $\mathcal{T}^+ \oplus A_k^{red}$. The maps v_k^+ and h_{-k}^+ are isomorphisms for large values of k and so represent multiplication by some non-negative power of U, say U^{V_k} and U^{H_k} respectively when restricted to the tower summand in each A_k^+. The non-negative integers V_k and H_k are concordance invariants of K which satisfy, by [NW15, Lemma 2.4] and [HLZ15, Lemma 2.5], the relations $H_k = V_{-k}$, $H_k = V_k + k$, and

$$V_k - 1 \leqslant V_{k+1} \leqslant V_k. \tag{2.6}$$

Furthermore, for each i, we have [Ras03b, Corollary 7.4]

$$V_i \leqslant \left\lceil \frac{g_4(K) - i}{2} \right\rceil. \tag{2.7}$$

The V_i also determine the correction terms or d invariants of surgery along the knot K:

Theorem 2.1.8. *[NW15, Proposition 1.6] For $p, q \geqslant 0$ and $0 \leqslant i \leqslant p-1$. we have:*

$$d(S^3_{p/q}(K), i) = d(L(p,q), i) - 2\max\{V_{\lfloor i/q \rfloor}, V_{\lfloor \frac{p+q-1-i}{q} \rfloor}\} \tag{2.8}$$

Now we explain how the maps v_k and h_k together with the quotient complexes A_k^+ determine the Heegaard Floer homology of p/q surgery along K. Since we are only interested in integer surgery in this paper, we write the theorem down in this case. The reader interested in the change to the case of fractional surgeries and a more detailed explanation of the notation should consult [OS11; Gai17]. To this end, let

$$\mathcal{A}^\circ_{i,p}(K) := \bigoplus_{n\in\mathbb{Z}} (n, A^\circ_{i+pn}), \qquad \mathcal{B}^\circ := \bigoplus_{n\in\mathbb{Z}} (n, B^\circ).$$

Then define a chain map $D^\circ_{i,p} : \mathcal{A}^\circ_{i,p} \to \mathcal{B}^\circ$ by $D^\circ_{i,p}(\{(k,a_k)\}_{k\in\mathbb{Z}}) = \{(k,b_k)\}_{k\in\mathbb{Z}}$ where $b_k = v^\circ_{i+pk}(a_k) + h^\circ_{i+p(k-1)}(a_{k-1})$. Letting $\mathcal{X}^\circ_{i,p}$ denote the mapping cone of $D^\circ_{i,p}$, we have

Theorem 2.1.9. *[OS11, Theorem 1.1] There is a relatively graded isomorphism of $\mathbb{F}[U]$-modules*

$$H_*(\mathcal{X}^\circ_{i,p}) \cong HF^\circ(S^3_p(K), i).$$

Next, we introduce the ν^+ invariant. as defined in [HW16, Definition 2.1].

Definition 2.1.10. *The invariant ν^+ is defined as follows: $\nu^+ := \min\{k \in \mathbb{Z} \mid v_k : A^+_k \to \widehat{CF}(S^3), v^+_k(1) = 1\}$, where $1 \in H_*(A^+_k)$ is a generator with lowest grading of the tower summand.*

Recall that $\nu^+(K) \leqslant g_s(K)$ [HW16, Proposition 2.4]. With the mapping cone formula we can give an alternative definition of ν^+. This definition is equivalent to the one just given since the integers V_k determine the map v^+_k on the non-torsion summand of A^+_k [NW15].

Lemma 2.1.11. $\nu^+(K) = \min\{k \in \mathbb{Z} \mid V_k = 0\}$.

We will also make use of the hat version ν as defined in [OS11, Definition 9.1]

Definition 2.1.12. *For a knot $K \subset S^3$, define $\nu(K) := \min\{s \mid (\hat{v}_s)_* \neq 0\}$.*

Then genus detection of knot Floer homology implies that

$$g(K) = \max\{\nu(K), \{s \mid \dim H_*(\widehat{A}_{s-1}) > 1\}\}. \tag{2.9}$$

2.2 Reducible Surgeries on Slice Knots

In this section we prove Theorems 2.1.3 and 2.1.6.

The d-invariants of Reducible Manifolds

Theorem 2.1.3 follows from the more general Theorem 2.2.1 below, which deals with d-invariants of knots which admit a reducible surgery.

Theorem 2.2.1. *Suppose K is a knot in S^3 such that pq is a reducing slope with $(p,q)=1$, $p>q$ and $S^3_{pq}(K) \cong Y_p \# Y_q$. Then for each $0 \leqslant \ell \leqslant \frac{(p-1)(q-1)}{2}$, the V_i's satisfy*

$$\sum_{i=0}^{q-1} \left(V_{\ell+i} - V_{\alpha(\ell+i+p)}\right) = \frac{(p-1)(q-1)}{2} - \ell, \tag{2.10}$$

Where $\alpha(j) = \min\{j, pq-j\}$.

Proof. Suppose K is a knot in S^3 with $S^3_{pq}(K) \cong Y_p \# Y_q$. We will write π_p for the projection map $\pi_{Y_p} : \mathrm{Spin}^c(S^3_{pq}(K)) \to \mathrm{Spin}^c(Y_p)$ and similarly for π_q. As $|H^2(Y_p;\mathbb{Z})| = p$ we have $\pi_p([p+i]) = \pi_p([i])$ for $[i],[p+i] \in \mathrm{Spin}^c(S^3_{pq}(K))$. Then by additivity of the d-invariants, for any $\ell \in \mathbb{Z}$ we have:

$$d(S^3_{pq}(K),[p+i+\ell]) - d(S^3_{pq}(K),[i+\ell]) = d(Y_q,\pi_q[p+i+\ell]) - d(Y_q,\pi_q[i+\ell]). \tag{2.11}$$

Our assumptions on p and q imply that $\alpha(\ell+i) = \ell+i$, so by Theorem 2.1.8 and Equation 2.4 we see that the left hand side difference in equation 2.11 equals

$$\frac{2(\ell+i)+p(1-q)}{q} + 2V_{\ell+i} - 2V_{\alpha(\ell+i+p)}.$$

Summing from $i=0$ to $i=q-1$ we see:

$$\sum_{i=0}^{q-1} d(S^3_{pq}(K),[\ell+i+p]) - d(S^3_{pq}(K),[\ell+i]) = \sum_{i=0}^{q-1}\left(\frac{2(\ell+i)+p(1-q)}{q}\right) + 2\sum_{i=0}^{q-1}\left(V_{\ell+i} - V_{\alpha(\ell+i+p)}\right). \tag{2.12}$$

On the other hand, by Equation (2.11) the left-hand side of Equation (2.12) is equal to

$$\sum_{i=0}^{q-1} d(Y_q,\pi_q[\ell+i+p]) - d(Y_q,\pi_q[\ell+i]).$$

Additionally, this sum is zero because the projection π_q induces bijections between $\mathrm{Spin}^c(Y_q)$ and both sets $\{\ell,\ldots,\ell+q-1\}$, $\{p+\ell,\ldots,p+\ell+q-1\}$.

Rearranging the sum in Equation 2.12, we see that

$$\sum_{i=0}^{q-1} \left(V_{\ell+i} - V_{\alpha(\ell+i+p)}\right) = \frac{(p-1)(q-1)}{2} - \ell.$$

□

Proof of Theorem 2.1.3. We first show that Theorem 2.2.1 implies Y is an integer homology sphere. Since $V_0 = 0$ by Equation 2.7 when K is slice, we have that $V_i = 0$ for all $i \geqslant 0$ due to their non-increasing behavior. Equation 2.10 with $\ell = 0$ implies $(p-1)(q-1) = 0$, so either $p = 1$ or $q = 1$. If $p = 1$, the positive solution of the two summands conjecture in the case where $V_i = 0$ for all $i \geqslant 0$ in [Mei17] implies that q was not a reducing slope since Y is irreducible. Therefore, under the assumption that we have a reducing slope, it follows that $q = 1$ and the reducible surgery is $S^3_p(K) \cong L(p,a)\#Y$ with Y an irreducible homology sphere.

To finish off the proof of Theorem 2.1.3, it remains to show that $a = 1$ and $d(Y) = 0$. Using Equation 2.5, we have

$$d(L(p,a),[i]) - d(L(p,a),[a+i]) = \frac{p-1-2[i]}{p}.$$

Notice that if i is a self-conjugate spin^c structure of $L(p,a)$, then $[i-a]$ and $[i+a]$ are conjugate for any a. Then $d(L(p,a),[i-a]) = d(L(p,a),[i+a])$ using [OS04c, Theorem 2.4]. Equation 2.5 used for the pairs $[i],[i+a]$ and $[i],[i-a]$ then yields

$$\frac{p-1-2[i]}{p} = -\frac{p-1-2[i-a]}{p}.$$

This implies that $2i \equiv a-1 \pmod{p}$, and so the self-conjugate Spin^c structure(s) of $L(p,a)$ correspond to the integers amongst $[\frac{a-1}{2}]$ and $[\frac{p+a-1}{2}]$. Both are realized as self-conjugate Spin^c structures when p is even, and precisely one of them is realized when p is odd (depending on the parity of a).

Recall that $S^3_p(K) = L(p,a)\#Y$ with Y a $\mathbb{Z}$-homology sphere, and let $[s] \in \text{Spin}^c(S^3_p(K))$ satisfy $\pi_L([s]) = \pi_L([0]) + a$. Equation 2.5 yields

$$d(S^3_p(K),[0]) - d(S^3_p(K),[s]) = d(L(p,a),\pi_L([0])) + d(Y) - (d(L(p,a),\pi_L([s])) + d(Y))$$

$$\begin{aligned} &= d(L(p,a),\pi_L([0])) - d(L(p,a),\pi_L([0])+a) \\ &= \frac{p-1-2\pi_L([0])}{p}. \end{aligned}$$

Additionally recall that $d(S^3_p(K),[i]) = d(L(p,1),[i]) - 2V_{\alpha(i)}$ due to Equation 2.8. This implies

$$\begin{aligned} d(S^3_p(K),[0]) - d(S^3_p(K),[s]) &= d(L(p,1),[0]) - d(L(p,1),[s]) - 2(V_0 - V_{\alpha(s+p)}) \\ &= d(L(p,1),[0]) - d(L(p,1),[s]) \\ &= \frac{s(p-s)}{p}, \end{aligned}$$

since $V_i = 0$ for all $i \geqslant 0$.

Now either $\pi_L([0]) = \frac{a-1}{2}$ or $\pi_L([0]) = \frac{p+a-1}{2}$. Provided the former, the two equations above yield $s(p-s) = p-a$. However $s(p-s) \geqslant p-1$, and so we must have $a = 1$ when $\pi_L([0]) = \frac{a-1}{2}$. If we suppose the latter so that $\pi_L[0] = \frac{p+a-1}{2}$, then these two equations yield the contradiction $s(p-s) = -a$. Thus $a = 1$, which forces $d(Y) = 0$ using Equation 2.8 with $s = 0$ and $V_0 = 0$.

□

Proof of Corollary 2.1.5. Suppose K is a knot in S^3 which admits a reducing slope of the form $r = pq$ with $S^3_{pq}(K) \cong Y_p \# Y_q$. Choosing $k = \frac{(p-1)(q-1)}{2} - 1$ for ℓ in Equation 2.10 shows

$$\sum_{i=0}^{q-1} V_{k+i} = 1 + \sum_{i=0}^{q-1} V_{\alpha(k+i+p)},$$

after rearranging terms. Thus, $V_k > 0$ since the V_i's are non-negative and non-increasing, and so $\nu^+(K) \geqslant k+1 = \frac{(p-1)(q-1)}{2}$ by Lemma 2.1.11. Since $\nu^+(K)$ is a lower bound for the slice genus of a knot [HW16], the result follows.

□

In this subsection we use the mapping cone formula for $\widehat{\mathrm{HF}}$ and the following lemma to prove Theorem 2.1.6. The lemma below follows immediately from the Künneth theorem for $\widehat{\mathrm{HF}}$ and the fact that lens spaces are L-spaces (for the proof and for the analogous statement for HF^+, see [HLZ15, Lemma 2.6] and Lemma 2.3.13.

Lemma 2.2.2. *Suppose Y is a three manifold and $Y \cong L(p,a)\#Y_q$ with $|H^2(Y_q,\mathbb{Z})| = q$. Then for any $\alpha \in H^2(Y)$ and $\mathfrak{s} \in \mathrm{Spin}^c(Y)$ we have* $\dim \widehat{\mathrm{HF}}(Y,\mathfrak{s}+q\alpha) = \dim \widehat{\mathrm{HF}}(Y,\mathfrak{s})$.

Proof of Theorem 2.1.6. Suppose $S^3_r(K) \cong L_r\#Y$ and $S^3_{r+1}(K) \cong L_{r+1}\#Z$ where $r \geqslant g(K)$, Y and Z are both integer homology spheres, and L_r is either a lens space or a connected sum of two lens spaces, and similarly for L_{r+1}. We assume the two reducing slopes are consecutive positive integers r and $r+1$ by mirroring the knot if necessary. Since both surgeries split off integer homology three spheres, and the complementary summand is an L-space, we see by Lemma 2.2.2 that

$$\dim(\widehat{\mathrm{HF}}(S^3_r(K),i)) = \dim(\widehat{\mathrm{HF}}(S^3_r(K),j))$$

for any two Spin^c structures i and j on $S^3_r(K)$. Similarly,

$$\dim(\widehat{\mathrm{HF}}(S^3_{r+1}(K),i)) = \dim(\widehat{\mathrm{HF}}(S^3_{r+1}(K),j)).$$

Note that if r is odd, we choose representatives $[i]$ of Spin^c satisfying $-\lfloor r/2\rfloor \leqslant i \leqslant \lfloor r/2\rfloor$. If r is even, choose representatives with $-\lfloor r/2\rfloor < i \leqslant \lfloor r/2\rfloor$. By the assumption $r \geqslant g(K)$ we have $r = g+i$ for $0 \leqslant i \leqslant g-2$, since a reducing slope on a hyperbolic knot is bounded above by $2g(K)-1$ by Equation (2.2) and $r+1$ is a reducing slope, we have $r+1 \leqslant 2g(K)-1$. In this case, the mapping cone formula implies that $\widehat{\mathrm{HF}}(S^3_r(K),k) \cong H_*(\widehat{A}_k)$ for $k = -i, -i+1, \ldots, 0, \ldots, i-1, i$. For all other k between 0 and $\lfloor r/2\rfloor$ we have

$$\widehat{\mathrm{HF}}(S^3_r(K),k) \cong H_*(\mathrm{Cone}(\widehat{A}_{k-i-g} \oplus \widehat{A}_k \to \mathbb{F})).$$

Note that $\widehat{\mathrm{HF}}(S^3_r(K),-k) \cong H_*(\mathrm{Cone}(\widehat{A}_{-k} \oplus \widehat{A}_{g+i-k}) \to \mathbb{F})$, so it suffices to consider only those k with $0 \leqslant k \leqslant \lfloor r/2 \rfloor$, since by [HLZ15, Lemma 2.3] $H_*(\widehat{A}_s) \cong H_*(\widehat{A}_{-s})$ and under this isomorphism the maps v_s and h_{-s} agree in the mapping cone.

Now, consider the mapping cone for $r+1$ surgery. Since $r+1 = g+i+1$, $\widehat{\mathrm{HF}}(S^3_{r+1}(K),k) \cong H_*(\widehat{A}_k)$ for $k = -i-1, -i, -i+1, \cdots, i-1, i, i+1$ and for all other k between 0 and $\lfloor (r+1)/2 \rfloor$ we have

$$\widehat{\mathrm{HF}}(S^3_{r+1}(K),k) \cong H_*(\mathrm{Cone}(\widehat{A}_{k-i-1-g} \oplus \widehat{A}_k \to \mathbb{F})).$$

Let $n_k = \dim(H_*(\widehat{A}_k))$. Then by Lemma 2.2.2, since r is a reducing slope with a $\mathbb{Z}$ homology sphere summand, we have

$$n_0 = n_1 = n_2 = \cdots = n_i = n_{i+1} + n_{1-g} + 1 - 2\mathrm{rank}(h_{1-g} \oplus v_{i+1}).$$

However, $r+1$ surgery reducible implies that $n_0 = n_{i+1}$, and so

$$n_{i+1} = n_{i+1} + n_{1-g} + 1 - 2\mathrm{rank}(h_{1-g} \oplus v_{i+1}). \tag{2.13}$$

Since $\mathrm{rank}(h_{1-g} \oplus v_{i+1}) = 0$ or 1, we either have $n_{1-g} = -1$ or $n_{1-g} = 1$ by Equation (2.13). The former case is impossible, so $\mathrm{rank}(h_{1-g} \oplus v_{i+1}) = 1$ and $H_*(\widehat{A}_{g-1})$ is one dimensional. This contradicts equation (2.9). □

Proof of Corollary 2.1.7. This follows immediately from Theorem 2.1.3 and Theorem 2.1.6.

□

2.3 Almost L-space knots and the Mapping Cone Formula

In this section we dive a bit deeper into the mapping cone formula and use it to both count the ranks of knot Floer homology of Dehn surgeries on almost L-space knots in each Spin^c-structure and determine relative gradings of generators of $\mathrm{HF}_{red}(S^3_p(K),[s])$. This will allow us to rule out many slopes p with $1 < |p| \leqslant 2g(K) - 1$ from being reducing slopes.

Facts about Almost L-space knots

Most of this section comes from [BS22] and [Bin23]. We review the necessary facts about almost L-space knots that will be used in the proofs. Since we are interested in producing obstructions to a knot admitting a reducible surgery, we restrict ourselves to considering almost L-space knots of genus $g \geqslant 2$ (since genus 1 knots satisfy the cabling conjecture [HLZ15; BZ96].) Recall that an L-space is a rational homology 3-sphere Y that satisfies $\dim(\widehat{\mathrm{HF}}(Y)) = |H_1(Y;\mathbb{Z})|$.

Definition 2.3.1. *[BS22, Definition 1.9] A closed 3-manifold Y is called an almost L-space if Y is a rational homology sphere and $\dim(\widehat{\mathrm{HF}}(Y)) = |H_1(Y;\mathbb{Z})| + 2$. A non-trivial knot $K \subset S^3$ is an almost L-space knot if $\dim(\widehat{\mathrm{HF}}(S^3_n(K))) = n + 2$ for all $n \geqslant 2g(K) - 1$.*

Theorem 2.3.2. *[BS22, Proposition 3.9] Suppose K is an almost L-space knot of genus $g \geqslant 2$, then K is fibered and $V_{g-1} \neq 0$*

A corollary of this theorem is that $V_i \neq 0$ for all $i \leqslant g-1$. In particular, $\hat{v}_i$ vanishes on the copy of $\mathbb{F}$ coming from the tower summand in A_i^+. We will also need the following lemmas:

Lemma 2.3.3. *[BS22, Lemma 3.8] For K an almost L-space knot, we have $\widehat{A}_i \cong \mathbb{F}$ for $i \neq 0$ and $\widehat{A}_0 \cong \mathbb{F}^3$. Moreover $A_i^+ \cong \mathcal{T}^+$ for $i \neq 0$ and $A_0^+ \cong \mathcal{T}^+ \oplus \mathbb{F}_2[U^{-1}]/U^{-n}$ for some $n \geqslant 1$.*

Proof. The proof of the above lemma follows from [BS22, Lemma 3.8], and the large surgery formula. □

Recall that there is a chain map $D^\circ_{i,p} : \mathcal{A}^\circ_{i,p}(K) \to \mathcal{B}^\circ_{i,p}$ defined by

$$D^\circ_{i,p}(\{k, a_k\}) = \{(k, b_k)\}$$

where $b_k = v^\circ_{i+pk}(a_k) + h_{i+p(k-1)} \circ (a_{k-1})$. If we let $\mathcal{X}^\circ_{i,p}$ denote the mapping cone of $D^\circ_{i,p}$, then we have the following result

Theorem 2.3.4. *There is a relatively graded isomorphism of $\mathbb{F}[U]$ modules*

$$H_*(\mathcal{X}^\circ_{i,p}) \cong \mathrm{HF}^\circ(S^3_p(K), i)$$

We can in fact be more explicit. In the following lemma $D^T_{i,p}$ denotes the restriction of the map $D^+_{i,p}$ to the tower summand of $\mathcal{A}^+_{i,p}$

Lemma 2.3.5. *For $p > 0$, the map $D^+_{i,p} : \mathcal{A}^+_{i,p} \to \mathcal{B}^+_{i,p}$ is surjective and* $\mathrm{HF}^+(S^3_p(K), [i]) \cong \ker(D^+_{i,p}) = \ker(D^T_{i,p}) \oplus A^{red}_i \cong \bigoplus_{i \equiv p} \ker(v^+_i + h^+_i)$

Proof. It follows from [NW15] and [Gai17, Corollary 14] that for positive surgeries the map $D^T_{i,p}$ is surjective for all i. Since we are dealing with an almost L-space knot, the result follows for $i \neq 0$ immediately. In the case $i = 0$, it follows from [Gai17, Proposition 15] that $\ker(D^+_{0,p}) = \ker(D^T_{0,p}) \oplus A^{red}_0$. □

Lemma 2.3.6. *In the case $p < 0$, the map $\widehat{v}_0$ vanishes on the summand of $\widehat{A}_0$ coming from A^{red}_0*

Corollary 2.3.7. *For $p < 0$ the map* $\mathrm{coker}(D^+_{i,p}) \cong \mathcal{T}^+$ *and* $\mathrm{HF}_{red}(S^3_p(K), [i]) \cong \ker(D^+_{i,p}) \cong \ker(D^T_{i,p}) \oplus A^{red}_i$

Proof. By [Gai17, Proposition 19] and Lemma 2.3.3, the result follows if we can show that $V_0(m(K)) = 0$. This can be done by analyzing the 3 cases in [Bin23]. In each case, the filtered homotopy type of CFK^∞ is given explicitly. The proof that $V_0(m(K)) = 0$ for K an almost L-space knot with $g(K) \geqslant 2$ is exactly the same as the proof that $V_0(m(K)) = 0$ for K an L-space knot. □

To obstruct reducible surgeries on almost L-space knots, first we will determine the rank of $\widehat{\mathrm{HF}}(S^3_p(K), [s])$ for each $[s]$. Following [HLZ15], we pass to a smaller, but quasi-isomorphic model, of the mapping cone. Recall that for $s \geqslant g(K)$, the map v_s induces an isomorphism on homology, similarly, for $s \leqslant -g(K)$, the map h_s also induces an isomorphism on the level of homology. Now, if we let $\mathbb{A}^\circ_{i,p} := H_*(A^\circ_{i,p})$, and similarly $\mathbb{B}^\circ_{i,p} := H_*(B^\circ_{i,p})$ and

$\mathbf{v}_{i,p} = (v_{i,p})_*$ and similarly for $h_{i,p}$, we see that the truncated mapping cone complex, defined as

$$\mathbb{X}_{i,p} := \left(\bigoplus_{1-g\leqslant i\leqslant \max\{g-1,g-1+p\}} \mathbb{A}^\circ_{i,p} \right) \oplus \left(\bigoplus_{1-g+p\leqslant s\leqslant g-1} \mathbb{B}^\circ_{i,p} \right)$$

With the induced differential, is quasi-isomorphic to the mapping cone $\mathcal{X}^\circ$. Since this model has only finitely many objects, it is simpler to work with.

Using the truncated mapping cone model, it is a simple task to count the rank of Heegaard Floer homology of Dehn surgery on an almost L-space knot in S^3.

Lemma 2.3.8. *Let K be a knot with a positive almost L-space surgery, and let p be an integral slope on K satisfying $1 < |p| \leqslant 2g(K) - 1$. Let $k \equiv 2g - 1 \mod p$ with $0 \leqslant k < |p|$. If $p > 0$, then for $s \in \mathbb{Z}$ with $g - k \leqslant s < g - k + p$ we have*

$$rk(\widehat{\mathrm{HF}}(S^3_p(K), s)) = \begin{cases} 2\lfloor \frac{2g-1}{p} \rfloor + 3 & g-k \leqslant s < g \quad \textit{and} \quad s \equiv 0 \mod p \\ 2\lfloor \frac{2g-1}{p} \rfloor + 1 & g-k \leqslant s < g \\ 2\lfloor \frac{2g-1}{p} \rfloor + 1 & g \leqslant s < g-k+p \quad \textit{and} \quad s \equiv 0 \mod p \\ 2\lfloor \frac{2g-1}{p} \rfloor - 1 & g \leqslant s < g-k+p \end{cases}$$

If $p < 0$, then

$$rk(\widehat{\mathrm{HF}}(S^3_p(K), [s])) = \begin{cases} 2\left\lfloor \frac{2g-1}{|p|} \right\rfloor + 3 & g-k \leqslant s < g \quad s \not\equiv 0 \mod p \\ 2\left\lfloor \frac{2g-1}{|p|} \right\rfloor + 5 & g-k \leqslant s < g \quad s \equiv 0 \mod p \\ 2\left\lfloor \frac{2g-1}{|p|} \right\rfloor + 3 & g \leqslant s < g-k+|p| \quad s \equiv 0 \mod p \\ 2\left\lfloor \frac{2g-1}{|p|} \right\rfloor + 1 & g \leqslant s < g-k+|p| \quad s \not\equiv 0 \mod p \end{cases}$$

Proof. This proof is exactly the same as the proof of [HLZ15, Lemma 3.2]. Indeed when $p > 0$ Lemma 2.3.3 shows that the maps $\widehat{v}_i$ vanish on the tower summands of A_i^+ and Lemma 2.3.14 shows that the rank of p surgery on K in Spin^c structure $[s]$ is the either the same as the rank of p surgery on an L-space knot if $[s] \neq [0]$ or is 2 more than the rank of p surgery on an L-space knot if $[s] = [0]$. The case for negative surgeries is also the same by Lemma 2.3.15 since $V_0(m(K)) = 0$ for K an almost L-space knot, we just need to add 2 to the rank of $\widehat{\mathrm{HF}}(S^3_p(K), [0])$. □

Now suppose that p is a reducing slope for the hyperbolic almost L-space knot K. Then we have $S^3_p(K) \cong L(a,b)\#R$ where $p = ar$ and $|H_1(R;\mathbb{Z})| = r$. Note that in particular this implies that $(a,r) = 1$. Since $L(a,b)$ is an L-space Lemma 2.2.2 implies that for any $s \in \text{Spin}^c(S^3_p(K))$ we have

$$\text{rank}(\widehat{\mathrm{HF}}(S^3_p(K), [s]) = \text{rank}(\widehat{\mathrm{HF}}(S^3_p(K), [s+r])$$

This shows that in order for p surgery to be reducible there must be some periodicity, so the rank of $\widehat{\mathrm{HF}}$ is any particular Spin^c structure cannot be the unique Spin^c structure with that rank (they at least come in pairs). We first deal with the case $k = 0$, and show that in this case p is not a reducing slope.

Lemma 2.3.9. *With the notation as in Lemma 2.3.8, for $k = 0$ there is no possible periodicity among the ranks of $\widehat{\mathrm{HF}}(S^3_p(K), [s])$*

Proof. When $k = 0$ we see from Lemma 2.3.8 that there is a unique $[s]$, anmely $[s] = [0]$, so that $g \leqslant s < g + p$ and $\text{rank}(\widehat{\mathrm{HF}}(S^3_p(K), [s])) = \left\lfloor \frac{2g-1}{|p|} \right\rfloor + 1$. The contradicts Lemma 2.2.2 □

In a similar way, we handle the cases where $1 < k < p - 1$.

Lemma 2.3.10. *For $1 < k < p-1$ there is no possible periodicity among the ranks of $\widehat{\mathrm{HF}}(S^3_p(K), [s])$.*

Proof. By Lemma 2.3.8 for $1 < k < p - 1$ we see that there are at least 2 Spin^c structures $[s]$ satisfying $g - k \leqslant s < g$ and at least 2 Spin^c structures

$[s]$ satisfying $g \leqslant s < g-k+p$. In any case either there is an $[s]$ with $g-k \leqslant s < g$ so that $s \equiv 0 \mod p$ or there is an $[s]$ so that $g \leqslant s < g-k+p$ and $s \equiv 0 \mod p$. In the former case Lemma 2.3.8 implies that there is a unique Spin^c structure with rank $2\left\lfloor \frac{2g-1}{|p|} \right\rfloor + 3$, contradicting Lemma 2.2.2. In the latter case, there are k consecutive Spin^c structures $[s]$, namely those s with $g-k \leqslant s < g$, with rank $2\left\lfloor \frac{2g-1}{|p|} \right\rfloor + 1$ and only one Spin^c structure $[s]$ with $g \leqslant s < g-k+p$ with the same rank. Again this contradicts Lemma 2.2.2 □

Recall that $k \equiv 2g(K)-1 \mod |p|$. Lemma 2.3.10 implies that if K admits a reducible surgery of slope p, then $k=1$ or $k=p-1 \equiv -1 \mod |p|$. Therefore we have the following Corollary

Corollary 2.3.11. *Suppose K is an almost L-space knot with a reducing slope p. Then either $p|g(K)$ or $p|2g(K)-2$ and p is even.*

Proof. By Lemmas 2.3.9 and 2.3.10 we see that the only possibilities are $k = 1 \equiv 2g(K)-1 \mod p$ and $k = p-1 \equiv 2g(K)-1 \mod p$. In the former case, we have that $p|2g(K)-2$ and in the latter case we have that $p|2g(K)$. If $k = p-1 \equiv 2g(K)-1 \mod p$, then by Lemma 2.3.8 we see that the Spin^c structure labelled g must satisfy $g \equiv 0 \mod p$, so actually $p|g(K)$ and in that case all the Spin^c structures have the same rank. If $p|2g(K)-2$, then we see that the Spin^c structure labelled $g-1$ cannot be equivalent to the Spin^c structure labelled $0 \mod p$. So in particular p does not divide $g(K)-1$. Hence p is even. Moreover, we have $g(K)-1 = \frac{p}{2}m$ where m is odd (if m were even then p would divide $g(K)-1$). □

Lemma 2.3.12. *Suppose that p is a reducing slope so that $p|2g(K)-2$. Then $g(K)$ is even and $S^3_p(K) \cong L(2,1)\#R$ with $|H_1(R;\mathbb{Z})| = \frac{p}{2}$*

Proof. In the proof of Corollary 2.3.11 we found that if p is a reducing slope then either $p|g(K)$ or $p|2g(K)-2$. If we are in the latter case then $[g-1]$ and $[g-1+r]$ have to be paired up where r divides p and $g-1+r$ is the unique Spin^c structure so that $[g-1+r] = 0$. By Corollary 2.3.11 we see

that $g-1+r=\frac{p}{2}m+r\equiv 0 \mod p$, so $r=\frac{p}{2}$. Hence $S^3_p(K)\cong L(2,1)\#R$ with $|H_1(R;\mathbb{Z})|=\frac{p}{2}$, and we necessarily have that $(2,\frac{p}{2})=1$, so that $\frac{p}{2}$ is odd. Again by Corollary 2.3.11 we find that $g(K)=\frac{p}{2}m+1$ for some $m\geqslant 1$ and odd. Since $\frac{p}{2}$ is also odd, we see that $g(K)$ is even. □

In summary, we showed that for p to be a reducing slope on an Almost L-space knot, we have either $p|g(K)$ or $p|2g(K)-2$ and p and $g(K)$ are both even.

Relative Gradings and Proper Divisors

In this section we use the gradings of elements of $\mathrm{HF}_{red}(S^3_p(K),[s])$ to further restrict the possible reducing slopes on almost L-space knots. The following is an upgraded version of Lemma 2.2.2 (see [HLZ15])

Lemma 2.3.13. *For $S^3_p(K)\cong L(a,s)\#R$, there is an isomorphism of relatively graded $\mathbb{F}[U]$-modules $\mathrm{HF}^+(S^3_p(K),[s])\cong\mathrm{HF}^+(S^3_p(K),[s+r])$.*

We will use this lemma in conjunction with a computation of the relative gradings from the mapping cone to rule out divisors of $g(K)$ and $2g(K)-2$ from being reducing slopes.

To extract the gradings of elements in $\mathrm{HF}_{red}(S^3_p(K),[s])$ we want to dive deeper into the mapping cone and identify certain cycles in the mapping cone that generate $\mathrm{HF}_{red}(S^3_p(K),[s])$.

The following is from Gainullin [Gai17], building on work of [NW15] [HLZ15] and [OS04b]

Lemma 2.3.14. *[Gai17, Proposition 15] Suppose $p>0$, then there is an isomorphism $\mathrm{HF}^+(S^3_p(K),[i])\cong\ker(D^+_{i,p})$ and*

$$\ker(D^+_{i,p})\cong\mathcal{T}^+\bigoplus_{n\geqslant 1}\tau(H_{i-np})\bigoplus_{n\geqslant 1}\tau(V_{i+np})\bigoplus\mathbb{A}_{i,red}$$

for $i\leqslant p-i$

and otherwise

$$\ker(D^+_{i,p}) \cong \mathcal{T}^+ \bigoplus_{n\geqslant 2} \tau(H_{i-np}) \bigoplus_{n\geqslant 0} \tau(V_{i+np}) \bigoplus \mathbb{A}_{i,red}$$

Lemma 2.3.15. *[Gai17, Lemma 18] Suppose $p < 0$ and K is a knot so that $V_i(m(K)) = 0$. Then $\operatorname{coker}(D^+_{i,p}) \cong \mathcal{T}^+$, and*

$$\mathrm{HF}_{red}(S^3_p(K), [i]) \cong \ker(D^+_{i,p}) \cong \ker(D^T_{i,p}) \oplus \mathbb{A}_{i,red}$$

In particular, we can identify the largest graded pieces of each tower in $\mathrm{HF}_{red}(S^3_p(K), [s])$ as follows. By Lemma 2.3.3, for each $s \neq 0$ $A^+_s \cong \mathcal{T}^+$. Define $x_s = U^{-\max\{V_s, H_s\}}$, $y_s = U^{-\min\{V_s, H_s\}}$ and $z_s = U^{-\min\{V_s, H_s\}+1}$. So that z_s is the top graded element in $\ker(v^+_s + h^+_s) \cong F[U^{-1}]/U^{-\min\{V_s, H_s\}}$. Knowing $\mathrm{HF}_{red}(S^3_p(K), [s])$ as a relatively graded $\mathbb{F}[U]$-module is equivalent to knowing the gradings of the z_t for $t \equiv s \mod p$. In the case $s = 0$ by Lemma 2.3.3 we have $A^+_0 \cong \mathcal{T}^+ \oplus \mathbb{F}[U^{-1}]/U^{-N}$, so we have x_0, y_0 and z_0 as above in the $\mathcal{T}^+$ summand, and we have and element a in $\mathbb{F}[U^{-1}]/U^{-N}$ so that $a \neq Ub$ for some b. Then by Lemmas 2.3.15 and 2.3.14 understanding $\mathrm{HF}_{red}(S^3_p(K), [0])$ as a relative graded $\mathbb{F}[U]$-module is equivalent to knowing the grading of both z_t for $t \equiv 0 \mod p$ and a. Expressed a different way, define the auxilliary object

$$\widetilde{\mathrm{HF}}(S^3_p(K), [s]) := \operatorname{coker}(U : \mathrm{HF}^+(S^3_p(K), [s]) \to \mathrm{HF}^+(S^3_p(K), [s]))$$

That is, $\widetilde{HF}(S^3_p(K), [s])$ picks off the top of each truncated tower in $\mathrm{HF}_{red}(S^3_p(K), [s])$, so when $[s] \neq [0]$ this is equivalent to picking of the $z'_t s$ with $t \equiv s \mod p$ and when $[s] = [0]$ this is picking out both the $z'_t s$ for $t \equiv 0 \mod p$ and the element $a \in \mathbb{F}[U^{-1}]/U^{-N}$ so that $a \neq Ub$ for any b by Lemmas 2.3.14 and 2.3.15. In particular, we see that for $[s] \neq [0]$ and $p > 0$, we have

$$\operatorname{rank}(\widetilde{\mathrm{HF}}_n(S^3_p(K), [s])) = \#\{t : t \equiv s \mod p, \frac{p}{2} < |t| \leqslant g(K) - 1, gr(z_t) = n\}$$

and for $p < 0$ and $[s] \neq [0]$, we have

$$\operatorname{rank}(\widetilde{\mathrm{HF}}_n(S^3_p(K), [s]) = \#\{t : t \equiv s \mod p, gr(z_t) = n\}$$

Moreover, if we let $gr^{[s]}_{top}$ denote the largest grading of an element of $\widetilde{\mathrm{HF}}(S^3_p(K), [s])$ and $gr^{[s]}_{bot}$ denote the smallest, then a consequence of Lemma 2.3.13 is that if p is a reducing slope with $S^3_p(K) \cong L(a,b)\#R$, then for for every $n \in \mathbb{Z}$

$$\operatorname{rank}(\widetilde{\mathrm{HF}}_{gr^{[s]}_{top}+n}(S^3_p(K), [s]) = \operatorname{rank}(\widetilde{\mathrm{HF}}_{gr^{[s+r]}_{top}+n}(S^3_p(K), [s+r])$$

and

$$\operatorname{rank}(\widetilde{\mathrm{HF}}_{gr^{[s]}_{bot}+n}(S^3_p(K), [s]) = \operatorname{rank}(\widetilde{\mathrm{HF}}_{gr^{[s+r]}_{bot}+n}(S^3_p(K), [s+r])$$

In summary, we want to understand the relative gradings of the elements z_t and z_{t+r} when these elements exist and when $[t]$ and $[t+r]$ are distinct non-conjugate Spin^c structures. With this in mind the following is [HLZ15, Lemma 3.8 and Lemma 3.9].

Lemma 2.3.16. *For x_t and y_t as above, we have $gr(x_t) - gr(y_t) = 2|t|$.*

Lemma 2.3.17. *For z_t as above we have:*

If $p > 0$

$$gr(z_{t+p}) - gr(z_t) = \begin{cases} 2t & t > 0 \\ 2(t+p) & t + p < 0 \\ 0 & t \leqslant 0 \leqslant t + p \end{cases}$$

If $p < 0$

$$gr(z_{t-|p|}) - gr(z_t) = \begin{cases} 2t & t - |p| \geqslant 0 \\ 2(t-|p|) & t \leqslant 0 \\ 2(2t-|p|) & t - |p| \leqslant 0 \leqslant t \end{cases}$$

We will us the above Lemma in conjunction with Lemma 2.3.13 to rule out proper divisors of $\pm g(K)$ and $\pm(2g(K)-2)$ from being reducing slopes.

Lemma 2.3.18. *Suppose K is an almost L-space knot and p is a slope with $p|g(K)$ and $p \neq g(K)$. If p is a reducing slope then $p = 2r$ or $p = -2r$ and $g(K)$ is even*

Proof. Let K be an almost L-space knot. Suppose $g(K) = pm$ for some m with $|m| \geqslant 2$. Further, suppose $S^3_p(K) \cong L(a,b)\#R$ with $p = \pm ar$ and $(a,r) = 1$. We first deal with the case $p > 0$. We will compare the relative gradings of elements in $\widetilde{\mathrm{HF}}(S^3_p(K),[0])$ and $\widetilde{\mathrm{HF}}(S^3_p(K),[-r])$. In Spin^c structure $[0]$ the elements a, z_0 z_p, and z_{-p} are all non-zero in the mapping cone and a, z_p and z_{-p} survive in $\widetilde{\mathrm{HF}}(S^3_p(K),[0])$ by Lemma 2.3.14, where a is the element in $\mathrm{HF}_{red}(S^3_p(K),[0])$ coming from the $A^+_{0,red}$ summand of Lemma 2.3.3. Note that Lemma 2.3.17 shows that $gr(z_0) = gr(z_p) = gr(z_{-p})$. Therefore, $\mathrm{rank}(\widetilde{\mathrm{HF}}_{gr(z_0)}(S^3_p(K),[0])) \geqslant 2$. Now consider Spin^c structure $[-r]$. In the mapping cone for Spin^c structure $[-r]$ the elements z_{-r}, z_{p-r} z_{2p-r} and z_{-r-p} are all non-zero, and z_{p-r}, z_{p+r} and z_{2p-r} are non-zero in $\widetilde{\mathrm{HF}}(S^3_p(K),[-r])$ by Lemma 2.3.14. By Lemma 2.3.17 we see that $gr(z_{2p-r}) - gr(z_{p-r}) = 2(p-r)$, $gr(z_{p-r}) = gr(z_{-r})$ and $gr(z_{-p-r}) - gr(z_{-r}) = 2r$. Therefore, the only way for there to be a relatively graded isomorphism is if these two elements are in the same relative grading, so we need $2(p-r) = 2r$. This implies that $p = 2r$.

Next, suppose $p < 0$. Then as before we have the elements z_0, z_p and z_{-p} in the mapping cone for Spin^c structure $[0]$, as well as the element a coming from A^{red}_0, but in this case all the z_i with $i \equiv p$ are non-zero in $\widetilde{\mathrm{HF}}(S^3_p(K),[0])$. Computing relative gradings we see that $gr(z_0) - gr(z_p) = gr(z_0) - gr(z_{-p}) = 2|p|$, so $\mathrm{rank}\widetilde{\mathrm{HF}}_{gr(z_0)-2|p|}(S^3_p(K),[r]) \geqslant 2$. Comparing with Spin^c structure $[r]$, we see that the elements z_r, z_{p-r}, z_{2p-r} and z_{-r-p} are all non-zero and contribute to $\widetilde{\mathrm{HF}}(S^3_p(K),[r])$. Computing relative gradings, we find that $gr(z_r) - gr(z_{r-p}) = 2(r-p)$, $gr(z_r) - gr(z_{r+p}) = -2(2r+p)$ and $gr(z_{r+p}) - gr(z_{r+2p}) = -2(r+2p)$. In $[r]$, the z_i with $i \equiv r \mod p$ are the only elements that contribute to $\widetilde{\mathrm{HF}}(S^3_p(K),[r])$ and so $gr^{[r]}_{top} = gr(z_r)$ and if there is a relative graded isomorphism $\mathrm{HF}^+(S^3_p(K),[0]) \cong \mathrm{HF}^+(S^3_p(K),[r])$ necessarily $-2(2r+p) = 2(2r+p)$, which implies $p = -2r$. Otherwise there are not two or more of the z_i in the same relative grading in Spin^c structure

$[r]$. Therefore, the only possible reducing slopes for an almost L-space knot that are proper divisors of $g(K)$ are $p = \pm 2r$ with $r \geqslant 1$ odd. □

Corollary 2.3.19. *If $g(K)$ is odd, then K does not admit any reducing slopes that are proper divisors.That is, if p is a reducing slope for an almost L-space knot with odd genus then $p = \pm g(K)$.*

Proof. We saw in Lemma 2.3.8 that the only possible reducing slopes for an almost L-space knot are divisors of $g(K)$ and even divisors of $2g(K) - 2$ when $g(K)$ is even. So if $g(K)$ is odd, only the former are possible. But by Lemma 2.3.18 we see that also the only possible reducing slopes are even divisors of $g(K)$, so in particular $g(K)$ is even. □

Now, we analyze the cases when $p = 2r$, $p|g(K)$ with $p \neq g(K)$ and $r > 1$.

Lemma 2.3.20. *Suppose $p > 0$, $p|g(K)$, $p \neq g(K)$ and $p = 2r$. If $r > 1$, then p is not a reducing slope.*

Proof. Suppose $p = 2r$ and consider Spin^c structures $[1]$ and $[1 + r]$. By Lemma 2.3.13 there is a relatively graded isomorphism $\mathrm{HF}^+(S^3_p(K), [1]) \cong \mathrm{HF}^+(S^3_p(K), [1+r])$. To this end, in Spin^c structure $[1]$ the elements z_1, z_{1+2r}, z_{1-2r} and z_{1-4r} are all non-zero in the mapping cone and z_{1+2r}, z_{1-2r} and z_{1-4r} contribute to $\widetilde{\mathrm{HF}}(S^3_p(K), [1])$. By lemma 2.3.17 we find $gr(z_{1+2r}) - gr(z_1) = 2$, $gr(z_{1-2r}) = gr(z_1)$ and $gr(z_{1-2r}) - gr(z_{1-4r}) = -2(2r - 1)$. We compare this with Spin^c structure $[1 + r]$ (here we use the fact that $r > 1$ so that $[1 + r] \neq [0]$). In that Spin^c structure we have the elements z_{1+r}, z_{1+3r}, z_{1-r} and z_{1-3r} are all non-zero in the mapping cone and by Lemma 2.3.14 all but z_{1+r} survive in $\widetilde{\mathrm{HF}}(S^3_p(K), [1 + r])$. Computing relative gradings, we find that $gr(z_{1+3r}) - gr(z_{1+r}) = 2(1 + r)$, $gr(z_{1+r}) = gr(z_{1-r})$ and $gr(z_{1-3r}) - gr(z_{1-r}) = 2(r-1)$. Therefore, in order for there to be a relatively graded isomorphism we must have $2 = 2(r - 1)$ and $2(1 + r) = 2(2r - 1)$. Hence $r = 2$. This contradicts Lemma 2.3.18 where we proved that in this case r is odd. □

Lemma 2.3.21. *Suppose $p < 0$, $p|g(K)$ with $p \neq g(K)$ and $p = -2r$. If $r > 1$ then p is not a reducing slope.*

Proof. In the mapping cone the elements z_1 and z_{1-2r} are non-zero and survive in $\widetilde{\mathrm{HF}}(S^3_p(K), [1])$. We compute $gr(z_{1-2r}) - gr(z_1) = 2(2-2r)$. In Spin^c structure $[1+r]$, the elements z_{1-r} and z_{1+r} are non-zero and survive in $\widetilde{\mathrm{HF}}(S^3_p(K), [1+r])$. Computing their relative grading difference we have $gr(z_{1-r}) - gr(z_{1+r}) = 4$. Hence either $2(2-2r) = 4$ or $2(2-2r) = -4$. So either $r = 0$, which is impossible, or $r = 2$. The latter contradicts $S^3_p(K) \cong L(2,1)\#R$. □

Lemma 2.3.22. *For K an almost L-space knot the slope. If $g(K) > 3$ then $p = -g(K)$ is not a reducing slope.*

Proof. Let $p = -g(K) = -ar$ and consider the mapping cone for Spin^c structure $[1]$

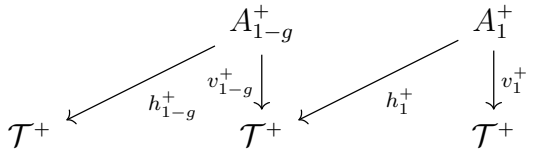

There are two generators in $\widetilde{\mathrm{HF}}(S^3_p(K), [1])$, z_{1-g} and z_1. We compute their relative grading difference:

$$gr(z_{1-g}) - gr(z_1) = 2(2-g)$$

By periodicity, there should be a relatively graded isomorphism between $\widetilde{\mathrm{HF}}(S^3_p(K), [1])$ and $\widetilde{\mathrm{HF}}(S^3_p(K), [1+r])$. When $r \neq 1$ are two non zero generators in $\widetilde{\mathrm{HF}}(S^3_p(K), [1+r])$, z_{1-g+r} and z_{1+r}. Their relative grading difference is

$$gr(z_{1-g+r}) - gr(z_{1+r}) = 2(2(1+r) - g)$$

Hence, in order for there to be a relatively graded isomorphism, we need either $4(1+r) - 2g = 2(2-g)$ or $2g - 4(1+r) = 4 - 2g$. In the former case we

find that $4 + 4r = 4$, hence $r = 0$ which is a contradiction. In the latter case we find that $g - 2(1 + r) = 2 - g$, this implies $g = 2 + r$. Since $p = -g(K)$ and $p = -ar$, we have that $-ar = 2 + r$ So $-r(a + 1) = 2$. Therefore either $r = 2$ and $a = -2$, which contradicts $(a, r) = 1$, or $r = 1$ and $a = -3$. This implies that $p = -3$. □

Lemma 2.3.23. *If $p > 0$, K is an almost L-space knot and $p|2g(K) - 2$ with $p \neq 2, 2g(K) - 2$. Then p is not a reducing slope.*

Proof. By Lemma 2.3.8, we see that $p = ar$ with $a = 2$ and $r = \frac{p}{2}$ odd. Therefore, we will compare relative gradings of elements in $[1]$ and $[1 - \frac{p}{2}]$. Now in Spin^c structure $[1]$ by Lemma 2.3.17 we have $gr(z_1) + 2 = gr(z_{1+p})$ and $gr(z_1) = gr(z_{1-p})$. In $[1 - \frac{p}{2}]$ we have $gr(z_{1+\frac{p}{2}}) = gr(z_{1-\frac{p}{2}}$ and $gr(z_{1-\frac{p}{2}}) + 2(\frac{p}{2} - 1) = gr(z_{1-\frac{3p}{2}})$. Therefore, in order for there to be a relatively graded isomorphism, we would need $1 = \frac{p}{2} - 1$, so $p = 4$. This is impossible since $(\frac{p}{2}, 2) = 1$.

□

Lemma 2.3.24. *Suppose $p < 0$, K is an almost L-space knot and $p|2g(K) - 2$ with $p \neq 2 - 2g, -2$. Then p is not a reducing slope.*

Proof. In this case the elements z_1, z_{1+p} and z_{1-p} are all non-zero in the mapping cone and survive in $\widetilde{\mathrm{HF}}(S^3_p(K), [1])$. By Lemma 2.3.17 we have that $gr(z_{1-p}) - gr(z_1) = -2(p - 1)$ and $gr(z_{1+p}) - gr(z_1) = 2(2 + p)$. Since $p \neq -2$, the Spin^c structures $[0]$ and $[1 - \frac{p}{2}]$ are distinct. We have the elements $z_{1-\frac{p}{2}}], z_{1-\frac{3p}{2}}$ and $z_{1+\frac{p}{2}}$. Computing their relative grading differences we find $gr(z_{1-\frac{p}{2}}) - gr(z_{1+\frac{p}{2}}) = -4$ and $gr(z_{1-\frac{3p}{2}}) - gr(z_{1-\frac{p}{2}}) = -2(\frac{3p}{2} - 1)$. Hence in order for there to be a relatively graded isomorphism from $[1]$ to $[1 - \frac{p}{2}]$, we would need either $2(2 + p) = 4$ or $2(2 + p) = -4$. In the former case we have $p = 0$, which obviously cannot happen, and in the latter we have $p = -4$, which cannot happen because by Lemma 2.3.8 $\frac{p}{2}$ is odd. □

Lemma 2.3.25. *Suppose $p = 2 - 2g$ and $p \neq -2$ (so $g(K) \neq 2$). Then p is not a reducing slope.*

Proof. Since $p \neq -2$, we have that $g \geqslant 4$ (recall that in the case when p divides $2g(K)-2$, the genus is even) and $[1]$ and $[2-g]$ are not conjugate.

We have that in each Spin^c structure $[s] \neq [0], [g-1]$ there is just one non-zero z_s. However, we can still compare the grading on this z_s to the bottom of the tower in two Spin^c structures in the same orbit, namely $[1]$ and $[2-g]$. In $[1]$, we have $gr(x_1) = d_1 + 1$, hence $gr(z_1) = d_1 - 3$. In $[2-g]$, we have $gr(z_{2-g}) = d_{2-g} - 1$. So there is no relatively graded isomorphism of $\mathbb{F}[U]$-modules.

□

In summary, we have shown that for p to be a reducing slope, p must satisfy either $p = \pm 2$, or $p = g(K)$, unless $g(K) = 3$ in which case $p = \pm g(K)$, or $p = (2g(K)-2)$ with p and g even. Hence if g is odd and greater than 3, then the only possible reducing slope is $g(K)$.

Corollary 2.3.26. *Almost L-space knots of genus $g(K) \geqslant 2$ do not admit multiple reducing slopes.*

CHAPTER 3

(1,1) PATTERNS

In this chapter we study the knot Floer homology of satellite knots with $(1,1)$-patterns from the perspective of bordered Floer homology and the immersed curve reformulation of the pairing theorem for satellite knots with $(1,1)$-patterns with a goal of computing various 3- and 4-dimensional invariants of satellite knots with patterns from two novel families of patterns. In Sections 3.1-3.6 we study a family of patterns which we denote by $P^{(p,1)}$. These patterns satisfy $w(P^{(p,1)}) = p+1$ and $P^{(p,1)}(U) \sim T_{2,3}$. We call such patterns *trefoil patterns*. We compute the three-genus, and bound the four-genus of these satellites. We show that all patterns in this family are fibered in the solid torus. This implies that satellites with fibered companions and patterns from this family are also fibered. We also show that satellites with thin fibered companions or companions K with $\tau(K) = \pm g(K)$ formed from these patterns have left or right veering monodromy. We then use this to show that satellites with fibered companion knots K so that $|\tau(K)| < g(K)$ formed from these patterns do not have thin knot Floer homology, using a recent result of [BNS22].

In Sections 3.7-3.11 we study a family of patterns denoted by $Q^{i,j}$ such that $w(Q^{i,j}) = j$ and $Q^{i,j}(U) \sim U$ (called *unknot patterns*) and the knot Floer homology of the *n-twisted satellites* that are formed from these patterns with arbitrary companions. Recall that an n-twisted satellite knot, denoted $P_n(K)$, is formed from a companion knot K and a pattern knot P where the longitude of the solid torus containing P is glued to the curve $n\mu + \lambda$ on $S^3 - \nu(K)$. We study how the invariants $g(Q^{i,j}_n(K))$, $\tau(Q^{i,j}_n(K))$ and $\epsilon(Q^{i,j}_n(K))$ behave under this twisting operation and find closed formulas for then in terms of i, j, n. We also investigate the function $n \mapsto \dim(\widehat{\mathrm{HFK}}(S^3, Q^{i,j}_n(K), g(Q^{i,j}_n(K))))$ and use this and fibered detection of knot Floer homology to understand when the n-twisted pattern $Q^{i,j}_n$ is fibered in the solid torus.

3.1 Introduction

Knot Floer homology, introduced by Rasmussen [Ras03a] and Ozsváth and Szabó [OS04b], is an invariant of null homologous knots in the three sphere. Its simplest instantiation takes the form of a bigraded Abelian group, $\widehat{\mathrm{HFK}}(S^3, K) \cong \bigoplus_{m,A} \widehat{\mathrm{HFK}}_m(S^3, K, A)$. Here m is called the *Maslov grading* and A is called the *Alexander grading*. Knot Floer homology contains information about the knot K and its complement $S^3 \backslash \nu(K)$. For example, it detects the three-genus [OS04a] and fiberedness of the knot [Juh08c; Ni07], contains information about the monodromy of fibered knots [Ni20], bounds the number of disjoint, non-isotopic Seifert surfaces in the knot complement [Juh08a], and bounds the four-genus of the knot [OS03b]. In this note, we use these detection properties to investigate three- and four-dimensional invariants of satellite knots formed from a family of $(1,1)$-patterns.

Recall that, given a knot $K \subset S^3$ and a pattern $P \subset S^1 \times D^2$, we can construct a new knot, called the (0-twisted) satellite knot with *companion* knot K and *pattern* knot P, denoted $P(K)$, by removing a tubular neighborhod of K and gluing in the pair $(S^1 \times D^2, P)$ so that $S^1 \times \{pt\}$ is identified with the Seifert longitude of K. A pattern knot P is a $(1,1)$-pattern if it admits a genus-1 doubly-pointed bordered Heegaard diagram, a concept that we recall in section 3.2.

Our main reason for restricting to $(1,1)$-patterns is computational. For an arbitrary pattern P, the bordered pairing theorem of [LOT18] expresses $\widehat{\mathrm{HFK}}(S^3, P(K))$ in terms two invariants: $\widehat{\mathrm{CFA}}(S^1 \times D^2, P)$ and $\widehat{\mathrm{CFD}}(S^3 \backslash \nu(K))$. For $(1,1)$-patterns, the work of Chen in [Che19] recasts this pairing theorem in terms of Lagrangian intersection Floer homology of two curves in the punctured torus. This facilitates computation in two ways: it allows one to vary the pattern within a family and it allows one to compute the decompositon into Alexander gradings much more efficiently than with the language of the original bordered pairing theorem.

Many of the computations of knot Floer homology of satellite knots that exist in the literature involve $(1,1)$-patterns. For example the cabling

patterns studied in [Hom14] (see also [HW19]), Mazur pattens studied in [Lev16] and [PW21], and Whitehead double patterns studied in [Hed07] are all $(1,1)$-patterns. Given this, it is interesting to compute knot Floer homology of satellites where the pattern comes from a family of $(1,1)$-patterns. In [Che19] this project is taken up and he examines the case where P is an arbitrary $(1,1)$-pattern P so that $P(U) \simeq U$, called an *unknot pattern*, and the companion knot is the right or left handed trefoil.

In the following, we use the immersed curve pairing theorem as stated in [Che19] to compute the knot Floer homology of satellites with arbitrary companion knots K and patterns P from a specific family of $(1,1)$-patterns with the property that $P(U) \simeq T_{2,3}$. We will refer to such patterns as *trefoil patterns*. In section 3.4 we introduce, for each $p > 1$, a trefoil pattern denoted $P^{(p,1)}$ which is closely related to the $(p,1)$ unknot cabling pattern. Our goal is to investigate various three- and four-dimensional properties of the satellite knots obtained from these trefoil patterns. First, for each $p > 1$ and for any knot K, we compute the invariant $\tau(P^{(p,1)}(K))$, an integer valued concordance invariant derived from the knot Floer homology package first defined by [OS03b], in terms of $\tau(K)$ and $\epsilon(K)$.

Theorem 3.1.1. *For the patterns $P^{(p,1)}$ and for an arbitrary companion knot $K \subset S^3$, we have*

- *If $\epsilon(K) = 1$, then $\tau(P^{(p,1)}(K)) = (p+1)\tau(K) + 1$*
- *If $\epsilon(K) = -1$, then $\tau(P^{(p,1)}(K)) = (p+1)(\tau(K) + 1)$*
- *If $\epsilon(K) = 0$, so $\tau(K) = 0$, then $\tau(P^{(p,1)}(K)) = \tau(T_{2,3}) = 1$.*

As shown in [OS03b, Corollary 1.3], the integer $\tau(K)$ satisfies $|\tau(K)| \leqslant g_4(K)$, where $g_4(K)$ is the smooth four-genus of a knot (the minimal genus of a surface properly embedded in B^4 with boundary $K \subset S^3$). This gives the following corollary concerning the slice genus of these satellite knots.

Corollary 3.1.2. *For any companion knot K with $\tau(K) \neq -1$ and $\epsilon(K) \neq -1$, the satellite knots $P^{(p,1)}(K)$ are not slice.*

Given a pattern in the solid torus, we can associate to it an integer $w(P)$, called the winding number of the pattern, by computing the algebraic intersection between the pattern P and a meridional disk $\{0\} \times D^2$. Given a pattern P with winding number r, we define a *relative Seifert surface* for P to be a surface $\tilde{\Sigma}$ in $S^1 \times D^2$ so that the interior of $\tilde{\Sigma}$ is disjoint from P, and the boundary of $\tilde{\Sigma}$ consists of P together with r coherently oriented longitudes. A pattern is *fibered* if the complement $S^1 \times D^2 \backslash \nu(P)$ is fibered over S^1 with fiber surface a relative Seifert surface for P. Furthermore, the genus of a pattern, $g(P)$, is defined to be the minimal genus of a relative Seifert surface for P.

For a satellite knot $P(K)$ with a *non-trivial* companion K a result of Schubert [Sch53] shows that the three-genus of the satellite knot $g(P(K))$ can be expressed in terms of $w(P)$, $g(K)$ and $g(P)$:

$$g(P(K)) = |w(P)|g(K) + g(P). \tag{3.1}$$

This has the consequence that for any non-trivial knot K, the value of $g(P(K))$ is determined by the value of $g(K)$ and $g(P)$. However, $g(P)$ depends only on the pattern. Hence, we can compute $g(P)$ if we can compute the three genus of some satellite with non-trivial companion K and pattern P, for example $P(T_{2,3})$. Using the fact that knot Floer homology detects the genus of knots, we prove

Lemma 3.1.3. *For any $p > 1$, the trefoil patterns $P^{(p,1)}$ have $g(P^{(p,1)}) = 1$.*

Now, given the value of $g(P)$, we can determine $g(P(K))$ in terms of $g(K)$ for any non-trivial companion knot K by using equation (3.1). This gives the following corollary. Note that the case $K = U$ follows since $g(U) = 0$ and $P^{(p,1)}(U) \simeq T_{2,3}$ has genus 1.

Corollary 3.1.4. *For any knot K and for any $p > 1$, $g(P^{(p,1)}(K)) = (p + 1)g(K) + 1$.*

In a similar vein, Hirasawa, Murasugi, and Silver proved in [HMS08] that a satellite knot with non-trivial companion is fibered if and only if both

the pattern and the companion knot are fibered. This has the consequence that to determine if a pattern P is fibered in the solid torus, it is enough to determine if the knot $P(T_{2,3})$ is fibered. Since knot Floer homology detects when a knot is fibered, to show that the pattern P is fibered, it is then enough to compute $\widehat{\mathrm{HFK}}(S^3, P(T_{2,3}), g(P(T_{2,3})))$ and show that it has rank 1.

Theorem 3.1.5. *For $p > 1$ the pattern knot $P^{(p,1)}$ is fibered in the solid torus.*

One motivation to understand fibered patterns is the result of Ni [Ni06, Theorem 1.2] that the knot Floer homology of satellites with fibered patterns in the top Alexander grading has the same dimension as the knot Floer homology of the companion in the top Alexander grading. That is

$$\mathrm{rk}\widehat{\mathrm{HFK}}(S^3, K, g(K)) = \mathrm{rk}\widehat{\mathrm{HFK}}(S^3, P(K), g(P(K))). \tag{3.2}$$

This theorem, when combined with the work of Juhasz in [Juh08c; Juh08a] which relates the knot Floer homology in the top Alexander grading to the sutured Floer homology of the complement of a Seifert surface for the knot K has the following consequences.

Proposition 3.1.6. *If K is a knot with $rk(\widehat{\mathrm{HFK}}(S^3, K, g(K))) < 4$ and P is a fibered pattern, then for all $i \geqslant 1$ the knots K and $P^i(K)$ have unique minimal genus Seifert surfaces.*

Proposition 3.1.7. *If K is a knot with $rk(\widehat{\mathrm{HFK}}(S^3, K, g(K))) = 3$ and P is a fibered pattern, then K and $P^i(K)$ admit depth $\leqslant 1$ taut foliations transverse to the boundary.*

Recall that fibered knots have unique minimal genus Seifert surfaces. These propositions can be viewed as generalizations of this fact. In particular, by Theorem 3.1.5, these propositions apply to the patterns $P^{(p,1)}$.

Finally we study the next to top Alexander graded piece of the knot Floer homology of these satellite knots. In the case that K is a fibered knot,

$\widehat{\mathrm{HFK}}(S^3, K, g(K)-1)$ contains information about the monodromy of the fibration, in the following sense.

Theorem 3.1.8 ([Ni20])**.** *If K is a fibered knot and $rk(\widehat{\mathrm{HFK}}(S^3, K, g(K)-1)) = 1$, then the monodromy of K is either left or right veering.*

Remark 3.1.9. *There is no analogue of equation (3.2) for the next to top Alexander graded piece of knot Floer homology of a satellite and its companion. In general, there is not even an inequality relating them, even for fibered patterns. For example $rk(\widehat{\mathrm{HFK}}(S^3, T_{2,3}, 0) = 1$ and $rk\widehat{\mathrm{HFK}}(S^3, (T_{2,3})_{2,1}, 1) = 2$ and as Theorem 3.1.10 shows, constructing satellites with certain patterns can decrease the rank in the next to top Alexander graded piece by an arbitrary amount. Note, certain families of patterns do preserve the property of having one dimensional Floer homology in the next to top Alexander grading, for example if K is an L-space knot and P is a pattern so that $P(K)$ is also an L-space knot (for example the (p, q) cable pattern with $\frac{q}{p} \geqslant 2g(K)-1$) then by [HW18] both K and $P(K)$ have one dimensional Floer homology in the next to top Alexander grading.*

Recall that the δ-grading on knot Floer homology is define by $\delta = m - A$. We call a knot K *Floer thin* (or *thin*) if the δ-grading is constant for all generators of $\widehat{\mathrm{HFK}}(S^3, K)$.

Theorem 3.1.10. *For each $p > 1$, and for any fibered knot K with $\tau(K) = \pm g(K)$, or for any fibered thin knot K, we have*

$$rk(\widehat{\mathrm{HFK}}(S^3, P^{(p,1)}(K), g(P^{(p,1)}(K))-1)) = 1.$$

Corollary 3.1.11. *For any fibered knot K with $\tau(K) = \pm g(K)$, or for any fibered thin knot K, the fibered knot $P^{(p,1)}(K)$ has left or right veering monodromy.*

Lastly, we use Theorem 3.1.10 to show that for some fibered companion knots K, the satellite knots $P^{(p,1)}(K)$ are not Floer thin. The main result we use is [BNS22, Corollary 1.7] which says that a fibered thin knot with $|\tau(K)| < g(K)$ cannot have left or right veering monodromy.

Proposition 3.1.12. *If K is a non-trivial fibered knot with thin knot Floer homology such that $|\tau(K)| < g(K)$, then the knot Floer homology of $P^{(p,1)}(K)$ is not thin.*

Since quasialternating knots have thin knot Floer homology by [MO08], we have the following consequence of Proposition 3.1.12.

Corollary 3.1.13. *For any $p > 1$ and for any thin fibered knot K with $|\tau(K)| < g(K)$, the knots $P^{(p,1)}(K)$ are not quasialternating.*

Organization

In section 3.2 we introduced the bordered pairing theorem from [LOT18] and recall the work of [HRW22] reinterpreting the bordered invariants in terms of immersed curves in the punctured torus. In section 3.3, we recall Chen's immersed curve version of the pairing theorem from [Che19]. In section 3.4 we prove Theorem 3.1.1. In section 3.5, we prove Theorem 3.1.5, as well as propositions 3.1.6 and 3.1.7. In section 3.6, we prove Theorem 3.1.10 and Proposition 3.1.12.

3.2 Bordered Floer Homology

In this section we introduced the necessary notation to state and interpret the pairing theorem for bordered Floer homology of [LOT18]. Bordered Floer homology is an invariant that is used to study Heegaard Floer homology of three manifolds that have been decomposed along essential embedded surfaces. In our case, studying satellite operators, we are interested in decomposing the ambient three manifold, S^3 together with a knot K, along an essential torus. Then one can compute certain algebraic invariants of both sides and the Floer homology of the ambient three manifold (together with the knot filtration) can be computed by suitably combining these invariants.

In [LOT18], Lipshitz, Oszváth and Thurston associate, to a three manifold with parameterized torus boundary, a type A and D structure over

the torus algebra $\mathcal{A}$. We now briefly describe these concepts. The torus algebra $\mathcal{A}$ is defined as follows. Over $\mathbb{F}$ it has a basis consisting of two mutually orthogonal idempotents ι_0 and ι_1 and six other nontrivial elements $\rho_1, \rho_2, \rho_3, \rho_{12}, \rho_{23}, \rho_{123}$. The non-zero products in the algebra are given as follows:

$$\rho_1\rho_2 = \rho_{12} \quad \rho_2\rho_3 = \rho_{23} \quad \rho_1\rho_{23} = \rho_{12}\rho_3 = \rho_{123}$$

$$\begin{array}{ccc} \rho_1 = \iota_0\rho_1\iota_1 & \rho_2 = \iota_1\rho_2\iota_0 & \rho_3 = \iota_0\rho_3\iota_1 \\ \rho_{12} = \iota_0\rho_{12}\iota_0 & \rho_{23} = \iota_1\rho_{23}\iota_1 & \rho_{123} = \iota_0\rho_{123}\iota_1 \end{array}$$

If we let $\mathcal{I} \subset \mathcal{A}$ denote the subring of idempotents, then a type D structure over $\mathcal{A}$ is a unital left $\mathcal{I}$ module N together with an $\mathcal{I}$ linear map $\delta : N \to \mathcal{A} \otimes_{\mathcal{I}} N$ such that

$$(\mu \otimes \mathbb{I}) \circ (\mathbb{I} \otimes \delta) \circ \delta = 0$$

A type A structure is a right unital $\mathcal{I}$ module M with a collection of maps $m_{i+1} : M \otimes \mathcal{A}^i \to M$, for $i \geqslant 0$ such that

$$0 = \sum_{i=1}^{n} m_{n-i}(m_i(x \otimes a_1 \otimes \cdots \otimes a_{i-1}) \otimes \cdots \otimes a_{n-1}) + \sum_{i=1}^{n-2} m_{n-1}(x \otimes \cdots \otimes a_i a_{i+1} \otimes \cdots \otimes a_n) \tag{3.3}$$

and so that

$$m_2(x, 1) = x$$
$$m_i(x, \cdots, 1, \cdots) = 0$$

Given a type A structure M and a type D structure N, we can form a chain complex, called as the box tensor product and denoted $M \boxtimes N$. The underlying vector space is the tensor product $M \otimes_{\mathcal{I}} N$, and the differential is defined by

$$\partial^{\boxtimes}(x \otimes y) = \sum_{i=0}^{\infty} (m_{i+1} \otimes \mathbb{I})(x \otimes \delta_i(y)) \tag{3.4}$$

In the case that the type D structure is bounded, as defined in in [LOT18, Section 2], then the above sum is finite and the box tensor complex is well defined.

In what follows, we are interested in the following version of the bordered pairing theorem.

Theorem 3.2.1. *[LOT18, Theorem 11.19] Suppose Y is a closed 3-manifold decomposed as $Y = Y_1 \cup Y_2$ with $\partial Y_1 \cong -\partial Y_2 \cong T^2$. Suppose further that $K \subset Y_1$ is a knot which becomes null homologous in Y. Then up to homotopy equivalence of chain complexes*

$$g\widehat{\mathrm{CFK}}(Y, K) \simeq \widehat{\mathrm{CFA}}(Y_1, K) \boxtimes \widehat{\mathrm{CFD}}(Y_2)$$

We will give the immersed curve interpretation of this pairing theorem due to [Che19] for $(1,1)$ patterns in section 3.3. First, we will describe in more detail how to compute and interpret $\widehat{\mathrm{CFD}}(S^3 \backslash \nu(K))$ and $\widehat{\mathrm{CFA}}(S^1 \times D^2, P)$ as immeresed curves in the punctured torus in the next two sections.

$\widehat{\mathrm{CFD}}(S^3 \backslash \nu(K))$ *from* $\mathrm{CFK}^-(K)$

In this section, we recall the algorithm from [LOT18, Section 11.5] for computing $\widehat{\mathrm{CFD}}(S^3 \backslash \nu(K))$ from $\mathrm{CFK}^-(K)$. For the definitions of reduced, filtered basis, we refer the reader to the original source (see also [HW18]). We call a filtered reduced basis over $\mathbb{F}[U]$ vertically simplified if for each basis element x_i exactly one of the following conditions is satisfied

- There is a unique incoming vertical arrow, and no outgoing vertical arrow, or
- There is a unique outgoing vertical arrow and no incoming vertical arrow, or

- There are no vertical arrows.

A horizontally simplified basis is defined similarly, replacing vertical by horizontal in the above. Given a knot K and a framing n, there exists a pair of bases $\tilde{\eta} = \{\tilde{\eta}_1, \dots, \tilde{\eta}_{2k}\}$ and $\tilde{\xi} = \{\tilde{\xi}_1, \dots, \tilde{\xi}_{2k}\}$ for $CFK^-(K)$ that are horizontally and vertically simplified respectively. They are indexed so that for every pair $\tilde{\eta}_{2i-1}$ and $\tilde{\eta}_{2i}$ there is a horizontal arrow of length $l_i \geqslant 1$ connecting them and similarly, there is a vertical arrow of length $k_i \geqslant 1$ connecting $\tilde{\xi}_{2i-1}$ to $\tilde{\xi}_{2i}$. There are corresponding bases $\xi = \{\xi_0, \dots, \xi_{2k}\}$ and $\eta = \{\eta_0, \dots, \eta_{2k}\}$ for $\iota_0\widehat{\mathrm{CFD}}(X_k, n)$ so that if $\tilde{\xi}_j = \sum_{i=0}^{2k} a_{ij}\tilde{\eta}_i$ and $\tilde{\eta}_j = \sum_{i=0}^{2k} b_{ij}\tilde{\xi}_i$, then the corresponding change of bases formulas hold with the coefficients restricted to $U = 0$. The summand $\iota_1\widehat{\mathrm{CFD}}$ has basis

$$\bigcup_{i=1}^{k}\{\kappa_1^i, \dots, \kappa_{k_i}^i\} \cup \bigcup_{i=1}^{k}\{\lambda_1^i, \dots, \lambda_{l_i}^i\} \cup \{\mu_1, \dots, \mu_{|2\tau(K)-n|}\}$$

There are non-zero coefficient maps induced from the horizontal and vertical arrows in the complex for CFK^- as follows. A length k_i vertical arrow from ξ_{2i-1} to ξ_{2i} induces type D operations, sometimes called coefficient maps:

$$\xi_{2i-1} \xrightarrow{\rho_1} \kappa_1^i \xleftarrow{\rho_{23}} \kappa_2^i \dots \xleftarrow{\rho_{23}} \kappa_{k_i}^i \xleftarrow{\rho_{123}} \xi_{2i}$$

Similarly, for each length l_i horizontal arrow from η_{2i-1} to η_{2i}, we get coefficient maps

$$\eta_{2i-1} \xrightarrow{\rho_3} \lambda_1^i \xrightarrow{\rho_{23}} \lambda_2^i \xrightarrow{\rho_{23}} \dots \xrightarrow{\rho_{23}} \lambda_{l_i}^i \xrightarrow{\rho_2} \eta_{2i}$$

Additionally, there are coefficient maps from ξ_0 to η_0 depending on the framing and the value of the invariant $\tau(K)$.

- $\xi_0 \xrightarrow{\rho_{12}} \eta_0 \quad \text{if} \quad n = 2\tau(K)$
- $\xi_0 \xrightarrow{\rho_1} \mu_1 \xleftarrow{\rho_{23}} \dots \xleftarrow{\rho_{23}} \mu_m \xleftarrow{\rho_3} \eta_0 \quad \text{if} \quad n < 2\tau(K) \quad m = 2\tau(K) - n$
- $\xi_0 \xrightarrow{\rho_{123}} \mu_1 \xrightarrow{\rho_{23}} \dots \xrightarrow{\rho_{23}} \mu_m \xrightarrow{\rho_2} \eta_0 \quad \text{if} \quad n > 2\tau(K), \quad m = n - 2\tau(K)$

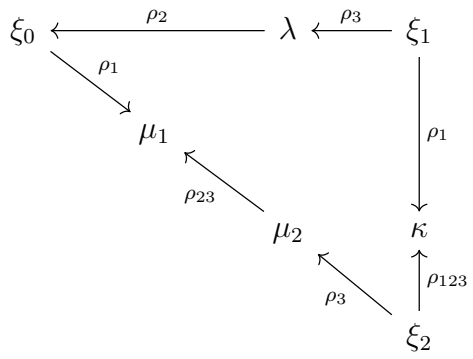

Figure 3.1. Type D structure for 0-framed right handed trefoil complement

For example, for the knot $K = T_{2,3}$, the right-handed trefoil, $\mathrm{CFK}^-(T_{2,3})$ has a simultaneously vertically and horizontally simplified $\mathbb{F}[U]$ basis $\{\tilde{\xi}_0, \tilde{\xi}_1, \tilde{\xi}_2\}$ with differential given by $\partial(\tilde{\xi}_1) = U\tilde{\xi}_0 + \tilde{\xi}_2$. Applying the above algorithm, we get the type D structure shown in Figure 3.1.

For any knot K in S^3, there is always a vertically distinguished element of a horizontally simplified basis, which is an element in a horizontally simplified basis with no incoming or outgoing vertical arrows. Similarly, there is a horizontally distinguished element of a vertically simplified basis. In [Hom14, Lemma 3.2], it is shown that it is always possible to find a horizontally simplified basis for $\mathrm{CFK}^\infty(K)$ so that one of the horizontal basis elements ξ_0 is the vertically distinguished generator of some vertically simplified basis. Note that the concordance invariant $\epsilon(K)$ can be defined in terms of the generator ξ_0: If ξ_0 occurs at the end of a horizontal arrow, then $\epsilon(K) = 1$, if ξ_0 occurs at the beginning of a horizontal arrow, then $\epsilon(K) = -1$. If there is no horizontal arrow to or from ξ_0, then $\epsilon(K) = 0$.

Immersed Curves for knot complements

Given a type D structure over the torus algebra, like $\widehat{\mathrm{CFD}}(S^3\backslash\nu(K), n)$, the work in [HRW22] shows how we can represent it as an immersed multicurve with local systems in the torus, which we now describe. The first

step is to construct a decorated graph from the type D structure. Let N be a type D structure over the torus algebra, and let $N_i = \iota_i N$. This gives a decomposition $N = N_0 \oplus N_1$. Given bases B_i of N_i, for $i = 0, 1$, we construct a decorated graph Γ as follows. The vertices of Γ are in correspondence with the basis elements and are labelled $\bullet$ or $\circ$ depending on if the vertex corresponds to a basis element in B_0 or B_1 respectively. Suppose now that we have two vertices corresponding to basis elements x and y such that $\delta(x) = \rho_I \otimes y + \cdots$, for $I \in \{\varnothing, 1, 2, 3, 12, 23, 123\}$. In this case we put an edge labelled ρ_I from x to y. A decorated graph is called reduced if no edge labelled by $\rho_\varnothing$ appears. The next step is to take a decorated graph and turn it into an immersed train track in the punctured torus. Let $T^2 = \mathbb{R}^2/\mathbb{Z}^2$ and let $w = (1 - \epsilon, 1 - \epsilon)$ be a basepoint. Let μ and λ be the images of the x and y axes respectively and embed the vertices of Γ into T^2 so that the $\bullet$ vertices lie on λ in the interval $\{0\} \times [\frac{1}{4}, \frac{3}{4}]$ and the $\circ$ vertices lie on λ in the interval $[\frac{1}{4}, \frac{3}{4}] \times \{0\}$. Then we embed the edges into the torus according to the rules shown in [HRW22, Figure 19] (see also Figure 3.2). In general this train track is not necessarily an immersed curve, but work in [HRW22] shows that for type D structures that arise from 3-manifolds with torus boundary one can always choose a nice basis so that the train track is an immersed curve (possibly with local systems). For example, we construct the immersed curve associated to the trefoil complement in Figure 3.2, where for example the arc from ξ_1 to κ indicates the presence of a ρ_1 edge from ξ_1 to κ in the decorated graph. We will denote this immersed curve by $\alpha(K)$.

Properties of Immersed Multicurves for Knot Complements

In this section we recall how the immersed curve $\alpha(K)$ encodes the concordance invariants $\tau(K)$ and $\epsilon(K)$ as well as the genus of the knot $g(K)$. In order to do this, we fix a representative of the lift of the immersed curve to the universal cover, called the *peg-board representative* of the immersed curve. This is discussed in [HRW22, Section 4.2]. In brief, we assume that we have chosen a minimal length representative of the immersed multicurve.

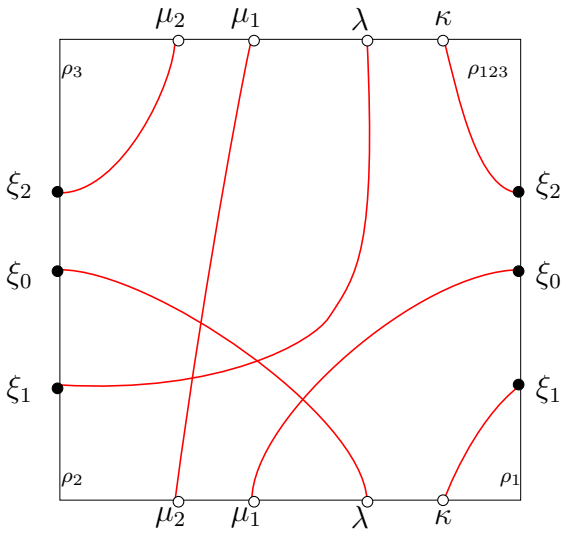

Figure 3.2. The immersed curve associated to the 0 framed trefoil complement

Given a peg-board representative of $\alpha(K)$, the genus of the knot is half the maximal number of pegs between the minimum and maximum height attained by the immersed curve. The invariants $\tau(K)$ and $\epsilon(K)$ are related to the essential component γ_0 of the immersed curve, see [HRW22] and [HW19, Proposition 2]. The essential component γ_0 is the unique non-vertical segment of the immersed curve, in the sense that all other components are supported in a neighborhood of the meridian, and the component γ_0 wraps once around the cylinder (in the covering of the torus corresponding to the longitudinal subgroup). As mentioned in [HRW17, Remark 50] this component does not carry any non-trivial local system as only one curve component can wrap around the cylinder (since otherwise the meridional filling would have rank $\geqslant 2$). This observation, together with the discussion surrounding [Hom14, Lemma 3.2] in Section 3.2 implies the following lemma concerning the shape of the essential component of $\alpha(K)$ lifted to the universal cover.

Lemma 3.2.2. *Suppose that K is a knot in S^3 and that γ_0 is the essential*

curve component of $\alpha(K)$ lifted to the universal cover.

- *If $\epsilon(K) = 1$ and $\tau(K) \geqslant 0$ γ_0 slopes upwards for $2\tau(K)$ rows and turns down at the top and up at the bottom*
- *If $\epsilon(K) = -1$ and $\tau(K) \geqslant 0$, then γ_0 slopes upwards for $2\tau(K)$ rows and turns up at the top and down at the bottom*
- *If $\epsilon(K) = 1$ and $\tau(K) \leqslant 0$ then γ_0 slopes downwards for $2\tau(K)$ rows and turns down at the bottom at up at the top*
- *If $\epsilon(K) = -1$ and $\tau(K) \leqslant 0$ then γ_0 slopes downwards for $2\tau(K)$ rows and turns up at the bottom and down at the top.*
- *If $\epsilon(K) = 0$, then $\tau(K) = 0$ and γ_0 is horizontal at height 0.*

In each case the remaining portion of the essential component of the immersed curve and any other component of the immersed curve are contained in a neighborhood of the meridian.

Proof. We will show that the immersed curve has the claimed form in the case that $\tau(K) > 0$ and $\epsilon(K) = 1$. The rest of the cases are similar. As mentioned above, in [Hom14], Hom constructs a horizontally simplified basis $\{\xi_0, \eta_0, \cdots, \eta_N\}$ so that ξ_0 is the distinguished element in a vertically simplified basis with no incoming or outgoing vertical arrows. In the case $\epsilon(K) = 1$, this generator appears at the end of a horizontal arrow. Suppose that $\eta_1 \to \xi_0$ is a length l arrow from η_1 to ξ_0. In this case, the portion of $\widehat{\mathrm{CFD}}(S^3\backslash\nu(K))$ has the following form: From the length l horizontal arrow from η_1 to ξ_0, the algorithm in [LOT18] produces a sequence of type D operations

$$\eta_1 \xrightarrow{\rho_3} \lambda_1^1 \xrightarrow{\rho_{23}} \lambda_2^1 \xrightarrow{\rho_{23}} \dots \lambda_l^1 \xrightarrow{\rho_2} \xi_0$$

(Note that this part of the type D operations or immersed curve is what changes when $\epsilon(K)$ changes sign)

Since $\tau(K) > 0$, the unstable chain takes the form

$$\xi_0 \xrightarrow{\rho_1} \mu_1 \xleftarrow{\rho_{23}} \cdots \xleftarrow{\rho_{23}} \mu_{2\tau(K)} \xleftarrow{\rho_3} \eta_0$$

(Note that this part of the type D operations or immersed curve is what changes when $\tau(K)$ changes sign)

Using the procedure described in [HRW17] and the previous section, this decorated graph becomes the portion of the immersed curve shown in Figure 3.3. As claimed, the immersed curve slopes upwards for $2\tau(K)$ rows, turns down at the top (from the ρ_2 from λ_l^1 to ξ_0) and turns up at the bottom by the symmetry of the immersed curve under the elliptic involution. The remaining bullet points follow similarly.

The fact that the remaining portion of the immersed curve is contained in a neighborhood of the meridian follows since the meridional filling of any knot complement has rank one. If any other component wrapped around the longitude, this would imply that the meridional filling has rank $\geqslant 2$. □

$\widehat{\mathrm{CFA}}(S^1 \times D^2, P)$ *for* $(1,1)$*-patterns* $P \subset S^1 \times D^2$

As we saw in the previous section, the type D structure from the pairing theorem can be obtained algorithmically from knowledge of $\mathrm{CFK}^-(K)$. For the type A side, there is no such algorithm for determining $\widehat{\mathrm{CFA}}(S^1 \times D^2, P)$ in terms of $\mathrm{CFK}^-(P(U))$. However, when the pattern $(S^1 \times D^2, P)$ admits a particular type of Heegaard diagram, called a genus-1 doubly-pointed bordered Heegaard diagram, we can compute $\widehat{\mathrm{CFA}}(S^1 \times D^2, P)$ directly. We now describe how to do this. First, we introduce the notation of a genus 1 doubly-pointed bordered Heegaard diagram.

Definition 3.2.3. *A genus-1 doubly-pointed bordered Heegaard diagram is a five tuple* $(\Sigma, \alpha^a, \beta, w, z)$*. Here* Σ *is a compact oriented surface of genus* 1 *with a single boundary component. The alpha arcs* $\alpha^a = (\alpha_1^a, \alpha_2^a)$ *are a pair of properly embedded, disjoint arcs in* Σ *with a fixed order to the intersections* $\alpha^a \cap \partial\Sigma$*. The basepoint* w *lies on the boundary of* Σ *in the complement of the endpoints of the* α *arcs; i.e.* $w \subset \partial\Sigma \backslash \partial\alpha^a$*. The resulting subdivision*

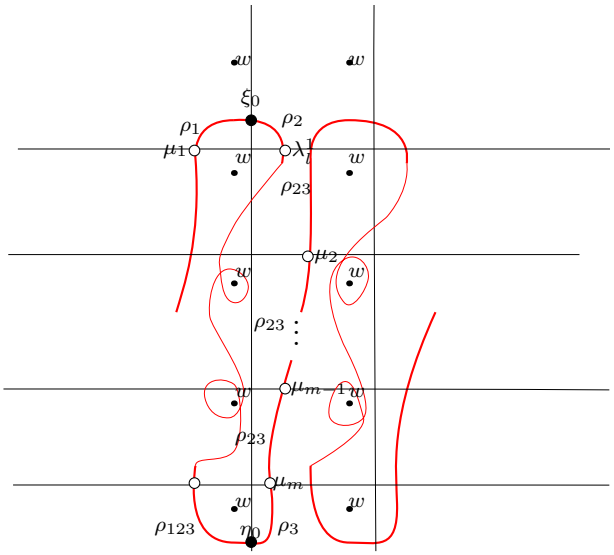

Figure 3.3. The essential component of the immersed curve for a knot K with $\tau(K) > 0$ and $\epsilon(K) = 1$. The curve crosses at heights $-\tau(K)$ and $\tau(K)$. The lighter portion of the curve indicates that γ_0 is potentially immersed in the punctured torus, but is contained in a small neighborhood of the meridian, along with all the other components of the immersed multicurve $\alpha(K)$

of $\partial\Sigma$ results in the data of a pointed matched circle. The β-curve is an embedded closed loop in Σ so that β is transverse to the α-arcs and the complement $\Sigma\backslash\beta$ is connected. Furthermore, we place a basepoint z in the interior of Σ without the α-arcs and β-circles, so that if we forget the z basepoint, the β curve is isotopic to α_2^a.

This data specifies a three manifold with torus boundary together with a knot. The three manifold and knot can be recovered by the following recipe. Attach a two-handle to $\Sigma \times [0,1]$ along $\beta \times \{1\}$. The knot is specified by connecting the z basepoint to the w basepoint in the complement of β and pushing the arc into the handlebody compressed by the β curve and connecting w to z in the complement of α^a in Σ. Note that the α-arcs are the cores of the 1-handles of the boundary torus. In our case, we have $\alpha_1^a = \lambda$

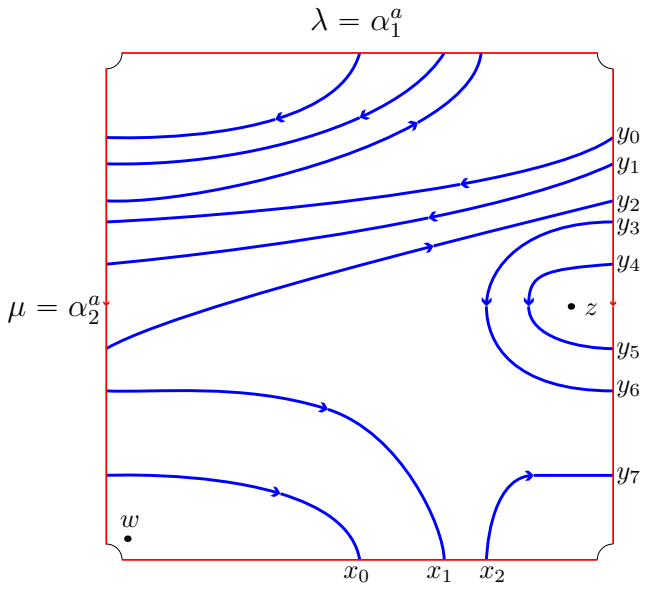

Figure 3.4. The genus 1 doubly pointed Heegaard diagram for the pattern $P^{(3,1)}$

and $\alpha_2^a = \mu$ the longitude and meridian of the torus boundary $\partial(S^1 \times D^2)$. See Figure 3.4 for an example of a genus 1 doubly pointed bordered Heegaard diagram. Note that by definition we have $\beta \cdot \mu = 0$ and $\beta \cdot \lambda = 1$ since if we forget the z basepoint the β curve is isotopic to the meridian. We orient the meridian as shown in Figure 3.4 and the β curve inherits an induced orientation from the meridian.

Now we describe how to obain $\widehat{\mathrm{CFA}}(S^1 \times D^2, P)$ from a given genus 1 doubly pointed bordered Heegaard diagram. As an $\mathbb{F}$ vector space $\widehat{\mathrm{CFA}}(S^1 \times D^2, P)$ is generated by elements of the set

$$\mathcal{G} = \{x | x \in \beta \cap \alpha^a\}.$$

For each $x \in \mathcal{G}$, we have the following right action of the idempotent subalgebra $\mathcal{I}$: $x \cdot \iota_0 = x$ if $x \in \alpha_1^a \cap \beta$ and $x \cdot \iota_0 = 0$ otherwise. Similarly, $x \cdot \iota_1 = x$ if $x \in \alpha_2^a \cap \beta$ and $x \cdot \iota_1 = 0$ otherwise.

Now, regard the surface-with-boundary Σ as $T^2\backslash D^2$. Let $\mathbb{R}^2 \to T^2$ denote the universal cover of the torus, and set $\tilde{\Sigma}$ to be the covering space obtained from $\mathbb{R}^2$ by removing the lifts of D^2. Using this covering space, we define the maps

$$m_{n+1} : M \otimes \mathcal{A}^{\otimes n} \to M$$

for $n \geqslant 0$ as follows.

$$m_{n+1}(x, \rho_{I_1}, \cdots, \rho_{I_n}) = \sum_{y \in \mathcal{G}} \#\mathcal{M}(x, y) y$$

where $\#\mathcal{M}(x, y)$ is the mod 2 count of index 1 immersed disks in $\tilde{\Sigma}$ such that, when we traverse the boundary of the disk we start from a lift of x and walk along an arc of some lift of α^a then along the arc ρ_{I_1} on some lift of ∂D^2, ..., then walk along some the arc ρ_{I_n} and then along some lift of α^a to y and finally along a lift of β from y to x.

For example, consider the doubly pointed genus 1 Heegaard diagram shown in Figure 3.4. The generators of $\widehat{\mathrm{CFA}}(P)$ in idempotent ι_0 (intersection of β with α_1^a) are labelled x_0, x_1, x_2 from left to right and the generators in idempotent ι_1 (intersections of β with α_2^a) are labelled $y_0, \cdots, y_7$ from top to bottom. We draw the lift to the cover $\tilde{\Sigma}$ in Figure 3.6 and indicate a few of the type A operations given by the disks shown. The gray disk gives a $m_3(x_0, \rho_{12}, \rho_1) = y_3$, the green disk gives $m_2(x_1, \rho_1) = y_1$ and the pink disk gives $m_3(y_1, \rho_2, \rho_1) = y_4$. The full type A module $\widehat{\mathrm{CFA}}(S^1 \times D^2, P^{(3,1)})$ is shown in Figure 3.5. In that figure, an arrow labelled $\rho_{I_1}, \rho_{I_2}, \ldots, \rho_{I_n}$ from x to y means there is an A_∞ operation $m_{n+1}(x, \rho_{I_1}, \ldots, \rho_{I_n}) = y$.

3.3 The pairing theorem for $(1, 1)$ patterns

The main result in [Che19] is a reinterpretation of the pairing theorem from [LOT18, Theorem 11.19] in terms of immersed curves when $\widehat{\mathrm{CFA}}(S^1 \times D^2, P)$ comes from a $(1, 1)$ pattern P. In this section we recall this theorem.

Let $\beta(P)$ denote the β curve in the data of a genus one doubly pointed Heegaard diagram and let $\alpha(K)$ denote the immersed curve for $S^3\backslash\nu(K)$ as

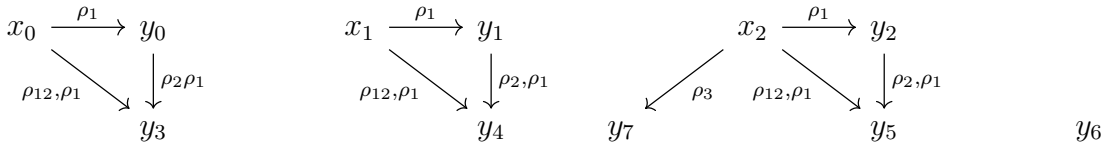

Figure 3.5. $\widehat{\mathrm{CFA}}(\mathcal{H})$ where $\mathcal{H}$ is the doubly pointed bordered Heegaard diagram shown in Figure 3.4

described in section 3.2. Chen's theorem says that to compute $\widehat{\mathrm{HFK}}(S^3, P(K))$ we can compute the intersection Floer homology of $\alpha(K)$ and $\beta(P)$, denoted $\widehat{\mathrm{CFK}}(\alpha, \beta)$, in the torus as follows. Let $T^2 = [0,1]^2/\sim$ and divide the square into four quadrants. Include the immersed curve $\alpha(K)$ into the first quadrant $[\frac{1}{2}, 1] \times [\frac{1}{2}, 1])$ and include $(\beta(P), w, z)$ into the third quadrant. Then extend both curves horizontally and vertically, so that α and β intersect in the second and fourth quadrants only. In this set up intersections in the second quadrant correspond to generators of $\widehat{\mathrm{CFA}}(S^3, P) \boxtimes \widehat{\mathrm{CFD}}(S^3 \backslash \nu(K))$ that come from pairing generators in idempotent ι_0 and intersection points in the fourth quadrant correspond to generators of $\widehat{\mathrm{CFA}}(S^3, P) \boxtimes \widehat{\mathrm{CFD}}(S^3 \backslash \nu(K))$ that come from pairing generators in the ι_1 idempotent. The main work in [Che19] is constructing from a differential in the Lagrangian Floer chain complex, $\widehat{\mathrm{CFK}}(\alpha, \beta)$, a type A operation in $\widehat{\mathrm{CFA}}(S^1 \times D^2, P)$ and a corresponding type D operation in $\widehat{\mathrm{CFD}}(S^3 \backslash \nu(K))$ so that these pair in the box tensor product to produce the given differential.

The data of the torus divided into quadrants, with the curves $\alpha(K)$ and $\beta(P)$ included as described, or this same picture lifted to the universal cover, will be referred to as a *pairing diagram* for the knot Floer homology of the satellite $P(K)$. For an example of a pairing diagram for the knot Floer homoloy of the satellite knot $P^{(3,1)}(T_{2,3})$ see Figure 3.7. From the picture we can see that $\widehat{\mathrm{CFK}}(S^3, P^{(3,1)}(T_{2,3}))$ has 41 generators. In that figure, we also indicate two differentials, in light and dark grey, that contribute to $\partial^{\boxtimes}$. The dark grey disk gives a differential in $\widehat{\mathrm{CFK}}(S^3, P^{(3,1)}(T_{2,3}))$ connecting $x_0 \boxtimes \xi_1$

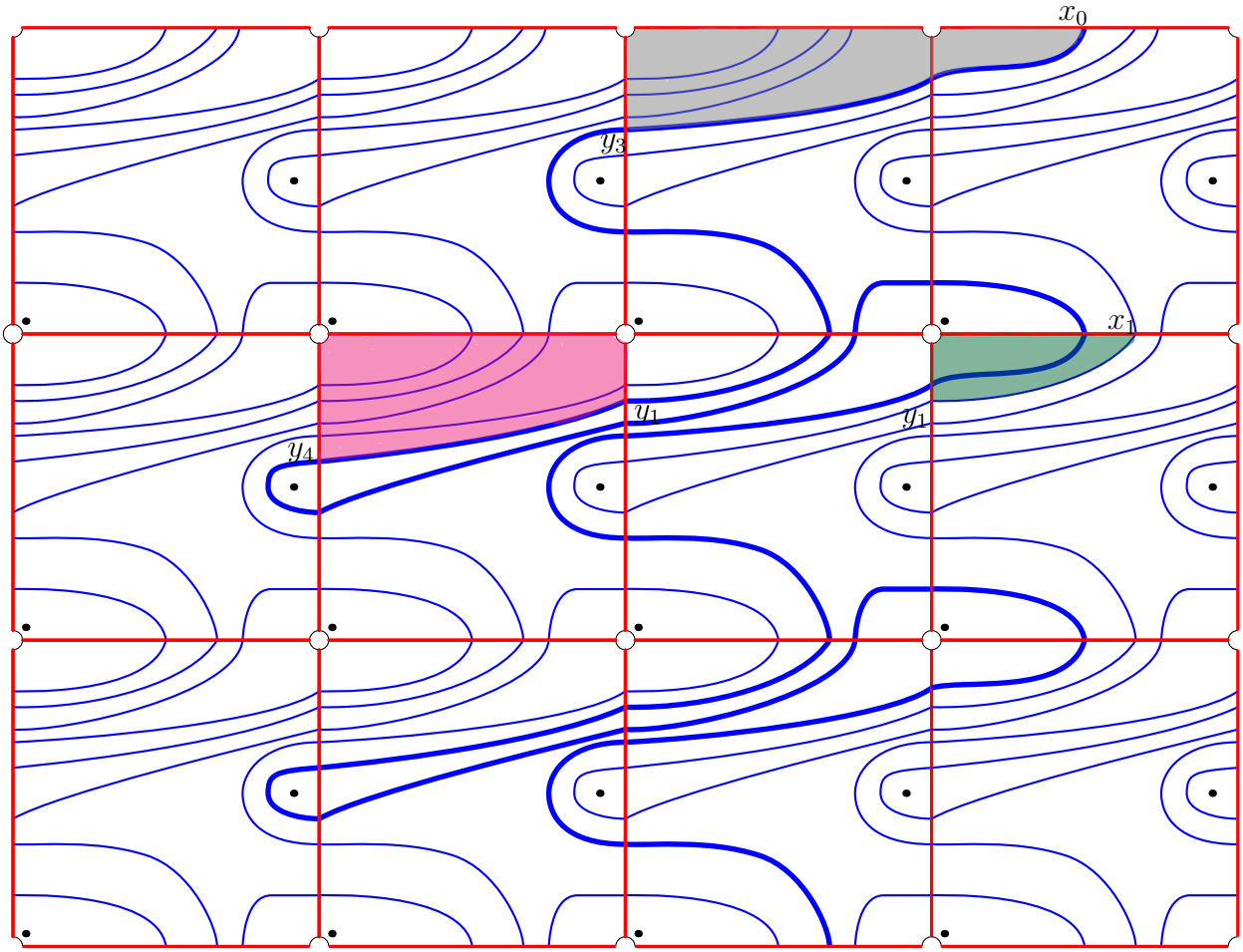

Figure 3.6. Lift of the pattern $P^{(3,1)}$ to the cover $\tilde{\Sigma}$ a single connected lift of β is shown in bold

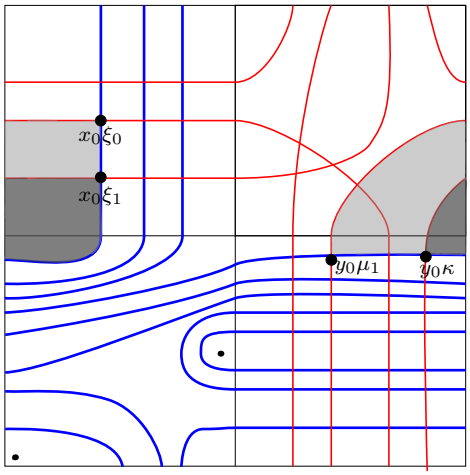

Figure 3.7. pairing diagram showing the trefoil pattern $P^{(3,1)}$ paired with 0 framed trefoil companion

to $y_0 \boxtimes \kappa$. This arises from pairing the type A operation $m_2(x_0, \rho_1) = y_0$ and the Type D operation $\delta(\xi_1) = \rho_1 \otimes \kappa$. The light grey disk represents a differential from $x_0 \boxtimes \xi_0$ to $y_0 \boxtimes \mu_1$ given by pairing the type A operation $m_2(x_0, \rho_1) = y_0$ and the type D operation $\delta(\xi_0) = \rho_1 \boxtimes \mu_1$.

For convenience we will usually draw pictures of single lifts of $\alpha(K)$ and $\beta(P)$ to the universal cover $\pi : \mathbb{R}^2 \to T^2$ of the torus. Here we choose a single lift of $\beta(P)$, call it $\tilde{\beta}$, and a lift of $\alpha(K)$, call it $\tilde{\alpha}$, so that $\tilde{\alpha}$ is in pegboard position with respect to a peg at the midpoint of the arc $\delta_{w,z}$ of large enough radius to contain both basepoints w and z. We also require that $\tilde{\alpha}$ and $\tilde{\beta}$ intersect transversely and there are no pairs of intersections that are connected by a Whitney disk that does not cross any basepoint. This is allowed, since intersection Floer homology is an isotopy invariant (a topic we come back to in the next section). These conditions ensure that $\widehat{\mathrm{CFK}}(\tilde{\alpha}, \tilde{\beta}) \simeq \widehat{\mathrm{HFK}}(S^3, P(K))$, where $\widehat{\mathrm{CFK}}(\tilde{\alpha}, \tilde{\beta})$ denotes the intersection Floer homology of the two curves in $\mathbb{R}^2 \backslash \{\pi^{-1}(w), \pi^{-1}(z)\}$. See Figure 3.8 for an example computing $\widehat{\mathrm{HFK}}(S^3, P^{(3,1)}(T_{2,3}))$ from a lifted pairing diagram.

This figure shows that $\mathrm{rk}(\widehat{\mathrm{HFK}}(S^3, P^{(3,1)}(T_{2,3}))) = 21$.

The last bit of information we want to extract from the pairing diagram is the Alexander grading on $\widehat{\mathrm{HFK}}(S^3, P(K))$. This is achieved by the following lemma.

Lemma 3.3.1. *[Che19, Lemma 4.1]*

Let x and y be two intersection points between α and β. Let ℓ be an arc on β from x to y, and let $\delta_{w,z}$ be a straight arc connecting w to z. Then

$$A(y) - A(x) = \ell \cdot \delta_{w,z}$$

For example, consider the intersection points labelled x and y in Figure 3.8. These intersection points are connected by an arc of the β curve that is shown in bold in the figure. When we traverse this arc, from x to y along the orientation of β, we cross five $\delta_{w,z}$ arcs positively. Then Lemma 3.3.1 implies $A(y) - A(x) = 5$.

Computing $\tau(P(K))$ from a pairing diagram

In this section, we recall from [Che19] the precedure for computing τ from the pairing diagram for $\widehat{\mathrm{CFK}}(P(K))$ when P is a $(1,1)$ pattern. Recall that the Alexander filtration on $\widehat{\mathrm{CFK}}(K)$ produces a spectral sequence converging to $\widehat{\mathrm{HF}}(S^3)$. The τ invariant is the minimal Alexander grading of the cycle that survives to the E^∞ page. In what follows we give a way of computing this spectral sequence in the pairing diagram for $\widehat{\mathrm{CFK}}(S^3, P(K))$ for $(1,1)$ patterns P. First, we recall the following well known lemma that gives us a way of thinking about passing from one page of the spectral sequence to the next as cancelling differentials that decrease filtration by the minimal amount, see [BHL19; Zha18].

Lemma 3.3.2. *[BHL19, Lemma 2.4] Suppose (C, d) is a chain complex over $\mathbb{F}_2$ freely generated by elements $\{x_i\}$. Let $d(x_i, x_j)$ be the coefficient of x_j in $d(x_i)$ and suppose $d(x_k, x_l) = 1$. Then the complex (C', d') wih generators $\{x_i | i \neq k, l\}$ and differential*

$$d'(x_i) = d(x_i) + d(x_i, x_l)d(x_k)$$

is chain homotopy equivalent to (C, d)

Now, suppose C is a filtered chain complex. The above lemma tells us how to compute the spectral sequence associated to the filtration in stages. The E_0 term of the spectral sequence is the associated graded $C = \bigoplus C_i$. Then, we pass from the E_0 to the E_1 page by cancelling the components of d that do not shift the grading, and arrive at a chain complex (E_1, d_1), where the d_1 differential is defined as in lemma 3.3.2. Continuing in this way, we pass from the E_1 page to the E_2 page by cancelling the components of the differential d_1 that shift grading by one, etc. In this way, the spectral sequence collapses when we have reached a chain complex filtered chain homotopy equivalent to the original one but whose differential is zero. For more details, see the discussion after Remark 2.5 in [BHL19].

In the spectral sequence induced by the Alexander filtration on $\widehat{\mathrm{CFK}}(\tilde{\alpha}, \tilde{\beta})$, the previous discussion shows that passing from one page to the next in this spectral sequence amounts to cancelling differentials that connect elements of minimal Alexander filtration difference. We now give an way to see that cancellation geometrically in the complex $\widehat{\mathrm{CFK}}(\tilde{\alpha}, \tilde{\beta})$. In the pairing diagram, differentials are given by Whitney disks that connect two intersection points and cross the z basepoint, but not the w basepoint and the filtration difference is the number of z basepoints enclosed. To cancel two generators connected by such a Whitney disk, we perform an isotopy of the β curve over the disk to a new curve β' thus cancelling those two intersection points in the diagram, together with possible more if the Whitney disk wasn't innermost, i.e. it contains arcs of the α curve in its interior. In any case, all the intersection points cancelled by isotoping away this Whitney disk will all have the same filtration difference, so it doesn't matter if we cancel pairs of generators of minimal filtration difference one at a time or in bulk. Once this isotopy is performed, we arrive at a new complex, with fewer generators. To remember the filtration difference after the cancellation, following

Chen we place small arrows on the β' curve, called A-bouys, that remember that an isotopy of a Whitney disk crossing some number of z basepoints was performed. Then, when we compute filtration differences of the remaining intersection points in the α and β' complex, we count both intersections of the β' curve with the $\delta_{w,z}$ arcs and the A-bouys.

It remains to observe that when we cancel two intersection points by isotoping the curve β to β', the differential d' on the Lagrangian Floer chain complex $\widehat{\mathrm{CFK}}(\tilde{\alpha}, \tilde{\beta}')$, which is given by counting holomorphic disks with boundary conditions on $\tilde{\alpha}$ and $\tilde{\beta}'$, is given by the formula $d'(a) = d(a) + d(a,y)d(x)$, where $d(a,y)$ is, as above, the coefficient of y in $d(a)$. To see this, recall that for a generator x of the Lagrangian Floer chain complex, the differential is given by

$$d(x) = \sum_y n(x,y)y$$

where $n(x,y)$ counts Maslov index 1 holomorophic disks connecting x to y in the α, β complex. Now, suppose that we isotope the curve β to a new curve β' where β' results from isotoping β over a Whitney disk that crosses the z basepoint and cancels the intersection points x and y of minimal filtration difference. Then by [SRS14][equation 59], the new holomorphic disk count in the α and β' complex is given by

$$n'(a,b) = n(a,b) + n(a,y)n(x,b)$$

Where $a, b \in \alpha \cap \beta'$. This implies that $d'(a) = d(a) + d(a,y)d(x)$ for $a \in \widehat{\mathrm{CFK}}(\tilde{\alpha}, \tilde{\beta}')$. Indeed, we have

$$d'(a) = \sum_b n'(a,b)b = \sum_b n(a,b)b + n(a,y)\sum_b n(x,b)b = d(a) + d(a,y)d(x).$$

This gives a diagramatic way to run the Alexander filtration spectral sequence in a pairing diagram. For example, consider Figures 3.8-3.11. In that sequence of figures we first see the pairing diagram for $\widehat{\mathrm{HFK}}(S^3, P^{(3,1)}(T_{2,3}))$ in Figure 3.8. In Figure 3.9, we have indicated all of the Whitney disks that

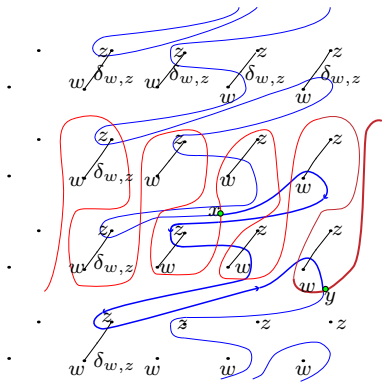

Figure 3.8. Pairing diagram for $\widehat{\mathrm{HFK}}(S^3, P^{(3,1)}(T_{2,3}))$. Intersection points labelled x and y satisfy $A(y) - A(x) = 5$ and $A(x) = 0$.

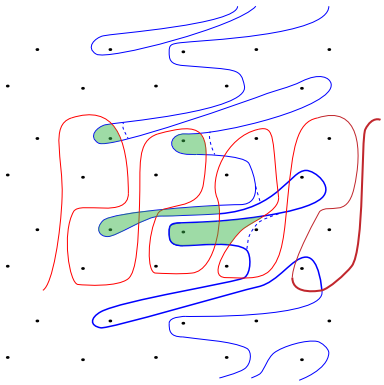

Figure 3.9. The disks shown represent all the differentials that lower filtration degree by one. Cancelling the disks by an isotopy, we end up with Figure 3.10

connect two intersection points of filtration difference one. When we cancel these disks by isotoping the β curve over these disks, we arrive at Figure 3.10. In that figure, we have indicated the disks that connect intersection points of minimal filtration difference. Cancelling these, we arrive at Figure 3.11, where we see three intersection points, two of which are connected by a Whitney disk, shown in the figure in purple. If we cancel these two generators we arrive at a pairing diagram with one intersection point. The Alexander grading of this intersection point is then $\tau(P^{(3,1)}(T_{2,3}))$ by the discussion above.

A convenient way to package the entire spectral sequence is shown in Figure 3.12. Here we see all of the disks we cancelled in the spectral sequence, and the A bouys that keep track of the Alexander filtration from the original complex in all of the subsequent pages. Note that if we draw it like

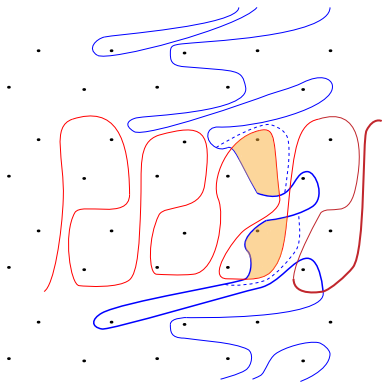

Figure 3.10. The result of cancelling the disks in Figure 3.9. There are two disks that connect generators of $\widehat{\mathrm{CFK}}(\tilde{\alpha}, \tilde{\beta}')$ of minimal filtration difference. Cancelling these disks we arrive at Figure 3.11

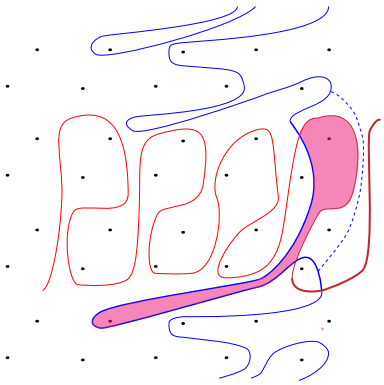

Figure 3.11. The result of isotoping β' in Figure 3.10, we arrive at a complex with three generators and one differential connecting two generators of minimal filtration difference

this, we have to cancel all intersection points with filtration difference one before cancelling any with filtration difference two, etc. We can find the absolute Alexander grading of the generator labelled a (the intersection point we found to survive the z-basepoint spectral sequence) as follows. By the symmetry under the elliptic involution, it is easy to see that $A(x) = 0$. Then using Lemma 3.3.1 we have $A(a) - A(x) = A(a) = 5$, so $\tau(P^{(3,1)}(T_{2,3})) = 5$

3.4 Trefoil patterns

In this section we will compute τ of satellite knots with arbitrary companion knot K and pattern P from a family of trefoil patterns that we will

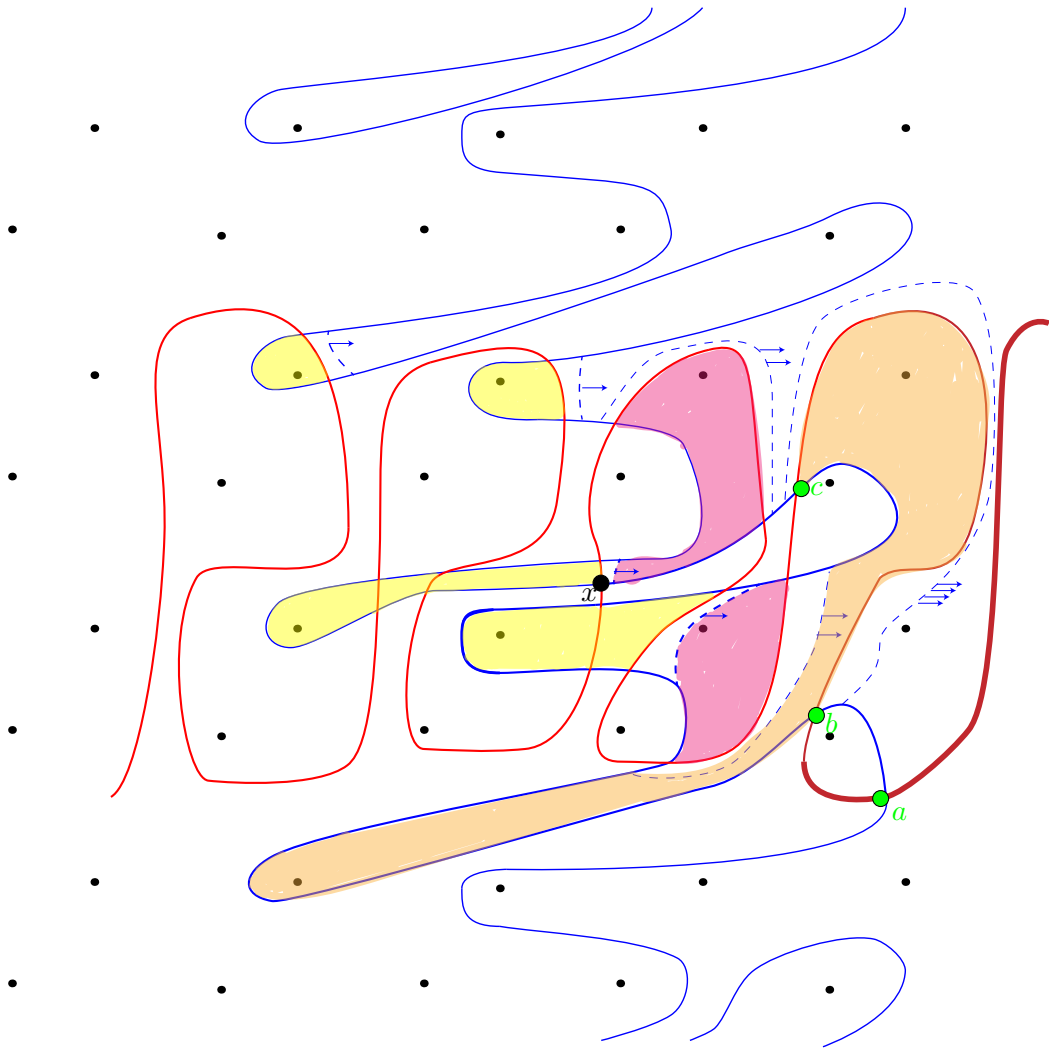

Figure 3.12. Cancelling all intersection points with filtration difference one (disk in yellow) and intersection points with filtration difference two (disks in pink) There are three intersection points remaining.

now describe.

Introducing the patterns

The $(1,1)$-patterns studied in this paper are constructed by isotoping the β curve on the doubly pointed bordered Heegaard diagram for the unknotted $(p,1)$-cable pattern so that we introduce only two extra intersection points between β and λ. To describe the isotopy, consider first the case $p = 3$. The unknotted $(3,1)$-cable pattern is shown in Figure 3.13. Isotope the β curve by taking the bottom-most horizontal strand and pushing it once across the longitude of the solid torus. Once we isotope β over the longitude, we follow the pattern around the meridian until we end up inside the bigon that contains the z basepoint, without crossing the longitude again. A intermediate stage of this isotopy is shown in Figure 3.14. If we push the β curve over the z basepoint, we arrive at the pattern shown in Figure 3.15, which we will denote by $P^{(3,1)}$.

In general, we take the bottom most horizontal strand of the β curve in the genus-1 doubly-pointed bordered Heegaard diagram for the $(p,1)$-cable pattern, push it once over the longitude, and then follow the pattern around the meridian until we end up inside the bygon that contains the z basepoint. If we push the β curve over the basepoint, we arrive at a $(1,1)$ diagram for a pattern that we denote $P^{(p,1)}$. The lift of the pattern $P^{(p,1)}$ is shown in Figure 3.19, where we see that it looks like the lift of the $(p,1)$ -cable pattern with one extra arm. By construction, since we only crossed the longitude λ once in our isotopy, we increased the number of intersections with the longitude by two. Therefore $\mathrm{rk}(\widehat{\mathrm{HFK}}(S^3, P^{(p,1)}(U))) = 3$ for all $p > 1$. Alternatively, pairing this pattern with $\widehat{\mathrm{CFD}}(S^3\backslash U)$ (whose immersed curve is a horizontal line) results in three intersection points and no differentials. As the rank of knot Floer homology detects the trefoil knot [HW18, Corollary 8], we know that $P^{(p,1)}(U)$ has the knot type of the trefoil in S^3. As mentioned in the introduction, we will call such a pattern $P \subset S^1 \times D^2$ a *trefoil pattern*. In the next section we will use the procedure described in section

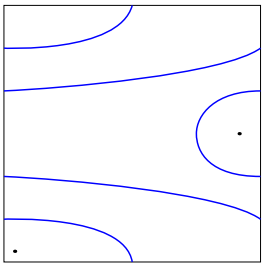

Figure 3.13. Doubly pointed Heegaard diagram for $(3,1)$ cable pattern

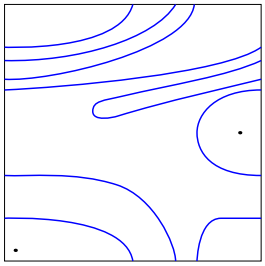

Figure 3.14. Midway through the isotopy

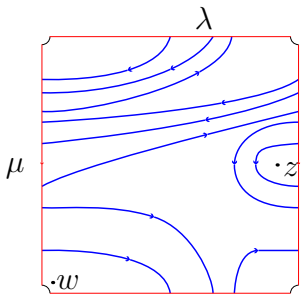

Figure 3.15. Doubly pointed bordered Heegaard diagram for the trefoil pattern $P^{(3,1)}$

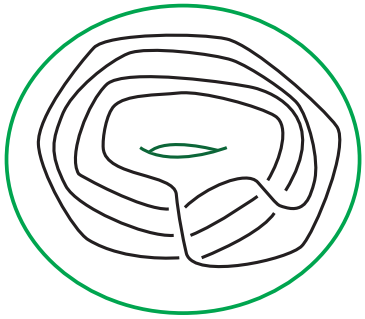

Figure 3.16. The trefoil pattern $P^{(3,1)}$ in the solid torus

3.3 to prove Theorem 3.1.1.

τ of 0-Framed Satellites With Arbitrary Companions

In the previous section we constructed, for each $p > 1$, a trefoil pattern in the solid torus. It follows from [Che19, Lemma 6.3] that $w(P^{(p,1)}) = p + 1$. The pattern $P^{(3,1)}$ is shown in the solid torus in Figure 3.16. In this section we show how to compute $\tau(P^{(p,1)}(K))$ for K an arbitrary knot in S^3. As we

will see, the answer only depends on the values of $\tau(K)$ and $\epsilon(K)$.

Proof of Theorem 3.1.1. We begin with a discussion of how to determine the absolute Alexander grading of intersection points representing generators of $\widehat{\mathrm{HFK}}(S^3, P^{(p,1)}(K))$ in the pairing diagrams in Figures 3.19 and 3.20. For example, in Figure 3.19 we see a lift of the β curve to the universal cover. The dotted portions of the β curve represents that the β curve crosses $p-3$ columns that are not drawn, and the β curve is completely horizontal. If we focus in on one row, for example the row highlighted in Figure 3.19, we can determine the relative Alexander grading of all the intersection points by Lemma 3.3.1. We then determine the relative Alexander grading of all the other generators by noting that by [Che19, Lemma 6.3], if x and x' are intersection points that occur on arcs of the β curve that differ by a meridional deck transformation (shifting the picture in the universal cover down a row), then their Alexander grading difference is $w(P)$, where $w(P)$ denotes the winding number of the pattern. For example in Figure 3.19 the intersection points x and x' lie on arcs of the β curve that are related by a meridional deck transformation. It is easy to see that $A(x) - A(x') = p + 1 = w(P)$. Now, to determine the absolute Alexander grading, note that the conjugation symmetry of knot Floer homology is witnessed in the pairing diagram by the hyperelliptic involution. That is, if we rotate the entire picture by π, and exchange the z and w basepoints, we will get the same complex. Therefore, if any intersection is fixed under this involution then it must have Alexander grading zero. In particular, we can see that the intersection that is fixed will occur along the arc of the β curve in Figure 3.19 that contains the point labelled x. Since all intersections along this arc will have Alexander grading zero by Lemma 3.3.1 it is enough to compute Alexander grading relative to any intersection between $\alpha(K)$ and β that lies on this arc. From now on, we assume that this has been done and the Alexander gradings that appear in Figure 3.19 are absolute and not relative.

Now, we turn to discuss how we determine which intersection point survives the z basepoint Alexander grading spectral sequence. By an isotopy of the β curve only crossing z basepoints, we can isotope β to the light blue

curve in Figures 3.19 and 3.20 in the far right of the diagram. From this observation, we see that there is a choice of cancelling disks in the pairing diagram so that when we run the spectral sequence, the last remaining intersection point lies in the far right column of the pairing diagram. This choice of cancelling disks echos the choice made in the example shown in Figure 3.12 above. Next, recall that the immersed curve $\alpha(K)$, for a general knot K, consists of two kinds of components. There is the essential curve component γ_0 with no non-trivial local systems which wraps around the longitude of the torus and there are (potentially) other components that are immersed with local systems which all lie in a neighborhood of the meridian. Since β can be isotoped away from a neighborhood of the meridian by crossing only z basepoints, the intersection point that survives the Alexander filtration spectral sequence is an intersection between the essential component γ_0 and $\beta(P)$. Therefore, since the essential curve component has the form described in Lemma 3.2.2 and depends only on the values of $\tau(K)$ and $\epsilon(K)$, it remains to analyse the following cases to determine the absolute Alexander grading of the generator that survives.

$\tau(K) > 0, \epsilon(K) = 1$: In this case, the part of the essential component of the immersed curve for K coming from the unstable chain slopes upward for $2\tau(K)$ rows and turns down at the top and up at the bottom. See Figure 3.17 for an example when $p = 3$ and $K = T_{2,3}$ and Figure 3.19 for the general case, where in that figure, we pay attention to the piece of the essential component that is dotted and we only draw the portion of the essential component of $\alpha(K)$ that carries the intersecion that survives the spectral sequence. In this case we see that the surviving intersection point is the one labelled a in Figure 3.19. To compute what this Alexander grading is, we use Lemma 3.3.1. When we follow the β curve from the generator with Alexander grading 0, labelled x in the figure, we travel down $\tau(K)$ rows and then cross one extra $\delta_{w,z}$ arc. The $\tau(K)$ rows results in a change in Alexander filtration by $w(P)\tau(K) = (p+1)\tau(K)$, and crossing one more $\delta_{w,z}$ arc gives the result:

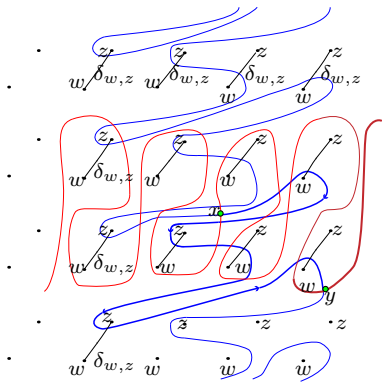

Figure 3.17. The lift of the trefoil pattern $P^{(3,1)}$ shown in Figure 3.15 paired with the right handed trefoil. We have $\tau(P^{(3,1)}(T_{2,3})) = A(y) = 5$.

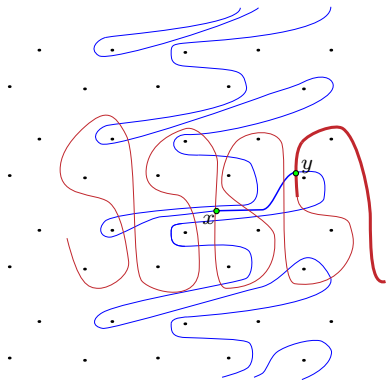

Figure 3.18. The lift of the trefoil pattern P_3 shown in Figure 3.15 paired with the left handed trefoil. We find $\tau(P^{(3,1)}(T_{2,-3})) = A(y) = 0$.

$$\tau(P^{(p,1)}(K)) = (p+1)\tau(K) + 1.$$

For example, in Figure 3.17, we saw earlier that $\tau(P^{(3,1)}(T_{2,3})) = 5$.

$\tau(K) > 0, \epsilon(K) = -1$: In this case, that part of the essential component of the immersed curve for K slopes upward for $2\tau(K)$ rows, but it turns down at the bottom and up at the top. See Figure 3.19, where we pay attention to the solid portion of the essential component of the immersed curve in the bottom right that turns down and contains the intersection point labelled b. Since b is the only intersection point remaining after isotoping β to the light blue curve, we see that $A(b) = \tau(P^{(p,1)}(K))$. Using Figure 3.19, we see that this intersection point occurs exactly $\tau(K)+1$ rows below the generator with Alexander grading zero. Using Lemma 3.3.1, we see that

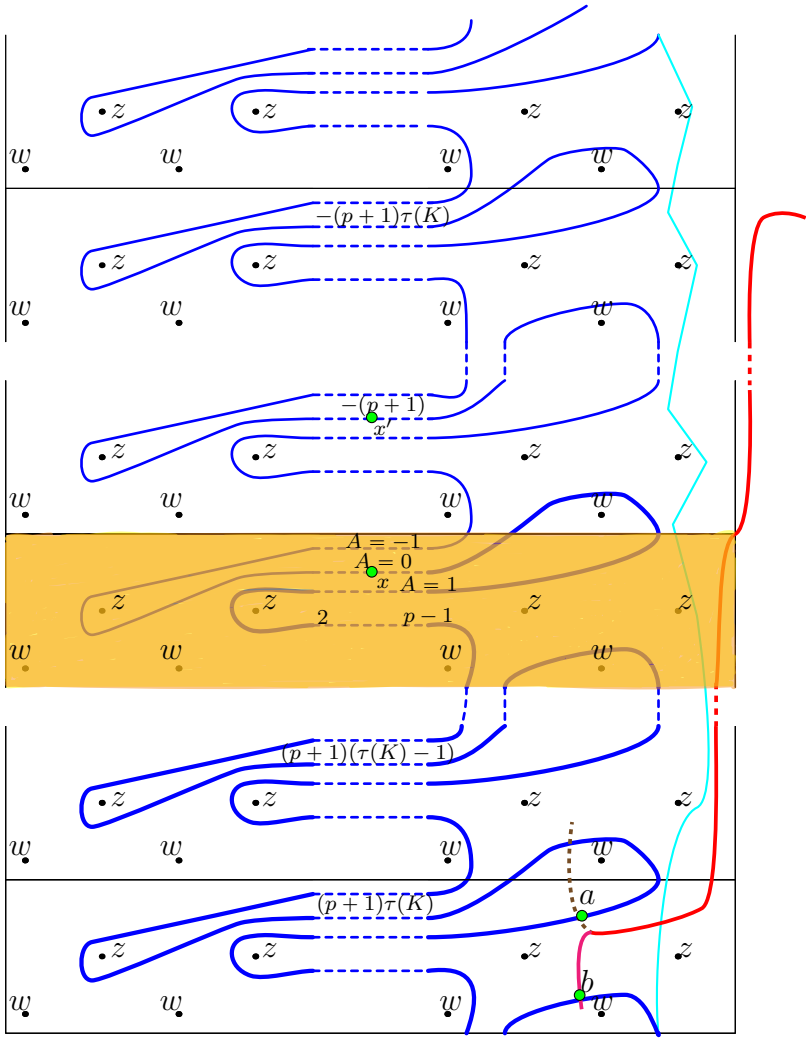

Figure 3.19. The general case with $\tau(K) > 0$ and $\epsilon(K) = \pm 1$. $\epsilon(K) = 1$ is shown as a dotted arc, and $\epsilon(K) = -1$ is shown as a solid arc

$$\tau((P^{(p,1)})(K)) = (p+1)(\tau(K)+1)$$

$\tau(K) < 0, \epsilon(K) = 1$: In this case, the essential component of the immersed curve α slopes downward for $2\tau(K)$ rows, and turns up at the top and down at the bottom, see Figure 3.20 where in the case $\epsilon(K) = 1$, we focus on the solid portion of the essential component of $\alpha(K)$ in the upper right, which contains the intersection point labeled a. Just as in the previous cases we see that a survives the z basepoint spectral sequence and we find the Alexander grading of a by counting how may rows above the generator with Alexander grading zero this intersection point lies. From Figure 3.20 we see that the intersection point y lives exactly $\tau(K)$ rows above the intersection point x with $A(x) = 0$. Therefore, by Lemma 3.3.1 $A(y) = w(P)\tau(K)$. Then, we see that $A(a) - A(y) = 1$, so we have

$$A(a) = \tau(P^{(p,1)}(K)) = (p+1)\tau(K) + 1.$$

$\tau(K) < 0, \epsilon(K) = -1$: This case is similar to the previous cases. Here the relevant portion of the α immersed curve slopes downward and turns down at the top and up at the bottom, see Figure 3.20 paying attention to the dotted portion of the curve in the upper right. The intersection point labelled b is the one that survives the z-basepoint spectral sequence. We count the number of rows above the central row that this intersection point occurs to compute $A(b)$. The result is

$$\tau(P^{(p,1)}(K)) = (p+1)(\tau(K)+1).$$

For an example, consider Figure 3.18. We see that the intersection point that survives the z basepoint spectral sequence lies on both the bold portion of the α curve and the bold portion of the β curve. It is easy to see from the picture that $\tau(P^{(3,1)}(T_{2,-3})) = 0$, since travelling along the bold potion of the β curve, we do not cross any $\delta_{w,z}$ arcs.

$\epsilon(K) = 0$: In this case, we also have $\tau(K) = 0$. Hence the essential curve component is horizontal. Therefore, the intersection point that survives the

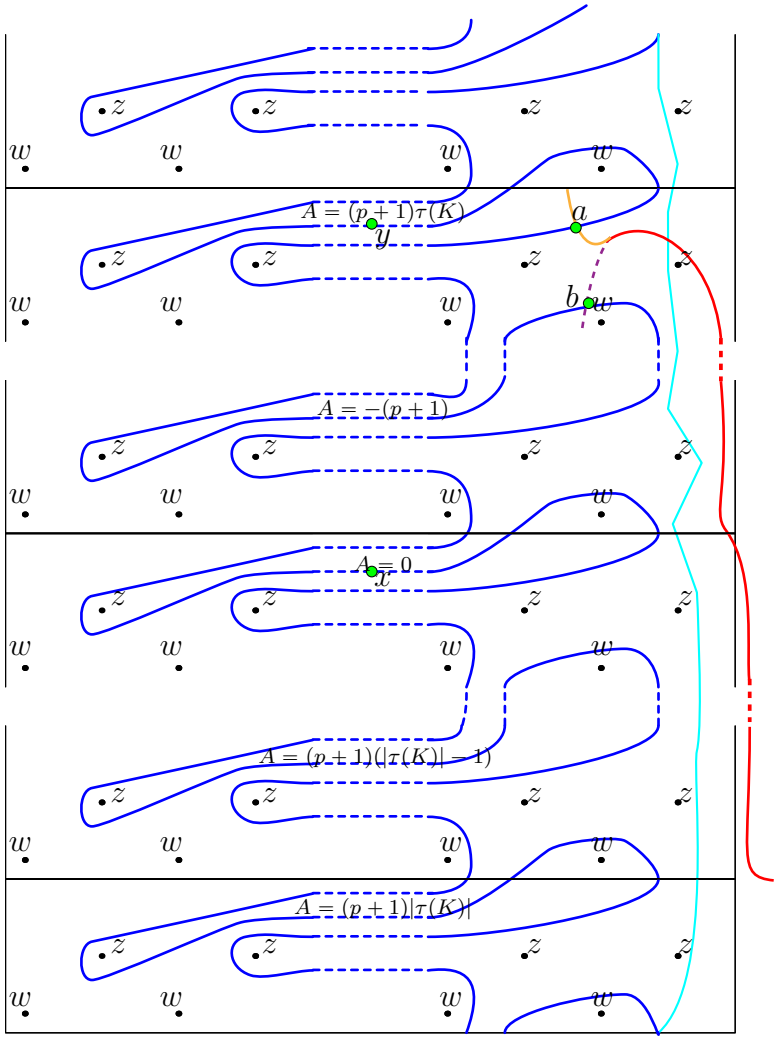

Figure 3.20. The general case with $\tau(K) < 0$ and $\epsilon(K) = \pm 1$. $\epsilon(K) = -1$ is shown as a dotted arc and $\epsilon(K) = 1$ is shown as a solid arc

z basepoint spectral sequence has Alexander grading 1, which is the same as $\tau(T_{2,3})$ as expected. □

3.5 Three Genus and Fiberedness

In this section we will prove theorem 3.1.5 from the introduction. Recall that the knot Floer homology detects both the three-genus and the fiberedness of a knot $K \subset S^3$ in the following sense. The genus of a knot is the largest Alexander grading supporting non-zero Floer homology by [OS04a]. Further, the knot is fibered if and only if the knot Floer homology is one dimensional in this top Alexander grading by [Juh08c].

Recall from [HMS08] that, for a non-trivial companion knot, the satellite knot $P(K)$ is fibered if and only in the companion knot K is fibered in S^3 and the pattern is fibered in the solid torus. Therefore, to prove theorem 3.1.5, it is enough to show that $P^{(p,1)}(T_{2,3})$ is fibered. Furthermore, for a non trivial knot K, we have the classical genus of a satellite formula

$$g(P(K)) = |w(P)|g(K) + g(P). \tag{3.5}$$

So, to compute $g(P)$ it is enough to compute $g(P(T_{2,3}))$.

Proof of Lemma 3.1.3. We will make use of the pairing diagram in Figure 3.21 which computes $\widehat{\mathrm{HFK}}(S^3, P^{(p,1)}(T_{2,3}))$. In the diagram, we see that the generator a has the largest Alexander grading of any intersection point, and we compute using Lemma 3.3.1 that $A(a) = p + 2$. Hence $g(P^{(p,1)}(T_{2,3})) = p + 2$. Then using equation 3.5 we have

$$p + 2 = g(P^{(p,1)}(T_{2,3})) = (p + 1)g(T_{2,3}) + g(P) = p + 1 + g(P),$$

which implies that $g(P) = 1$.

□

With Lemma 3.1.3 in hand, we can prove that the for all $p > 1$, patterns $P^{(p,1)}$ are fibered.

Proof of Theorem 3.1.5. Since knot Floer homology detects fibered knots, and a satellite knot is fibered if and only if the pattern and comanion are fibered, to show that the pattern $P^{(p,1)}$ is fibered it is enough to show that $\mathrm{rk}(\widehat{\mathrm{HFK}}(S^3, P^{(p,1)}(T_{2,3}), p+2)) = 1$ for all $p > 1$. To this end, consider the pairing diagram for $\widehat{\mathrm{HFK}}(S^3, P^{(p,1)}(T_{2,3}))$. By the proof of Lemma 3.1.3, we know that a has the largest Alexander grading of any intersection point. To show that $P^{(p,1)}(K)$ is fibered, we will show that for any other intersection point x in the pairing diagram, we have $A(x) < A(a)$. To this end, note that the Alexander grading is weakly decreasing as we travel up the pairing diagram on the β curve. It follows from lemma 3.3.1 that $A(a) - A(b) = 1$ and that $A(x) \leqslant A(b)$ for any other intersection point x. Therefore $\widehat{\mathrm{HFK}}(S^3, P^{(p,1)}(T_{2,3}), p+2)$ is one dimensional for all $p > 1$, and so the satellite knot $P^{(p,1)}(T_{2,3})$ is fibered for all $p > 1$. Since a satellite knot with non trivial companion is fibered if and only if both the pattern is fibered and the companion is fibered [HMS08], it follows that P is a fibered pattern. □

Recall from the introduction that fibered knots have unique minimal genus Seifert surfaces. Hence, for a fibered pattern P and a fibered knot K, the satellite knot $P(K)$ also has a unique minimal genus Seifert surface. Given this, one might wonder when the operation of taking a satellite of a non-trivial knot can increase or decrease the number of non-isotopic Seifert surfaces in the knot complement. In this direction, we prove Propositions 3.1.6 and 3.1.7 from the introduction, which imply that for knots with small rank knot Floer homology in the top Alexander grading the process of taking a satellite with a fibered pattern preserves the property of having a unique minimal genus Seifert surface as well as the property of having a depth at most one codimension one taut folitation of the complement.

Proof of Proposition 3.1.6. Suppose K is a knot with $\mathrm{rk}(\widehat{\mathrm{HFK}}(S^3, K, g(K))) < 4$ and P is a fibered pattern. Then by [Juh08a, Theorem 2.3] it follows that K has a unique minimal genus Seifert surface up to isotopy. By equation 3.2 we have $\mathrm{rk}(\widehat{\mathrm{HFK}}(S^3, P(K), g(P(K)))) < 4$. Hence $P(K)$ also has a unique minimal genus Seifert surface by [Juh08a][Theorem 2.3]. Repeating

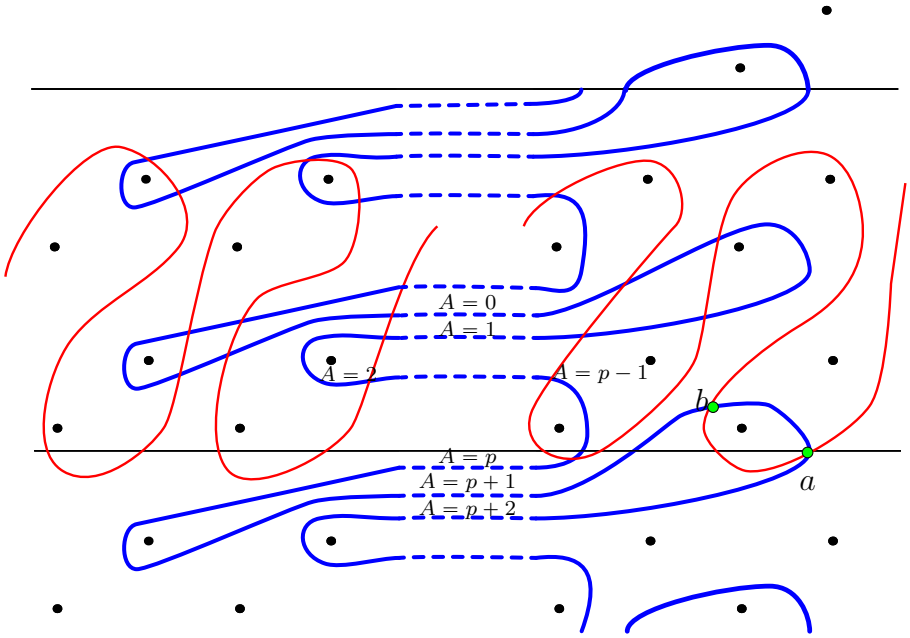

Figure 3.21. The pairing diagram computing $\widehat{\mathrm{HFK}}(S^3, P^{(p,1)}(T_{2,3}))$

the above argument, we see that $P^i(K)$ has a unique minimal genus Seifert surface up to isotopy for all $i \geqslant 1$. □

Proof of Proposition 3.1.7. Suppose K is a knot with $\mathrm{rk}(\widehat{\mathrm{HFK}}(S^3, K, g(K))) = 3$. So $a_{g(K)}$, the coefficient of $(t^g + t^{-g})$ in the symmetrised Alexander polynomial for K, is equal to $\chi(\widehat{\mathrm{HFK}}(S^3, K, g(K)))$ so is non zero. It follows from [Juh08c, Theorem 1.8] that $S^3 \backslash \nu(K)$ has a depth $\leqslant 1$ taut foliation transverse to $\partial(\nu(K))$. Then, equation 3.2 implies that $\mathrm{rk}(\widehat{\mathrm{HFK}}(S^3, P(K), g(P(K)))) = 3$, and so $a_{g(P(K))} = \chi(\widehat{\mathrm{HFK}}(S^3, P(K), g(P(K)))) \neq 0$, where $a_{g(P(K))}$ is the analogous coefficient of the Alexnader polynomial for $P(K)$. So $S^3 \backslash P(K)$ has a depth $\leqslant 1$ taut foliation transverse to $\partial\nu(K)$ again by [Juh08c, Theorem 1.8]. This argument can be repeated to show that $S^3 \backslash P^i(K)$ also has a depth $\leqslant 1$ taut foliation transverse to $\partial\nu(P^i(K))$ for all $i \geqslant 1$. □

3.6 Next to top Alexander grading

In this section we prove Theorem 3.1.10 from the introduction. First, we recall the notion of right and left veering monodromy following [BNS22]. Suppose that Σ is a surface with non-empty boundary and a and b are two properly embedded arcs in Σ. We say that a is to the right of b at p, denoted $a \geqslant_p b$ if p is a common endpoint of both arcs and either a is isotopic to b rel boundary, or after isotoping a rel boundary so that it intersects b minimally, a is to the right of b in a neighborhood of p. Now, suppose that $\phi : \Sigma \to \Sigma$ is a homeomorphism of Σ which restricts to the identity on a boundary component B of Σ. Then we say that ϕ is right veering at B if

$$\phi(a) \geqslant_p a$$

for every properly embedded arc $a \subset \Sigma$ and every $p \in \partial a \cap B$. A map ϕ is called right veering if it is right veering at every boundary component of Σ. We call a map ϕ left veering if its inverse is right veering.

Recall from Theorem 3.1.8 that, for a fibered knot, we can detect when the monodromy of a fibration is right or left veering by computing the next

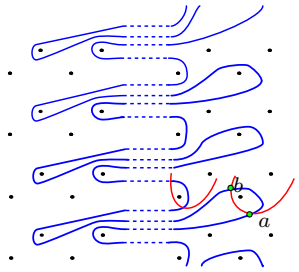

Figure 3.22. $P^{(p,1)}$ paired with a fibered knot with $\tau(K) = g(K)$

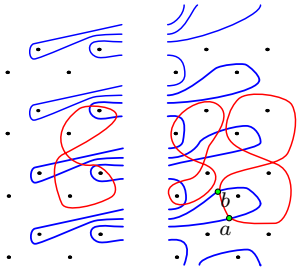

Figure 3.23. $P^{(p,1)}$ paired with a fibered thin knot K with $|\tau(K)| < g(K)$

to top Alexander graded piece of the knot floer homology to be one dimensional.

Lemma 3.6.1. *If K is a fibered knot with $\tau(K) = \pm g(K)$, then*

$$rk(\widehat{\mathrm{HFK}}(S^3, P^{(p,1)}(K), g(P^{(p,1)}(K)) - 1)) = 1.$$

Proof. Since K is a fibered knot with $\tau(K) = \pm g(K)$, we must have $\epsilon(K) = sgn(\tau(K))$ and the essential curve component has the form described in Lemma 3.2.2. Since the knot is fibered, there are no other components of the immersed curve that pass through at height $-g(K)$, so the red arcs shown in Figure 3.22 are representative of what the immersed curve of a general fibered knot with $\tau(K) = \pm g(K)$ looks like near the bottom row of the lifted pairing diagram. As we showed in the proof of Theorem 3.1.1, the knot $P^{(p,1)}(K)$ has one dimensional Floer homology in the top most Alexander grading, and the intersection point labelled a carries this Alexander grading. Continuing with this reasoning we have that $A(b) = g(P^{(p,1)}(K)) - 1$ by Lemma 3.3.1, since starting from a, we encounter one $\delta_{w,z}$ arc before we reach the intersection point labelled b. Now, no other intersections between the β curve and $\alpha(K)$ occur before we reach another $\delta_{w,z}$ arc while traversing β up the diagram. Since the Alexander grading is weakly decreasing as we travel up the β curve, it follows that b is the unique intersection point

with Alexander grading $g(P^{(p,1)}(K))-1$, hence $\widehat{\mathrm{HFK}}(S^3, P^{(p,1)}(K), g(P^{(p,1)}(K))-1)$ is one dimensional, as desired. □

Lemma 3.6.2. *Suppose K is a fibered thin knot with $|\tau(K)| < g(K)$. Then*

$$rk(\widehat{\mathrm{HFK}}(S^3, P^{(p,1)}(K), g(P^{(p,1)}(K)) - 1)) = 1$$

Proof. First, recall from [Pet13] that CFK^∞ has a simultaneously vertically and horizontally simplified basis with repect to which it decomposes as a direct sum of a staircase summand and boxes, and all horizontal and vertical differentials have length one. In this case the immersed curve $\alpha(K)$ consists of the essential component together with figure eight components, as shown in figure 3.23. Since $|\tau(K)| < g(K)$, the essential component of the immersed curve doesn't pass through at height $\pm g(K)$ and the portion that does consists of a single figure eight component, as shown in Figure 3.23. We know that the intersection point a represents the sole generator with Alexander grading $g(P^{(p,1)}(K))$, and the generator b has Alexander grading $g(P^{(p,1)}(K)) - 1$. Similar to the proof of Lemma 3.6.1, we see from the diagram that any other intersection point has Alexander grading $< g(P^{(p,1)}(K)) - 1$. Therefore b is the sole intersection point with Alexander grading $g(P^{(p,1)}(K)) - 1$ so $\widehat{\mathrm{HFK}}(S^3, P^{(p,1)}(K), g(P^{(p,1)}(K)) - 1)$ is one dimensional, as desired. □.

Proof of Theorem 3.1.10. If K is any fibered knot such that $\tau(K) = \pm g(K)$, then Lemma 3.6.1 implies that $P^{(p,1)}(K)$ has left or right veering monodromy. If K is any fibered thin knot such that $|\tau(K)| < g(K)$, then Lemma 3.6.2 implies that $P^{(p,1)}(K)$ has left or right veering monodromy. □

Finally, we prove Proposition 3.1.12 from the introduction.

Proof of Proposition 3.1.12. Suppose K is a non-trivial fibered thin knot with $|\tau(K)| < g(K)$. By Theorem 3.1.10, the fibered knot $P^{(p,1)}(K)$ has right or left veering monodromy. Therefore, by [BNS22, Corollary 1.7] to show that $P^{(p,1)}(K)$ is not thin it is enough to show for each $p > 1$ that $|\tau(P^{(p,1)}(K)| < g(P^{(p,1)}(K))$. By Corollary 3.1.4 we know that $g(P^{(p,1)}(K)) =$

$(p+1)g(K)+1$. In the case $\epsilon(K)=0$, Theorem 3.1.1 implies $\tau(P^{(p,1)}(K)) = 1 < (p+1)g(K)+1 = g(P^{(p,1)}(K))$, since $g(K) > 0$. In the case $\epsilon(K)=1$, Theorem 3.1.1 implies $|\tau(P^{(p,1)}(K))| \leqslant (p+1)|\tau(K)|+1 < (p+1)g(K)+1 = g(P^{(p,1)}(K))$, where the strict inequality is by assumption. In the case $\epsilon(K) = -1$ we have that $-g < \tau(K) < g$. Then $|\tau(P^{(p,1)}(K))| = (p+1)|\tau(K)+1| < (p+1)g(K) < (p+1)g(K)+1 = g(P^{(p,1)}(K))$. □

3.7 n-Twisted Satellites with Generalized Mazur Patterns

In this section, we study the immersed curve pairing theorem in the case that the knot complement has framing n, or equivalently when we add full twists around the meridian to the pattern knots. We compute the genus and determine the fiberedness and the Heegaard Floer concordance invariants τ and ϵ of satellite knots with arbitrary companions K and patterns from a family of knots in the solid torus, which we denote $Q_n^{i,j}$, shown in Figure 3.24. Here $j \in \mathbb{Z}_{>0}$ is the winding number of the pattern, $n \in \mathbb{Z}$ is the number of full twists around the meridian, and $i \in \mathbb{Z}_{\geqslant 0}$ denotes the number of full twists added to the clasp region in the box labelled i in Figure 3.24. We refer to the patterns $Q_n^{i,j}$ as *n-twisted generalized Mazur patterns*, since $Q_0^{0,1}$ is the Mazur pattern and $Q_0^{i,1}$ is a generalized Mazur pattern in analogy with the generalized Whitehead doubles of [Tru16] (See recent work of [PX24] for a similar family of patterns also called generalized Mazur patterns). Given a knot K, the satellite knot with n-twisted generalized Mazur pattern $Q_n^{i,j}(K)$ can either be viewed as a 0-twisted satellite with pattern $Q_n^{i,j}$ or as an n-twisted satellite with pattern $Q_0^{i,j}$. In this paper, we mostly adopt the latter perspective.

In [Lev16], Levine computed τ and ϵ of 0-twisted satellites with Mazur pattern and arbitrary companions by explicitly determining the bordered bimodule $\widehat{\mathrm{CFDA}}(X_Q)$ associated to the complement of the Mazur pattern in the solid torus and using the bordered pairing theorem of [LOT18]. Levine used this to compute τ and ϵ of 0-twisted satellites with Mazur pattern. More recently, in [CH23], Chen and Hanselman showed that the $UV = 0$ quotient of the full knot Floer complex of satellite knots with $(1,1)$-patterns can be computed using the immersed curve pairing theorem. They then recovered, in a more direct way, Levine's computation of τ and ϵ of 0-twisted satellites with Mazur pattern [CH23, Theorem 6.9].

One consequence of Levine's computation of ϵ of satellites with Mazur pattern is that the Mazur pattern does not act surjectively on the smooth concordance group. Levine then used this to construct a knot in the bound-

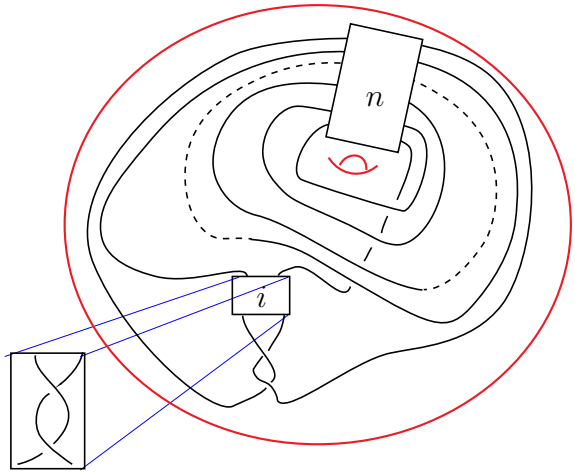

Figure 3.24. The pattern $Q^{i,j}$. In the box labelled i, there are i full twists on two strands as shown in the box on the bottom left. In the box labelled n insert n full twists on $j+2$ strands

ary of a contractible 4-manifold that does not bound a PL disk there or in any other contractible 4-manifold with the same boundary, answering a question of Kirby and Akbulut [Lev16, Theorem 1.2].

In this work, we extend these computations to determine τ and ϵ of n-twisted satellites with patterns $Q^{i,j}$. As a special case of our work, we show that τ of an n-twisted satellite knot with Mazur pattern and companion K depends only on the value of n relative to $2\tau(K)$, which echos the computations of τ of n-twisted Whitehead doubles [Hed07]. Interestingly this is not the case for τ of satellites with patterns $Q^{i,j}$ with winding number $j > 1$, where we show that the value of τ depends linearly on n and quadratically on j. Further, we show that for any companion knot K, $\epsilon(Q^{i,j}_n(K)) \neq -1$. This shows that for all $i \geqslant 0$, $j > 0$ and $n \in \mathbb{Z}$ the patterns $Q^{i,j}_n$ do not act surjectively on the smooth concordance group. See [PX24] for another family of patterns that have a similar property.

In another direction, we extend recent computations of Petkova and Wong in [PW21], where they showed that the genus and fiberedness of the

n-twisted Mazur pattern in the solid torus can be determined from the bordered type A structure $\widehat{\mathrm{CFA}}(S^1 \times D^2, Q^{0,1})$, using the bordered pairing theorem and classical results about the genus and fiberedness of satellites knots [Sch53; HMS08]. We expand on these computations and give closed formulas for the genus of n-twisted satellite knots with patterns $Q^{i,j}$ and arbitrary companions, and we determine for which i, j and n the pattern knots $Q^{i,j}_n$ are fibered in the solid torus. We also show that for any non-trivial companion K the satellite knot $Q^{i,j}_n(K)$ is not Floer thin.

Statement of Results

Recall that for the n-twisted satellite knot $P_n(K)$ with non-trivial companion knot K, we have [Sch53]

$$g(P_n(K)) = |w(P)|g(K) + g(P_n), \tag{3.6}$$

where $w(P_n) = (P_n \cap (\{pt\} \times D^2))$ is the winding number of the pattern and $g(P_n)$ is the genus of a relative Seifert surface for P_n. A consequence of this formula is that to determine $g(P_n(K))$ for an arbitrary non-trivial companion knot K, it is enough to determine $g(P_n(T_{2,3}))$. We use this observation together with the fact that knot Floer homology detects the genus of knots in S^3 to prove the following:

Theorem 3.7.1. *For K be a non-trivial knot in S^3, $j \in \mathbb{Z}_{>0}$, $i \in \mathbb{Z}_{\geqslant 0}$ and $n \in \mathbb{Z}$*

$$g(Q^{i,j}_n(K)) = \begin{cases} jg(K) + \dfrac{j(j+1)}{2}n + 1 & n \geqslant 0 \\ jg(K) + \dfrac{j(j+1)}{2}|n| + (1-j) & n < 0 \end{cases}$$

Equation 3.6, and so the proof of Theorem 3.7.1, requires the companion knot to be non-trivial. However, a similar computation gives $g(Q^{i,j}_n(U))$:

Theorem 3.7.2. *For $j \in \mathbb{Z}_{>0}$, $i \in \mathbb{Z}_{\geqslant 0}$ and $n \in \mathbb{Z}$*

$$g(Q_n^{i,j}(U)) = \begin{cases} \frac{j(j+1)}{2}n + 1 & n > 0 \\ 0 & n = 0 \\ \frac{j(j+1)}{2}|n| + 1 - j & n < 0 \end{cases}$$

Note that when $j = 1$ and $i = 0$ Theorem 3.7.1 and Theorem 3.7.2 recover [PW21, Theorem 1.0.5]

Recall from [HMS08] that a satellite knot $P_n(K)$ is fibered if and only if the companion knot K is fibered in S^3 and the pattern knot P_n is fibered in $S^1 \times D^2$. This implies that to show that a satellite knot $P_n(K)$ is fibered, it is enough to show that the satellite knot $P_n(T_{2,3})$ is fibered. Since a knot $K \subset S^3$ with $g(K) = g$ is fibered in S^3 if and only if $\text{rank}(\widehat{\text{HFK}}(S^3, K, g)) = 1$ [Ni07; Juh08b], we see that to determine if a pattern P_n is fibered it is enough to compute the top Alexander graded piece of the knot Floer homology of $P_n(T_{2,3})$. For $P = Q^{i,j}$, in Lemma 3.9.2 we compute the rank of the top Alexander graded piece of the knot Floer homology of $Q_n^{i,j}(T_{2,3})$ and show

Theorem 3.7.3. *Let K be a non-trivial fibered knot in S^3. Then the satellite knot $Q_n^{i,j}(K)$ is fibered if and only if either $j \geqslant 2$, $i = 0$ and $n \neq 0$ or $j = 1$, $i = 0$ and $n \neq -1, 0$.*

Note that the case $j = 1$ and $i = 0$ of Theorem 3.7.3 recovers [PW21, Theorem 1.0.6]. The proof of Theorem 3.7.3 actually shows that for any companion knot K, the rank of $\widehat{\text{HFK}}(S^3, Q_n^{i,j}(K), g(Q_n^{i,j}(K)))$ is greater than or equal to $i + 1$.

Recall that a knot is called Floer thin if all the generators of the knot Floer homology are supported in the same δ grading, where $\delta(x) = M(x) - A(x)$. We show

Theorem 3.7.4. *For any non-trivial companion knot K, the satellite knots $Q_n^{i,j}(K)$ are not Floer thin.*

We also consider the case when the companion knot is trivial.

Theorem 3.7.5. *For $K = U$ the satellite knots $Q_n^{i,j}(U)$ are Floer thin if and only if $j = 1$ and $n = -1$.*

Note that Theorems 3.7.4 and 3.7.5, in the case $i = 0$ and $j = 1$, recover [PW21, Theorem 1.01].
In [OS03b] and [Hom14] two smooth concordance invariants of knots derived from the $UV = 0$ quotient of the full knot Floer complex CFK^∞ are introduced, called $\tau(K)$ and $\epsilon(K)$. These invariants have proved fruitful in the study of the knot concordance group [Hed07; Hom14; Lev16]. We give an explicit computation of τ and ϵ of satellite knots with arbitrary companion knots K and patterns $Q_n^{i,j}$.

Theorem 3.7.6. *If K is a knot in S^3 with $\epsilon(K) = -1$, then for all $i \geqslant 0$, $j \geqslant 1$ and $n \in \mathbb{Z}$*

$$\tau(Q_n^{i,j}(K)) = j(\tau(K) + 1) + \frac{j(j-1)}{2}n.$$

If K is a knot in S^3 with $\epsilon(K) = 1$, then for all $i \geqslant 0$, $j \geqslant 1$ and $n \in \mathbb{Z}$

$$\tau(Q_n^{i,j}(K)) = \begin{cases} j\tau(K) + \dfrac{j(j-1)}{2}n + 1 & n < 2\tau(K) \\ j\tau(K) + \dfrac{j(j-1)}{2}n & n \geqslant 2\tau(K) \end{cases}$$

If K is a knot in S^3 with $\epsilon(K) = 0$, then for all $i \geqslant 0$, $j \geqslant 1$ and $n \in \mathbb{Z}$

$$\tau(Q_n^{i,j}(K)) = \begin{cases} \dfrac{j(j-1)}{2}n & n \geqslant 0 \\ \dfrac{j(j-1)}{2}n + j & n < 0 \end{cases}$$

Theorem 3.7.7. *For any knot K and for any $i \geqslant 0$, $j \geqslant 1$ and $n \in \mathbb{Z}$, we have $\epsilon(Q_n^{i,j}(K)) \in \{0, 1\}$.*

The invariant ϵ is a concordance invariant, and takes values in $\{0, 1, -1\}$. If we let $\mathcal{C}_\mathbb{Q}$ denote the rational homology knot concordance group (for the definition see [Lev16]) then an immediate Corollary of Theorem 3.7.7 is

Corollary 3.7.8. *For all $i \geqslant 0$, $j \geqslant 1$ and $n \in \mathbb{Z}$, the satellite operators $Q_n^{i,j} : \mathcal{C}_\mathbb{Q} \to \mathcal{C}_\mathbb{Q}$ are not surjective.*

As mentioned above, this shows that when we add full twists to the clasp region of the Mazur pattern (by increasing the parameter i) and when we add meridian twists to the Mazur pattern (by changing the framing n) we get a bi-infinite family of winding number 1 patterns that do not act surjectively on the smooth (or $\mathbb{Q}$-homology) concordance group and thus gives infinitely many examples of knots in homology spheres that do not bound PL disks in any contractible 4-manifold. See the recent work of [PX24] for another infinite family of winding number 1 unknot patterns with the same property. Our construction also gives many patterns of arbitrarily large winding number and various knot types in S^3 that also are not surjective satellite operators, and in particular shows that for these patterns, the image of the concordance invariant ϵ is not sensitive to twisting the pattern or changing the framing of the pattern knot complement.

3.8 Background

In this section we review some concepts from the immersed curve reformulation of bordered Floer homology and the bordered pairing theorem for $(1,1)$-patterns. We assume the reader is familiar with the various flavors of knot Floer homology and the work of [LOT18]. We quickly review the necessary background to state the immersed curve reformulation of the bordered invariants and bordered pairing theorem from [Che19; CH23; HRW22]. In Section 3.8 we introduce some notation and prove a structure theorem for the immersed curve associated to an n framed knot complement. Then in Section 3.8 we discuss $(1,1)$-patterns and the work of [Che19] with an eye towards extracting the $UV = 0$ quotient of the knot Floer complex from the pairing diagram as in [CH23], and then in Section 3.8 we discuss the specific family of $(1,1)$-patterns that gives rise to the patterns knots $Q^{i,j}$.

Immersed Curves for n-Framed Knot Complements

Note that the pair $(S^3, P_n(K))$ can be obtained by gluing $S^3 - \nu(K)$ with framing n to $(S^1 \times D^2, P)$ or by gluing $S^3 - \nu(K)$ with framing 0 to

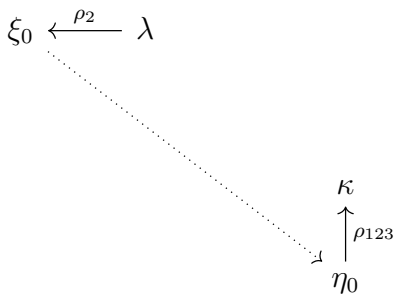

Figure 3.25. Type D structure for complement of knot K with $\tau(K) > 0$ and $\epsilon(K) = 1$, where we replace the dotted arrow from ξ_0 to η_0 by the appropriate unstable chain

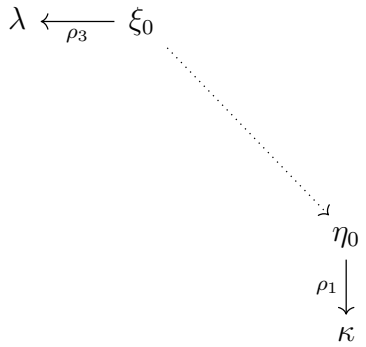

Figure 3.26. Type D structure for complement of knot K with $\tau(K) > 0$ and $\epsilon(K) = -1$, where we replace the dotted arrow from ξ_0 to η_0 by the appropriate unstable chain

the pair $(S^1 \times D^2, P_n)$. We want to study the pairing $\widehat{\mathrm{CFD}}(S^3 - \nu(K), n) \boxtimes \widehat{\mathrm{CFA}}(S^1 \times D^2, P)$ which computes $\widehat{\mathrm{CFK}}(S^3, P_n(K))$ from the perspective of immersed curves. With this goal in mind, we want to understand the essential component of the immersed curve associated to an n-framed knot complement. This lemma is a generalization of Lemma 3.2.2 to the case when the framing of the knot complement is arbitrary.

Definition 3.8.1 ([HRW22; HRW17; HW19])**.** *Given a knot $K \subset S^3$, let $\alpha(K, n)$ denote the immersed multi-curve representing the type D structure $\widehat{\mathrm{CFD}}(S^3 - \nu(K), n)$.*

As in [HW19, Proposition 2] we single out a special component of the immersed multi-curve $\alpha(K, n)$, denoted γ_0 and called the *essential component* of the immersed curve (See also [HRW22, pp 43-44]). As mentioned there, if we lift the curve to $\mathbb{R}^2$ and consider the vertical axes $\mathbb{Z} \times \mathbb{R}$, then the essential component is the only component of the immersed curve that

crosses from $\{i\} \times \mathbb{R}$ to $\{i+1\} \times \mathbb{R}$ and in the case when the framing $n = 0$, this potion of the essential component of the immersed curve component has slope $2\tau(K)$ (That is is spans $2\tau(K)$ rows) and it either turns up, down or continues straight after passing through $\{i+1\} \times \mathbb{R}$ if $\epsilon(K) = -1, 1$ or 0 respectively. We extend these observations to a structure theorem for a portion of γ_0 of n framed knot complements.

Lemma 3.8.2. *Suppose $\tau(K) \geqslant 0$ and $\epsilon(K) = 1$. If $n < 2\tau(K)$, then the essential component of the immersed curve has slope $2\tau(K) - n$ and turns down immediately after passing through $\{i+1\} \times \mathbb{R}$, see Figure 3.27. If $n \geqslant 2\tau(K)$, then the essential component of the immersed curve has slope $2\tau(K) - n$ and turns down immediately after crossing through $\{i+1\} \times \mathbb{R}$, see Figure 3.28.*

Proof. When $\epsilon(K) = 1$, by [Hom14] there is a reduced horizontally simplified basis so that the vertically distinguished generator ξ_0 of $\mathrm{CFK}^-(K)$ is an element of this horizontally simplified basis and occurs at the end of a horizontal arrow (symmetrically the horizontally distinguished generator η_0 occurs at the end of a vertical arrow). If $\tau(K) \geqslant 0$ then the algorithm from [LOT18, Theorem 11.26] shows that the type D structure contains the portion shown in Figure 3.25, where the dotted arrow is replaced by the appropriate unstable chain.

Then the algorithm in [HRW17, Sections 2.3-2.4] shows that the essential component of the immersed curve lifted to the cover $\mathbb{R}^2 \backslash \pi^{-1}(z)$ has the form shown. In Figure 3.27 and 3.28 we see the resulting curves for $n < 2\tau(K)$ and $n \geqslant 2\tau(K)$ respectively and indicate how the curves are built from the type D structure. Intersections with the vertical lines in the figure correspond to generators of $\iota_0 \widehat{\mathrm{CFD}}(S^3 - \nu(K), n)$ and the intersections with the horizontal lines correspond to generators of $\iota_1 \widehat{\mathrm{CFD}}(S^3 - \nu(K), n)$. If $\delta(x) = \rho_I \otimes y + \cdots$, then there is an arc ρ_I from x to y, as described in the figures. □

Similarly, we can show

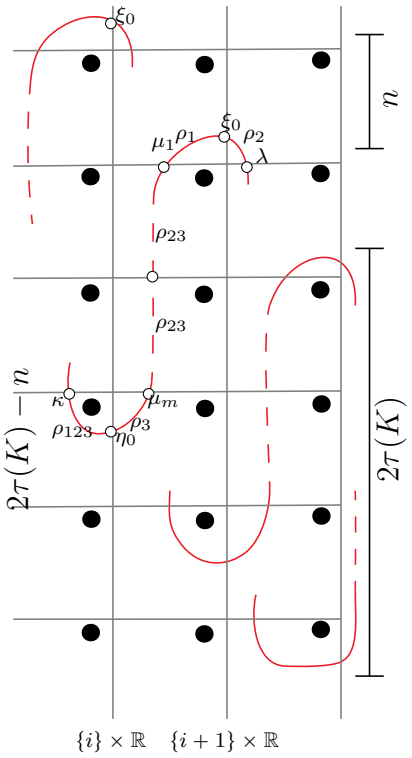

Figure 3.27. The unstable portion of $\alpha(K, n)$ with $\tau(K) \geqslant 0$ and $\epsilon(K) = 1$ and $2\tau(K) > n$

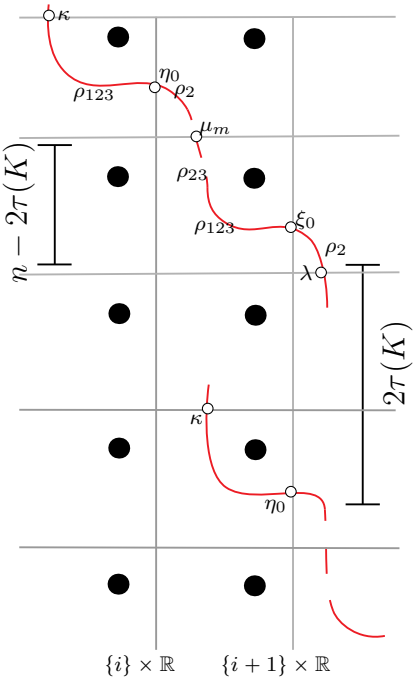

Figure 3.28. The unstable portion of $\alpha(K, n)$ with $\tau(K) \geqslant 0$ and $\epsilon(K) = 1$ and $n \geqslant 2\tau(K)$

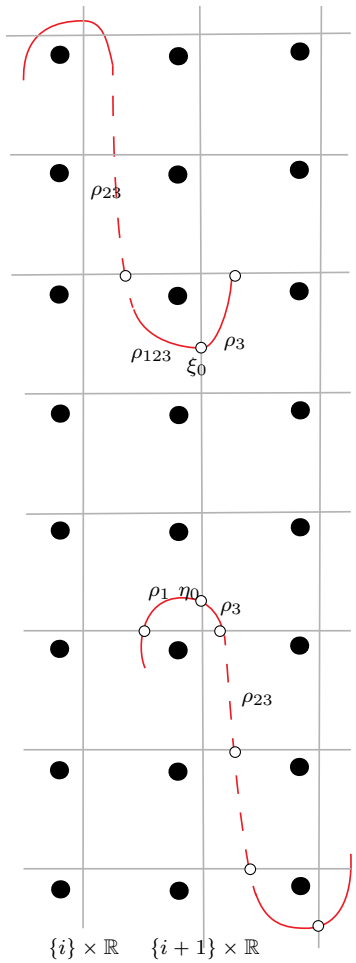

Figure 3.29. The unstable portion of $\alpha(K, n)$ with $\tau(K) \geqslant 0$ and $\epsilon(K) = -1$ and $n \geqslant 2\tau(K)$

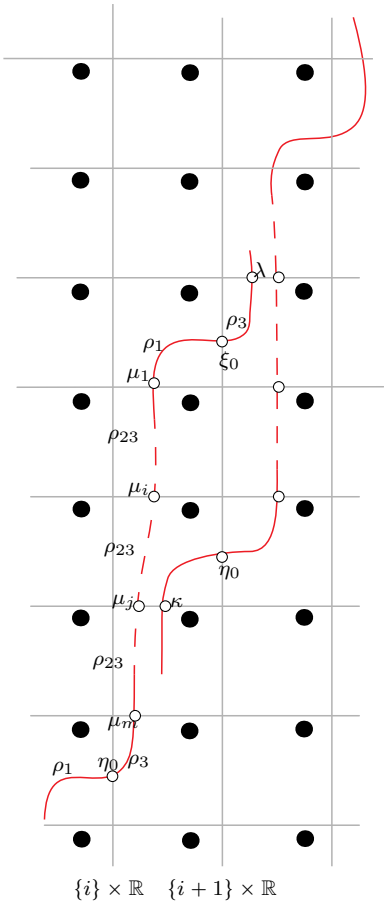

Figure 3.30. The unstable portion of $\alpha(K, n)$ with $\tau(K) \geqslant 0$ and $\epsilon(K) = -1$ and $n \leqslant 0 \leqslant 2\tau(K)$

Lemma 3.8.3. *Suppose $\tau(K) \geqslant 0$ and $\epsilon(K) = -1$. If $n \geqslant 2\tau(K)$, then the essential component of the immersed curve has slope $2\tau(K) - n$ and turns up after crossing through $\{i+1\} \times \mathbb{R}$, see Figure 3.29. If $n < 2\tau(K)$, then the essential component of the immersed curve has slope $2\tau(K) - n$ and turns up after crossing through $\{i+1\} \times \mathbb{R}$, see Figure 3.30.*

The statements about the form of the essential component of the immersed curve in the case $\tau(K) \leqslant 0$ are similar. In summary, the essential component of the immersed curve has slope $2\tau(K) - n$ and turns up, down or continues straight depending on whether $\epsilon(K) = -1, 1$ or 0.

(1,1)-Unknot Patterns

In this section, we review some notation and results about $(1,1)$ unknot patterns. In the case that the $(1,1)$ pattern knot P is an unknot pattern, meaning that $P(U) \sim U$, Chen showed that the β curve for the genus 1 doubly-pointed Heegaard diagram for P can be encoded by two integers (r,s), where $\gcd(2r-1, s+1) = 1$ [Che19, Theorem 5.1]. In this parametrization, r denotes the number of rainbows and s denotes the number of stripes (see [Che19, Figure 15]). The pattern described by the pair (r,s) corresponds to the two bridge link $\mathfrak{b}(2|s| + 4|r|, \epsilon(r)(2|r| - 1))$ [Che19, Theorem 5.4].

For example, see Figure 3.31 where we have drawn the doubly pointed Bordered Heegaard diagram for the unknot pattern described by the pair $(r,s) = (4,2)$, and Figure 3.32 where we have drawn the same genus 1 bordered Heegaard diagram with the pattern knot that it determines. In general, the knot determined by the $(1,1)$ unknot pattern given by the pair (r,s) has a presentation with $r-1$ rainbow arcs and $s+1$ stripes, see Figure 3.38.

As above, let $\widehat{\mathrm{CFK}}(\alpha, \beta, z, w)$ denote the intersection Floer homology of the two curves α and β in $T^2 \backslash \{z, w\}$ as described in [Che19, Theorem 1.2]. The generators of $\widehat{\mathrm{CFK}}(\alpha, \beta, z, w)$ are the intersection points of the two curves, and the differential counts embedded bigons with left boundary on the β curve and right boundary on the α curve. As proved in [CH23], we

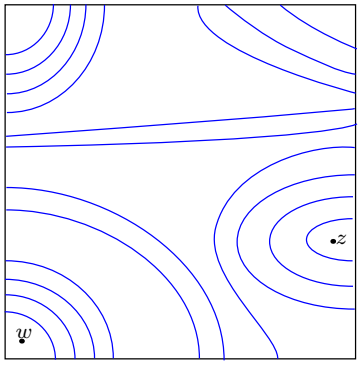

Figure 3.31. The $(1,1)$ pattern determined by the pair $(r,s) = (4,2)$

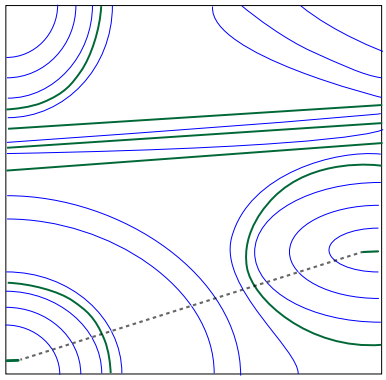

Figure 3.32. The knot in green in $S^1 \times D^2$ determined by the $(1,1)$ pattern with β curve the blue curve

can recover the $UV = 0$ quotient of the full knot Floer complex by considering disks that contain either z or w basepoints (but not both) and label them by V and U respectively. The component of the differential induced by counting bigons crossing the z basepoint will be called *vertical* differentials and denoted ∂^v, and those crossing the w basepoint *horizontal* differentials and denoted ∂^h.

Now, if $\pi : \mathbb{R}^2 \to T^2$ denotes the universal cover of the torus, let $\tilde{\beta}$ be a connected component of $\pi^{-1}(\beta)$ in $\mathbb{R}^2 \backslash (\pi^{-1}\{z,w\})$ and let $\tilde{\alpha}(K,n)$ be a lift of $\alpha(K,n)$ to $\mathbb{R}^2$, as in Figures 3.27-3.30. Then by [Che19, Proof of Theorem 1.2] $\widehat{\mathrm{CFK}}(\tilde{\alpha},\tilde{\beta},\pi^{-1}(z),\pi^{-1}(w)) \cong \widehat{\mathrm{CFK}}(\alpha,\beta,z,w)$. Indeed, it is easy to see that there is a correspondence at the level of generators, and it is similarly straightforward to see that differentials on both sides agree. See Figures 3.33, 3.35, and 3.36. Throughout we work with the lifted pairing diagram. We assume that the intersection between the two curves is *reduced*, meaning that the only bigons contributing to the differential are the bigons that cross either the z or the w basepoint, this is easily obtained by an isotopy of

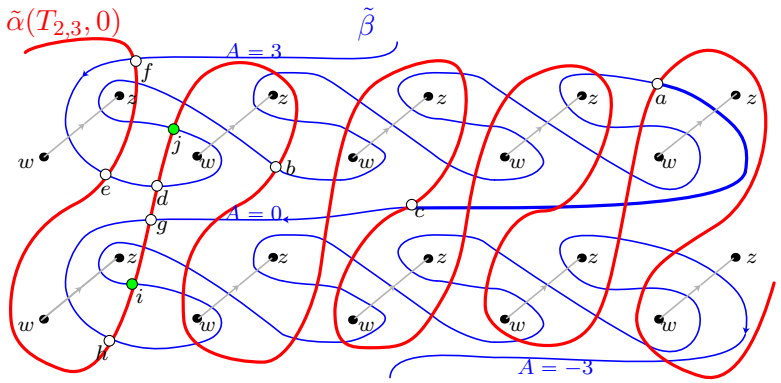

Figure 3.33. The lifted pairing diagram for $\widehat{\mathrm{CFK}}(\tilde{\alpha}(T_{2,3},0),\tilde{\beta},w,z)$

$\alpha(K,n)$ across the Whitney disks that don't contain a basepoint. With these conventions, the following is proved in [Che19, Theorem 1.2 and Lemma 4.1] and [CH23, Theorem 6.1]:

Theorem 3.8.4. *For P a $(1,1)$ pattern, $\widehat{\mathrm{HFK}}(S^3,P_n(K)) = \widehat{\mathrm{CFK}}(\tilde{\alpha}(K,n),\tilde{\beta}(P))$ and moreover $\mathrm{CFK}_{\mathbb{F}[U,V]/UV}(S^3,P_n(K)) \cong (\widehat{\mathrm{CFK}}(\tilde{\alpha}(K,n),\tilde{\beta},z,w),\partial^v,\partial^h)$. Furthermore, given two intersection points x and y between $\tilde{\alpha}(K,n)$ and $\tilde{\beta}(P)$, $A(y)-A(x) = \ell_{x,y}\cdot\delta_{w,z}$, where $\ell_{x,y}$ is an arc on the β curve that goes from x to y and A denotes the Alexander grading of generators of the knot Floer homology.*

See Figure 3.33 for an example, where we have drawn the lifted pairing diagram for the satellite knot $Q_0^{0,3}(T_{2,3})$. In that figure, we have labelled some intersection points, and drawn the $\delta_{w,z}$ arcs. Theorem 3.8.4 implies that the intersection points are in bijection with the generators of the knot Floer homology $\widehat{\mathrm{HFK}}(S^3,Q_0^{0,3}(T_{2,3}))$. Moreover, by taking an arc along the β curve from c to a, for example, we see that $A(a)-A(c) = -1$. The knot Floer homology has a symmetry given by $\widehat{\mathrm{HFK}}(S^3,K,A) \cong \widehat{\mathrm{HFK}}(S^3,K,-A)$, and we can see this symmetry in the pairing diagram by rotating the whole picture by π and exchanging the w and z basepoints. It follows that $A(c) = 0$ and we can always upgrade the relative Alexander grading given by Theo-

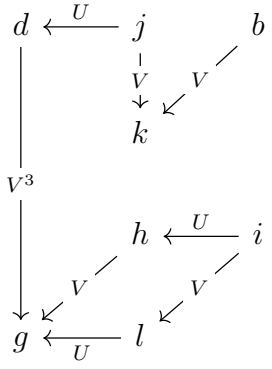

Figure 3.34. The piece of the complex $\mathrm{CFK}_{\mathbb{F}[U,V]/UV}(S^3, Q_0^{0,3}(T_{2,3}))$ that contains the intersection point d with $A(d) = \tau(Q_0^{0,3}(T_{2,3}))$ and $d + h$ generates $\widehat{\mathrm{HF}}(S^3)$.

rem 3.8.4 to an absolute Alexander grading. In Figure 3.33 we find $A(b) = 3$, $A(e) = A(d) = 4$ and $A(f) = 3$.

Another consequence of Theorem 3.8.4 is that since we can recover the $UV = 0$ quotient of the full knot Floer complex, we can compute both τ and ϵ of satellite knots with $(1,1)$-patterns. We return to this in Section 3.11 later, but we remark here that by counting disks that cross only the z basepoint in Figure 3.33, the intersection points d, g, and h form a subcomplex of $\widehat{\mathrm{CFK}}(Q_0^{0,3}(T_{2,3}))$ such that the cycle $d + h$ generates $\widehat{\mathrm{HF}}(S^3)$ (obtained by setting $V = 1$ in the above subcomplex). This cycle can be extended to a vertically simplified basis of $\mathrm{CFK}^-(Q_0^{0,3}(T_{2,3}))$ in the sense of [Hom14, Section 2]. Moreover, the intersection points i and j satisfy $\partial^h(i + j) = d + h$, so the distinguished element of the vertically simplified basis is in the image of the horizontal differential and this implies [Hom14, Section 3] that $\epsilon(Q_0^{0,3}(T_{2,3})) = 1$. Further, it is easy to see that the intersection point d satisfies $A(d) = \tau(Q_0^{0,3}(K))$. See Figure 3.34, where we have indicated a portion of the complex over $\mathbb{F}[U,V]/UV$. Note that the above argument only involved intersection points between the unstable portion of the curve $\alpha(T_{2,3}, 0)$ in the first column and the β curve. We return to this observation in section 3.11, where we see that this holds in general for the patterns given

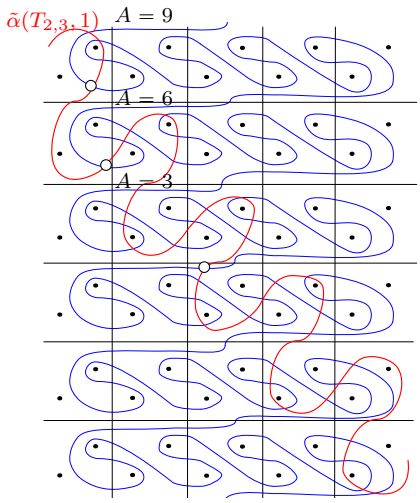

Figure 3.35. The pairing diagram for $\widehat{\mathrm{CFK}}(\alpha(T_{2,3},1),\beta(Q^{0,3}))$

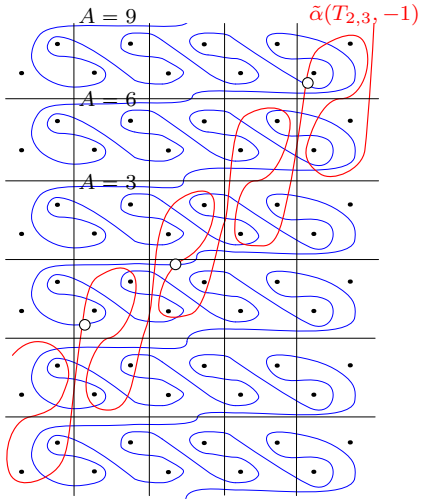

Figure 3.36. The pairing diagram for $\widehat{\mathrm{CFK}}(\alpha(T_{2,3},-1),\beta(Q^{0,3}))$

by the β curve $\beta(i,j)$.

The pairing diagrams and their lifts become more complicated when we consider knots with non-zero framing since the unstable chain gets longer for most values of n, which we need for computing the knot Floer homology of satellites with n-twisted patterns. For example, see Figures 3.35 and 3.36 where we have the pairing diagram for $Q^{0,3}_{-1}(T_{2,3})$ and $Q^{0,3}_{1}(T_{2,3})$. In those figures, the intersection point c satisfies $A(c) = 0$ and we have indicated some of the Alexander gradings of intersection points.

The Curves $\beta(i,j)$

In this section we introduce the specific $(1,1)$-patterns that give rise to the pattern knots $Q^{i,j}$ shown in Figure 3.24.

Definition 3.8.5. *Let $\beta(i,j)$ denote the β curve for the $(1,1)$ pattern which in the parameterization of [Che19] is given by $(r,s) = (2+j+2(j+1)i, j)$.*

The doubly pointed bordered Heegaard diagram associated with $\beta(i,j)$

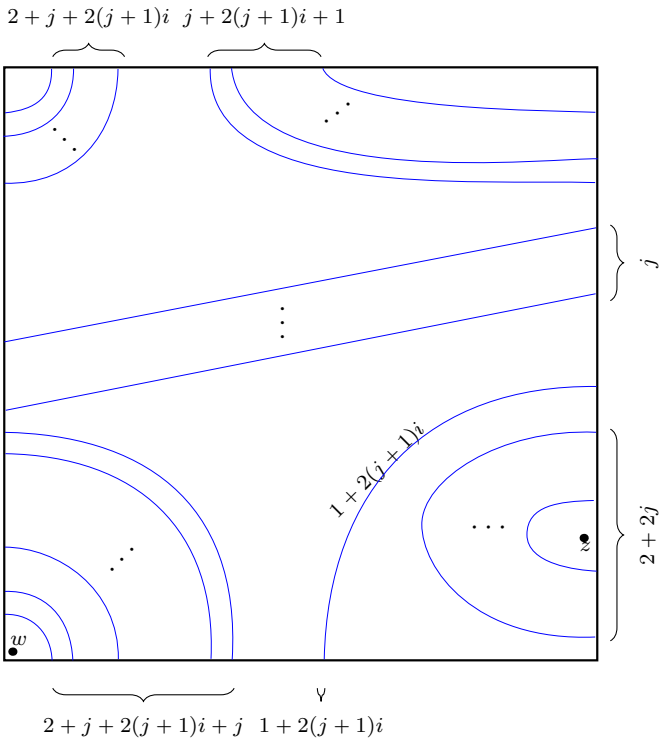

Figure 3.37. The $(1,1)$ pattern that determines the pattern knot $Q^{i,j}$. Figure 3.31 shows the case $i = 0$ and $j = 2$

is shown in Figure 3.37, and from that description it is easy to see that knot determined by the $(1,1)$ pattern with β curve $\beta(i,j)$ is shown in Figure 3.38. In that figure there are $r - 1 = 1 + j + 2i(1 + j) = (2i + 1)(1 + j)$ rainbows and $s + 1 = j + 1$ stripes. Each pair of strands represents $j + 1$ parallel strands, as indicated, and there are $2i(j + 1)$ of them. If we pull the $(2i + 1)(1 + j)$ rainbows from the left side of the figure around the orange arc, we end up with Figure 3.39. In that figure the bold line represents j consecutive strands. We isotope the j strands by pulling i the bold piece of the knot, and end up at Figure 3.40. Here there are j strands winding around the hole of the torus and $2i + 1$ rainbows. It is straightforward to verify that this is the knot $Q_0^{i,j}$ shown in Figure 3.24.

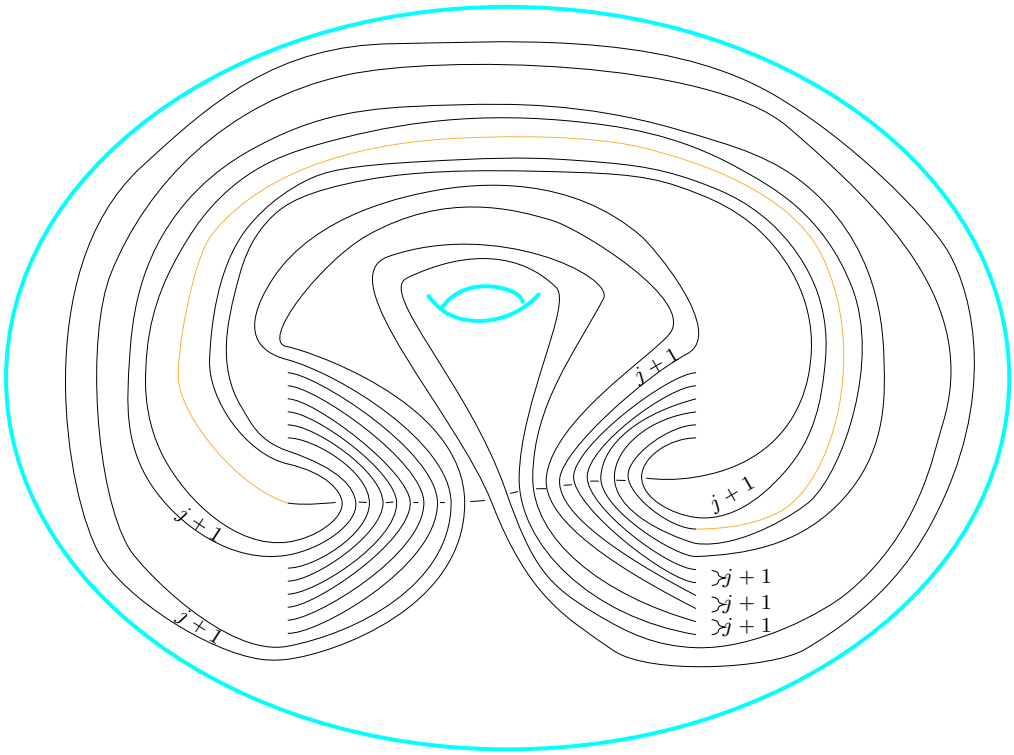

Figure 3.38. The knot in $S^1 \times D^2$ determined by the $(1,1)$ pattern with $\beta = \beta(i,j)$

In order to understand the pairing diagram for $\widehat{\mathrm{CFK}}(\tilde{\alpha}(K,n), \tilde{\beta}(i,j))$ we make some observations about the lifted β curve $\tilde{\beta}(i,j)$. When $i = 0$ the curve $\beta(0,j)$ is determined by the pair $(r,s) = (2+j, j)$. In this case, it is easy to see that the lift $\tilde{\beta}(0,j)$ has the form shown in Figure 3.41 top row. Indeed, each "wave" contributes one to the count of rainbows, and there are $j+1$ "waves", and there is one extra rainbow at the left end. Said another way, the lifted β curve $\tilde{\beta}(0,j)$ is obtained from $\tilde{\beta}(0,j-1)$ by the finger move shown in Figure 3.41 and this isotopy introduces one more rainbow and one more stripe to $\tilde{\beta}(0,j-1)$.

Next we claim that the transition from $\tilde{\beta}(0,j)$ to $\tilde{\beta}(1,j)$ corresponds to "twisting up" each wave, which is shown in Figure 3.43. Indeed, here we see

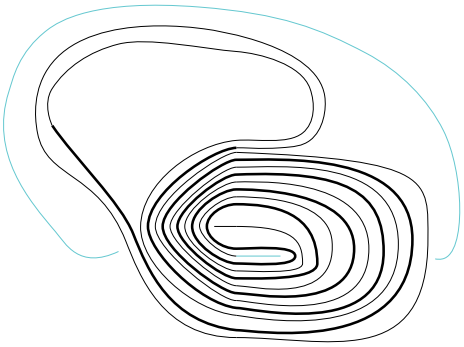

Figure 3.39. The knot from Figure 3.38 after an isotopy

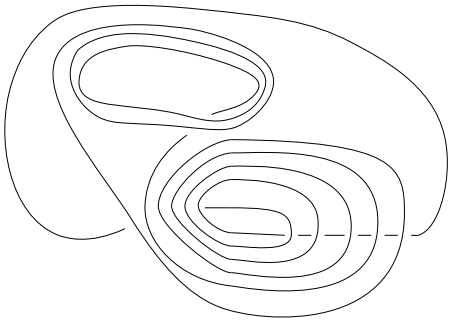

Figure 3.40. Isotope the j consecutive strands that are bold in Figure 3.39 to obtain this knot, which is $Q_0^{i,j}$

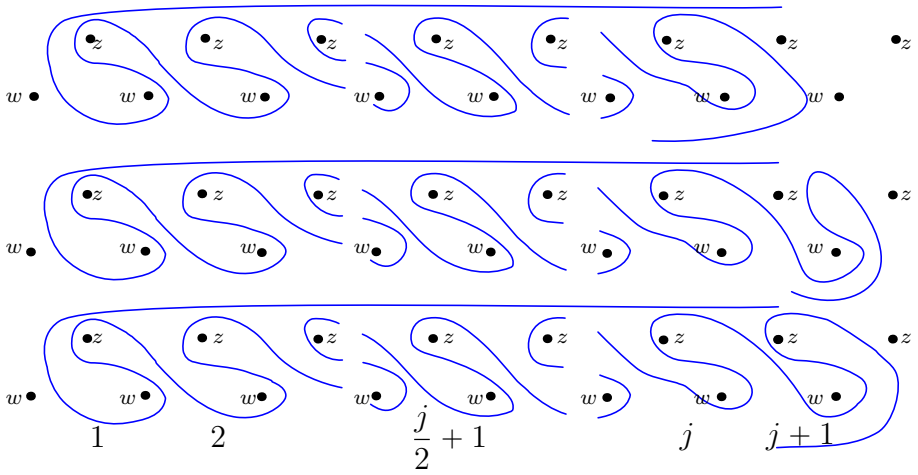

Figure 3.41. The isotopy that produces $\beta(0, j+1)$ from $\beta(0, j)$.

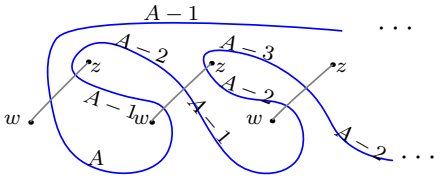

Figure 3.42. The curve $\tilde{\beta}(0, j)$ for the knot $Q^{0,j}$

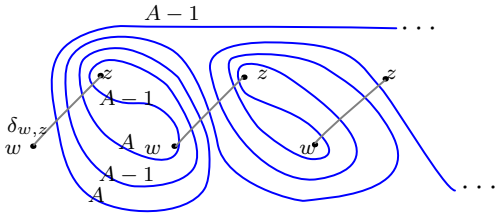

Figure 3.43. twist up the curve $\tilde{\beta}(0, j)$ to get the curve $\tilde{\beta}(1, j)$ for the knot $Q^{1,j}$

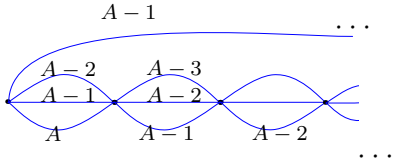

Figure 3.44. The collapsed $\tilde{\beta}(0, j)$ curve for the knot $Q^{0,j}$

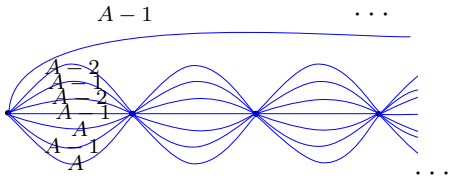

Figure 3.45. The collapsed $\tilde{\beta}(1, j)$ curve for the knot $Q^{1,j}$

that twisting up adds an extra 2 rainbows for each wave region, and thus $2(j + 1)$ new rainbows in total. In general, $\tilde{\beta}(i, j)$ is obtained from $\tilde{\beta}(0, j)$ by twisting up each wave region i times, and we see that this corresponds to adding $2(j + 1)i$ new rainbows, and no new stripes, to the lifted β curve.

For convenience we label the arcs of the β curves between lifts of the $\delta_{w,z}$ arcs by relative Alexander gradings that an intersection between $\alpha(K, n)$ and $\beta(i, j)$ on that arc would carry if there were intersections on that arc. It is straightforward to see that these Alexander grading labels increase as we move from right to left and bottom to top along the lift $\tilde{\beta}(i, j)$. Moreover, from the description of twisting up and [Che19, Lemma 4.1] the following lemma is immediate (see Figures 3.42-3.43).

Lemma 3.8.6. *For any knot K and for any $i > 0$, we have*

$$\{A : \widehat{\mathrm{HFK}}(S^3, Q_n^{i,j}(K), A) \neq 0\} = \{A : \widehat{\mathrm{HFK}}(S^3, Q_n^{0,j}(K), A) \neq 0\}$$

In order to simplify arguments and pictures in the next section, we introduce a modified version of the lifted β curve, called the collapsed β curve.

Definition 3.8.7. *Let $B(i,j)$ denote the curve $\tilde{\beta}(i,j)$ after collapsing the lifts of the arcs $\delta_{w,z}$ to a single point*

See Figure 3.44 and 3.45 where we draw $B(0,j)$ and $B(1,j)$ together with the Alexander gradings of arcs. The following lemma is immediate.

Lemma 3.8.8. *As an $\mathbb{F}$-vector space, pairing with the collapsed β curve is the same as pairing with the β curve: $\widehat{\mathrm{CFK}}(\tilde{\alpha}(K,n), B(i,j)) \cong \widehat{\mathrm{CFK}}(\tilde{\alpha}(K,n), \tilde{\beta}(i,j))$ and moreover, we can recover the Alexander grading of any intersection point in the collapsed pairing diagram.*

Although twisting up does not change the set of Alexander gradings labelling arcs of the β curves by Lemma 3.8.6, twisting up does change the number of arcs of the collapsed β curve that are labelled with a fixed Alexander grading. We will return to this observation in section 3.9 (see Lemma 3.9.2).

3.9 Three-Dimensional Invariants

In this section we compute the genus of the patterns $Q_n^{i,j}$, determine the set of triples (i,j,n) so that the pattern $Q_n^{i,j}$ is fibered in the solid torus, and show that whenever K is a non-trivial companion the satellite knots $Q_n^{i,j}(K)$ are not Floer thin.

Three-Genus and n-twisted Satellites

In this section we use Theorem 3.8.4 and the collapsed pairing diagram for n-framed satellite knots to prove Theorems 3.7.1 and 3.7.2 from the introduction. Recall that our strategy is to determine $g(Q_n^{i,j}(T_{2,3}))$ directly

from the pairing diagram and deduce the forumla for a general non-trivial companion from Equation 3.6. An immediate Corollary of Theorem 3.7.1 is a computation of the genus of the n-twisted pattern knot $Q_n^{i,j}$ in $S^1 \times D^2$.

Corollary 3.9.1. *For $n \in \mathbb{Z}$, $i \in \mathbb{Z}_{\geqslant 0}$ and $j \in \mathbb{Z}_{>0}$, the pattern knot $Q_n^{i,j}$ in $S^1 \times D^2$ has genus*

$$g(Q_n^{i,j}) = \frac{j(j+1)}{2}|n| + \begin{cases} 1 & n \geqslant 0 \\ 1-j & n < 0 \end{cases}$$

Proof. Equation 3.6 shows that

$$g(Q_n^{i,j}) = g(Q_n^{i,j}(T_{2,3})) - jg(T_{2,3}) = g(Q_n^{i,j}(T_{2,3})) - j.$$

□

To prove Theorems 3.7.1 and 3.7.2, we will make use of the collapsed pairing diagram. Note first that since $g(K) = \max\{A : \widehat{\mathrm{HFK}}(S^3, K, A) \neq 0\}$, Lemma 3.8.6 implies that $g(Q_n^{0,j}(K)) = g(Q_n^{i,j}(K))$, so it is enough to consider the case $i = 0$.

In Figures 3.46-3.48, we see the top half of the lifted pairing diagram $\widehat{\mathrm{CFK}}(\tilde{\alpha}(T_{2,3}, n), \tilde{\beta}(0, j))$. The other half is determined by the symmetry of the pairing diagram coming from the symmetry of knot Floer homology. We work with the collapsed pairing diagram to simplify the pictures, since we are not interested in any of the differentials and only in the Alexander gradings in this section. Note that by [Che19, Lemma 6.3], the Alexander grading of intersection points of $\alpha(T_{2,3})$ and $\beta(0, j)$ increase by $-w(Q_n^{0,j}) = j$ as we go up one row in the pairing diagram, so to determine the largest Alexander grading of an intersection point in the pairing diagram, it is enough to determine the number of rows between the central intersection point c (with $A(c) = 0$) and the top of the pairing diagram.

Proof of Theorem 3.7.1. As mentioned, by Lemma 3.8.6, it is enough to determine the genus in the case $i = 0$, and by Equation 3.6 it is enough to compute $g(Q_n^{0,j}(T_{2,3}))$. To this end, consider first the case $n \geqslant 0$. It is

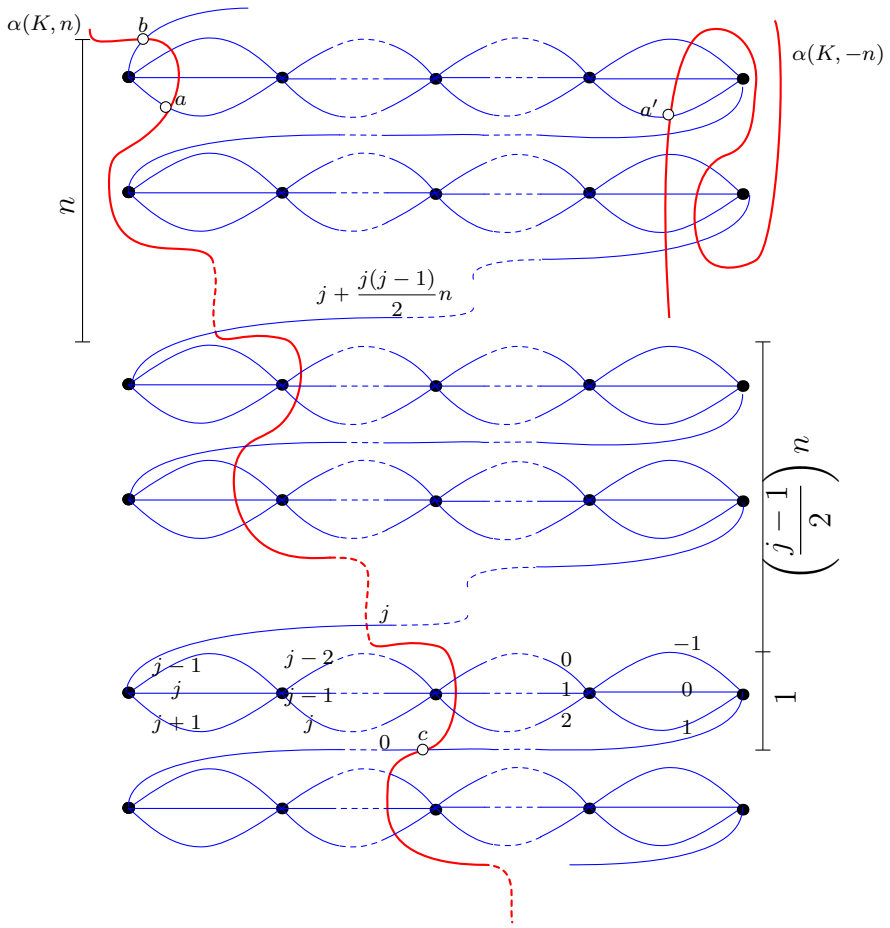

Figure 3.46. The pairing diagram for $Q_n^{0,j}$ when j is odd and $n > 0$

easy to see that the intersection point labelled a in Figures 3.46-3.48 has the largest Alexander grading. Indeed, the Alexander gradings increase by j for each row we go up in the pairing diagram and the Alexander gradings labelling each arc in the collapsed pairing diagram increase by one for each column we go over from right to left in the pairing diagram. To determine $A(a)$, note that there are a total of $2(j+2)+(n-2)(j+1)$ lifts of the curve $\beta(0,j)$ needed to account for all the intersections between $\alpha(T_{2,3},n)$ and $\beta(0,j)$. Indeed there are $(j+2)$ lifts of the $\mathrm{CFK}^\infty(T_{2,3})$ region (which occupies 2 rows) and there are $(j+1)$ lifts of the unstable region, which spans $n-2$ rows. There are then three cases to distinguish. If j is odd, then there are an even number of rows and the central intersection point occurs between these rows. Moreover, since there are an odd number of $\mathrm{CFK}^\infty(T_{2,3})$ regions, by symmetry of the pairing diagram the central intersection point occurs in the middle of the central CFK^∞ region of the curve. See Figure 3.46. If j is even, then there are an odd number of lifts of the unstable region and so the central intersection point occurs somewhere along the unstable region. If n is even or odd, then the number of rows is either even or odd. If n is even, we are in the situation pictured in Figure 3.48 and if n is odd, we are in the situation pictured in Figure 3.47. In any case, to determine $A(a)$ it is enough to count the number of rows between the central intersection point c and the intersection point labelled b. In all the cases the number of rows are indicated in the figure. We describe the case j even and n odd in detail and leave the rest to the reader.

In Figure 3.47 the central intersection point c occurs on the central lift of the unstable chain. There are $\dfrac{n-1}{2}$ rows between that intersection point and the intersection point labelled d in Figure 3.47. Then, there are $\dfrac{j-2}{2}n$ rows between the interesction point d and the intersection point e, and $n+1$ rows between e and b. Therefore,

$$A(b)-A(c)=j\left(\frac{n-1}{2}+\frac{j-2}{2}n+n+1\right).$$

Then it is straightforward to verify that $A(a)-A(b)=\dfrac{j}{2}+1$. Simplifying,

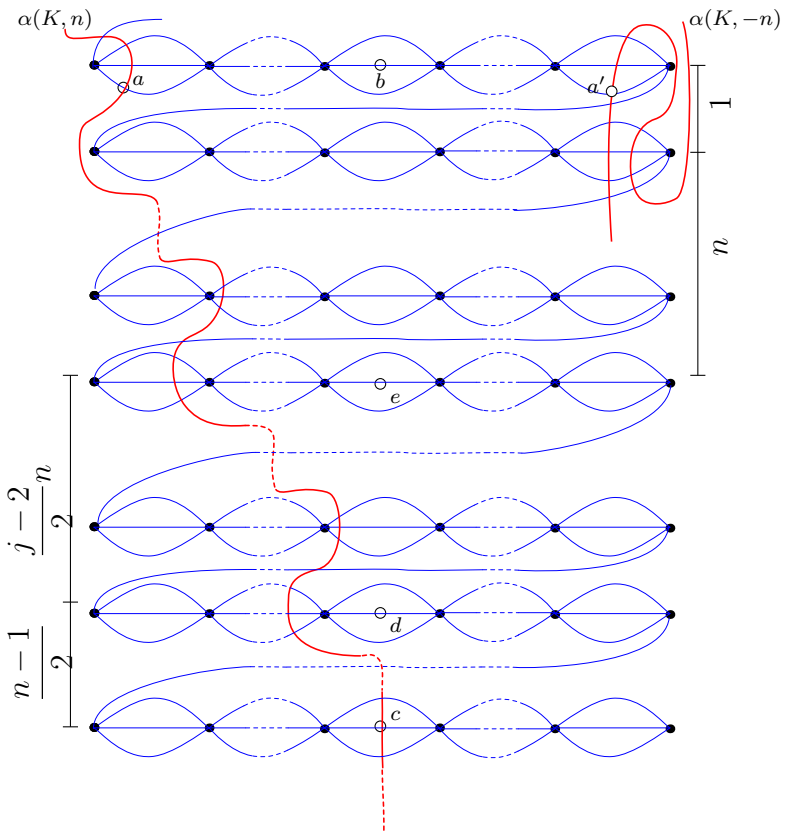

Figure 3.47. The general pairing diagram for j even and n odd

we see that when $n \geqslant 0$

$$g(Q_n^{i,j}(T_{2,3})) = A(a) = j + \frac{j(j+1)}{2}n + 1$$

This finished the proof in the case $n \geqslant 0$. When $n < 0$, Figures 3.46-3.48 show both the curve $\alpha(K,n)$ and the curve $\alpha(K,-n)$ and we can see that the difference $g(Q_{-n}^{i,j}(T_{2,3})) - g(Q_n^{i,j}(T_{2,3})) = j$. For example in Figure 3.47, the intersection point with the largest Alexander grading in the pairing with $\alpha(K,-n)$ is labelled a': $A(a') = g(Q_{-n}^{0,j}(K))$. Then $A(a) - A(a') = \ell_{a',a} \cdot \delta_{w,z} = j$. Therefore when $n < 0$, we have $g(Q_n^{i,j}(T_{2,3})) = j + \frac{j(j+1)}{2}|n| + 1 - j$ $\square$

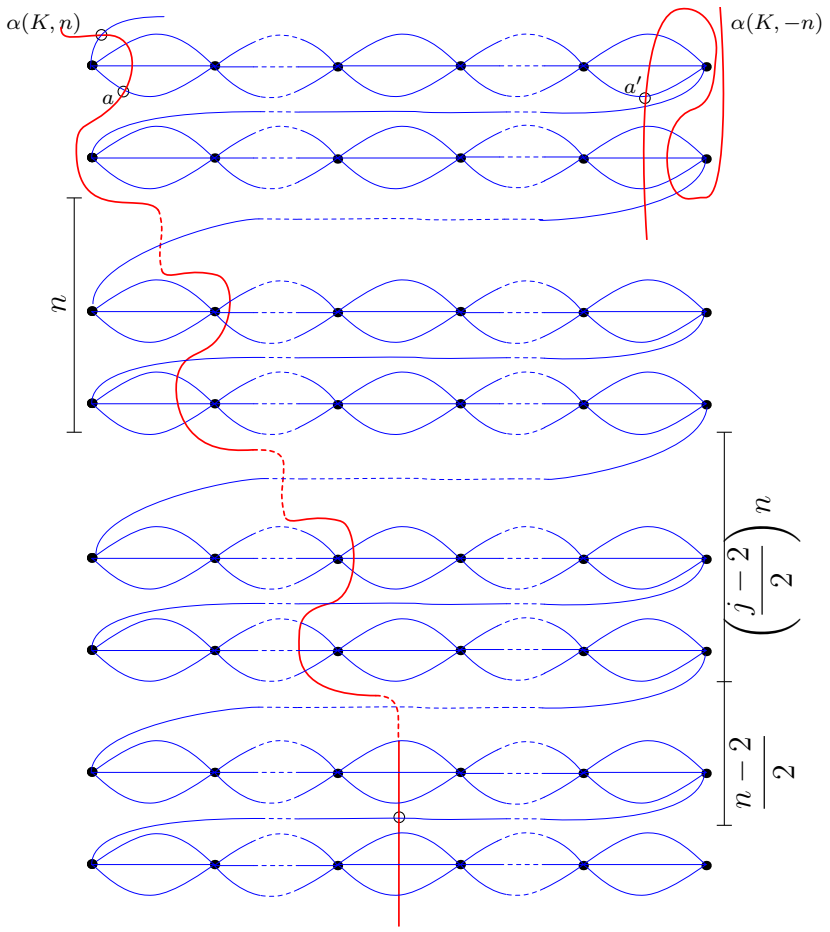

Figure 3.48. The general pairing diagram for j even and n even

Proof of Theorem 3.7.2. The computation of the genus when the companion knot is the unknot is similar to the proof of Theorem 3.7.1 and left to the reader (see Case 0 in the proof of Theorem 3.7.6 for the relevant pairing diagram). □

Fiberedness

In this section we prove Theorem 3.7.3. By [HMS08] a necessary condition for a satellite to be fibered is for the companion to be fibered and to

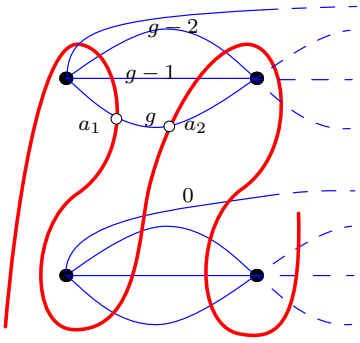

Figure 3.49. The lifted pairing diagram for $\widehat{\mathrm{HFK}}(Q_0^{0,j}(T_{2,3}))$

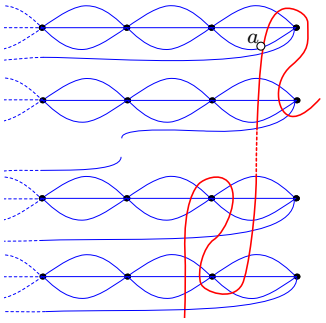

Figure 3.50. The pairing diagram for $Q_n^{0,j}(T_{2,3})$ when $n < -1$. The Alexander grading labels of the β arcs are as in Figure 3.51

determine the fiberedness of any satellite $Q_n^{i,j}(K)$ with fibered companion, it is enough to determine if the satellite knot $Q_n^{i,j}(T_{2,3})$ is fibered.

Now, recall that a knot K in S^3 is fibered if and only if $\widehat{\mathrm{HFK}}(S^3, K, g(K))$ has rank one [Ni07; Juh08b]. In the previous section we determined that largest Alexander grading, so the genus, of any satellite knot with pattern $Q_n^{i,j}$ and companion K. In this section, we will determine the rank of the knot Floer homology of $Q_n^{i,j}(T_{2,3})$ in Alexander grading $g(Q_n^{i,j}(T_{2,3}))$. Using this, we will show when this has rank one. In the following, let $g = g(Q_n^{i,j}(T_{2,3}))$

Lemma 3.9.2.

$$\dim(\widehat{\mathrm{HFK}}(S^3, Q_n^{i,j}(T_{2,3}), g)) = \begin{cases} 2(i+1) & \text{if } n = 0 \text{ and } j \geqslant 1 \\ 2(i+1) & \text{if } n = -1 \text{ and } j = 1 \\ (i+1) & \text{else} \end{cases}$$

Proof. We will first determine the rank of $\widehat{\mathrm{HFK}}(S^3, Q_n^{0,j}(T_{2,3}), g)$ then we will see how the rank changes when we increase i by twisting up the β curve.

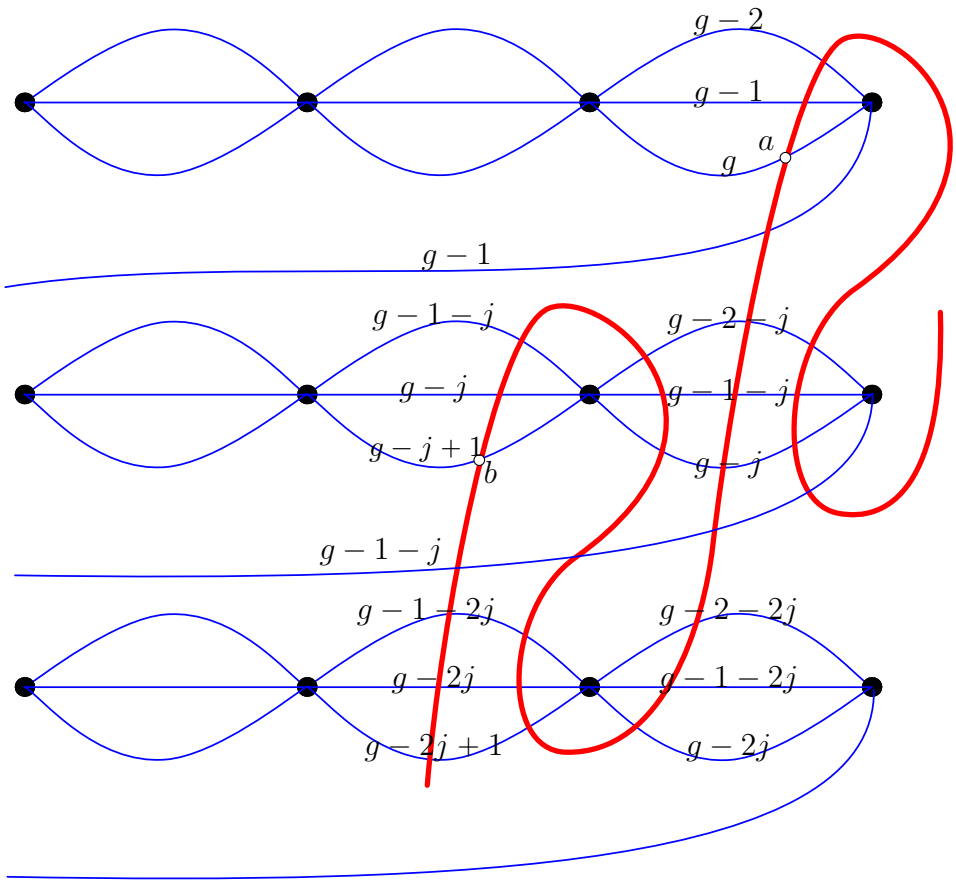

Figure 3.51. The general pairing diagram showing intersection points with largest possible Alexander grading when $i = 0$ and $n = -1$. For each increase in i, there is one more arc in the top right with Alexander grading label g, and one more arc in the second to top row and second to right column with label $g - 1 + j$

Suppose first that $n = 0$, In this case there are two intersection points in the top row of the pairing diagram that contribute to $\widehat{\mathrm{HFK}}(S^3, Q_0^{0,j}(T_{2,3}), g)$, shown in Figure 3.49 and labelled a_1 and a_2. Direct inspection shows that there are no other intersection points in this Alexander grading. Therefore $\dim(\widehat{\mathrm{HFK}}(S^3, Q_0^{0,j}(T_{2,3}))) = 2$.

Suppose now that $n < 0$. We first deal with the case $n < -1$. The pairing diagram for this case is shown in Figure 3.50. In that figure we see that there is one intersection point with Alexander grading $g(Q_n^{0,j}(T_{2,3}))$ labelled a in the top row of that figure. Inspection of the pairing diagram shows that all the intersection points in the lower rows of the pairing diagram all carry Alexander gradings $< g$ regardless of the value of j. Hence $\dim(\widehat{\mathrm{HFK}}(S^3, Q_n^{0,j}(T_{2,3}), g)) = 1$ when $n < -1$ and $j \geqslant 1$.

The pairing diagram for the case $n = -1$ is shown in 3.51. In that figure, we see that there is one intersection point in Alexander grading g in the top row of the pairing diagram, labelled a. All other arcs of the β curve in this row (and thus all other intersection points in this row) carry an Alexander grading label $< g$. Consider the next to top row of the pairing diagram. The largest possible Alexander grading is the Alexander grading of the intersection point labelled b, which is $g - j + 1$. This is always strictly less than g unless $j = 1$. Further, regardless of the value of j, all other intersection points carry an Alexander grading $\leqslant g - 1$. So in the case that $n = -1$, we see that $\dim(\widehat{\mathrm{HFK}}(S^3, Q_{-1}^{0,1}(T_{2,3}), g)) = 2$ and $\dim(\widehat{\mathrm{HFK}}(S^3, Q_{-1}^{0,j}(T_{2,3}), g)) = 1$ when $j > 1$.

The case that $n \geqslant 1$ is similar. In that case we see that for all $j \geqslant 1$ and $n \geqslant 1$, $\mathrm{rk}(\widehat{\mathrm{HFK}}(S^3, Q_n^{0,j}(T_{2,3}), g)) = 1$.

This proves the theorem in the case $i = 0$. To deal with the cases $i > 0$, recall that the lifted curve $\tilde{\beta}(i, j)$ is obtained from the lifted curve $\tilde{\beta}(i - 1, j)$ by twisting up, as shown in Figure 3.43. We see in Figures 3.52 and 3.53 that for each intersection point of $\tilde{\alpha}(T_{2,3}, n)$ with $\tilde{\beta}(i - 1, j)$ in Alexander grading g, there is one more intersection point of $\tilde{\alpha}(T_{2,3}, n)$ with $\tilde{\beta}(i, j)$ in that same Alexander grading. The theorem follows. □

With Lemma 3.9.2 in hand, we can prove Theorem 3.7.3 from the intro-

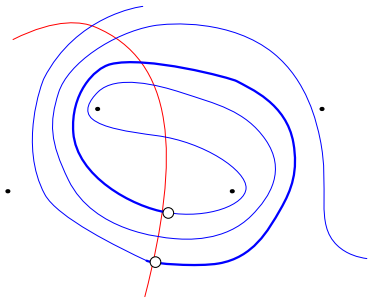

Figure 3.52. The top left of the pairing diagram when $n > 0$ and $i = 2$. The intersection points connected by a spiral are in Alexander grading $g = g(Q_n^{i,j}(K))$

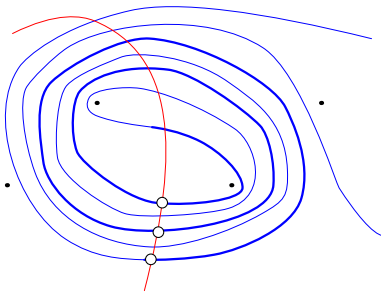

Figure 3.53. The top left of the pairing diagram when $n > 0$ and $i = 3$. The intersection points connected by a spiral are in the same Alexander grading $g = g(Q_n^{i,j}(K))$

duction.

Proof of Theorem 3.7.3. By [HMS08], the pattern knot $Q_n^{i,j}$ is fibered in $S^1 \times D^2$ if and only if the satellite knot $Q_n^{i,j}(T_{2,3})$ is fibered in S^3. By the computation in lemma 3.9.2 and the fact that a knot in S^3 is fibered if and only if $\operatorname{rank}(\widehat{\mathrm{HFK}}(S^3, K, g(K))) = 1$ [Ni07], we see that the pattern knot $Q_n^{i,j}$ is fibered for $j \geqslant 2$ if and only if $i = 0$ and $n \neq 0$ and when $j = 1$ $Q_n^{i,1}$ is fibred if and only if $i = 0$ and $n \neq 0, -1$. □

3.10 Thickness and unknotting number of generalized Mazur satellites with non-trivial companions

In this section we give lower bounds on the thickness and torsion order for n-twisted satellites with patterns $Q^{i,j}$ and arbitrary non-trivial companions. Recall that a knot K is called Floer thin if for all pairs of generators x and y of $\widehat{\mathrm{HFK}}(S^3, K)$ $M(x) - A(x) = M(y) - A(y)$. Equivalently, if we define the δ-grading as $\delta(x) = M(x) - A(x)$ a knot is thin if the δ grading

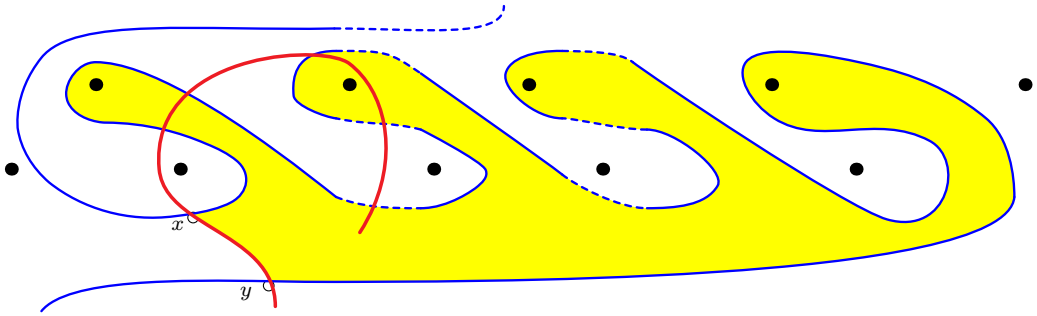

Figure 3.54. Illustration of two intersection points in the pairing diagram with a length $j+1$ vertical differential between them. The red arc is a portion of $\alpha(K,n)$ that exhibits the genus detection of knot Floer homology

is constant for all generators. This concept was introduced in [MO08], where they showed that all quasi-alternating knots have thin knot Floer homology.

Suppose that there is a length k vertical arrow between two distinct generators x and y of the knot Floer homology. Then $A(y) = A(x) - k$ and $M(y) = M(x) - 1$. In this case, if we consider the collapsed δ grading we see that $\delta(x) = M(x) - A(x)$ and $\delta(y) = M(x) - 1 - (A(x) - k) = \delta(x) + k - 1$. So if $k > 1$, these two generators are supported in distinct δ gradings, and so the knot K is not Floer homologically thin.

Theorem 3.10.1. *Suppose that K is a non-trivial companion knot. Then the satellite knots $Q_n^{i,j}(K)$ are not thin.*

The proof of Theorem 3.10.1 relies on the observation that, since knot Floer homology detects the genus of knots, if a knot K is non-trivial there is always a portion of the immersed curve in each column that exhibits this. We are only interested in the portion of the immersed curve in the second column of the pairing diagram which is shown in figure 3.54.

Proof. Suppose K is a non-trivial companion knot. Then the curve $\alpha(K,n)$ contains a portion as shown in Figure 3.54 by the genus detection of knot Floer homology. We see that there are two intersection points, denoted x

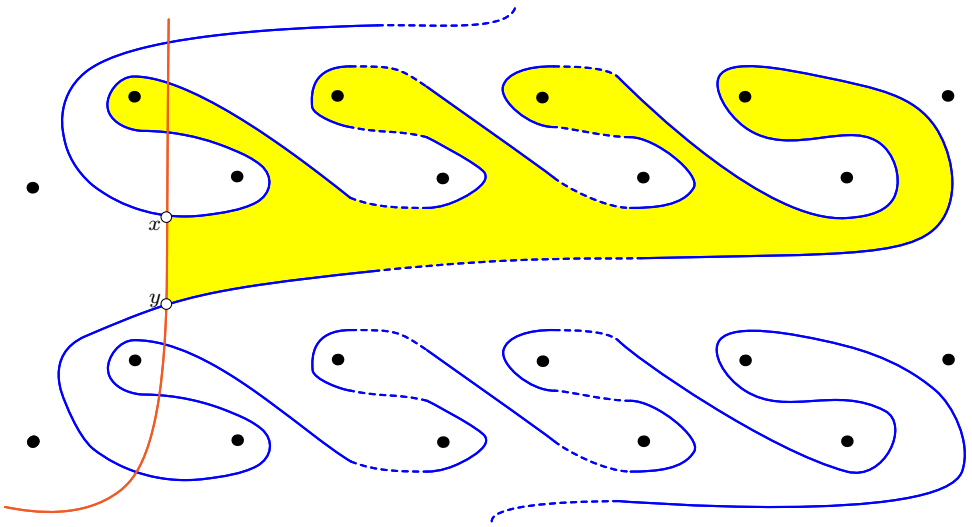

Figure 3.55. The pairing $\widehat{\mathrm{CFK}}(\alpha(U,n),\beta(i,j))$ when $n<-1$

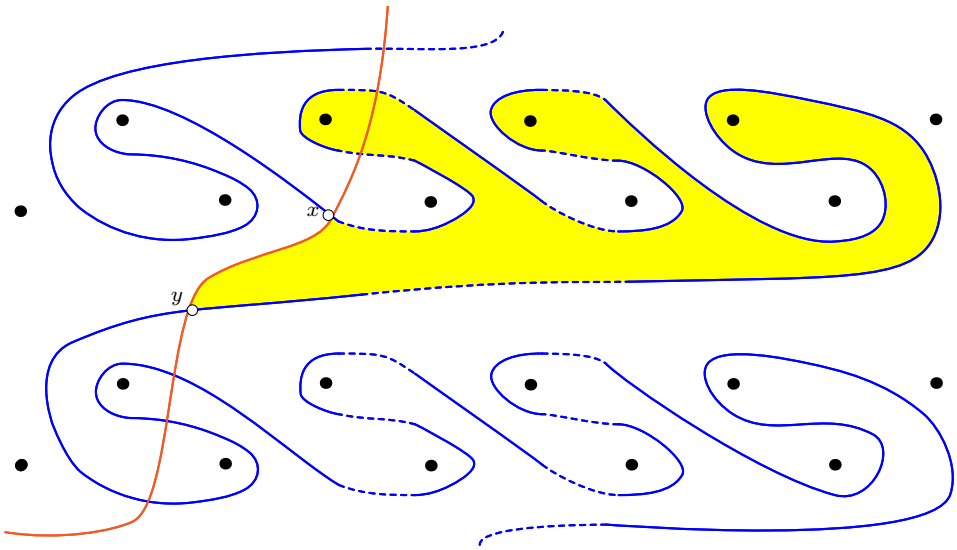

Figure 3.56. The pairing $\widehat{\mathrm{CFK}}(\alpha(U,-1),\beta(i,j))$

and y, that are connected by a length $j+1$ vertical differential. Hence the knot $Q_n^{i,j}(K)$ is not Floer thin. □

Next, we investigate what happens when the companion knot K is the

unknot. In that case, since $Q_0^{i,j}(U) \sim U$, it is clear that the 0-twisted satellite is Floer thin. In all other cases, we prove the following

Theorem 3.10.2. *The satellite knot $Q_n^{i,j}(U)$ is not Floer thin unless $n = -1$ and $j = 1$.*

Note that Theorems 3.10.1 and 3.10.2 in the case $j = 1$ recover [PW21, Theorem 1.01].

Proof. Since $K = U$, the pairing diagram $\widehat{\mathrm{CFK}}(\alpha(U,n), \beta(i,j))$ has the form shown in Figures 3.55 and 3.56. Figure 3.55 shows the case when $n < -1$ and Figure 3.56 shows the case when $n = -1$. The case when $n > 0$ is similar and left ot the reader. In the case $n < -1$ inspecting Figure 3.55 we see that there is a length $j + 1$ vertical differential between the intersection points labelled x and y. In the case $n = -1$, Figure 3.56 shows that there is a length j vertical differential between the intersection points labelled x and y. Inspection of the pairing diagram shows that these are the longest possible vertical differentials in the complex $\widehat{\mathrm{CFK}}_{\mathbb{F}[U,V]/UV}(S^3, Q_n^{i,j}(U))$. Therefore, when $n < -1$, the satellite knot $Q_n^{i,j}(U)$ is never thin and when $n = -1$, the satellite knot $Q_n^{i,j}(U)$ is thin if and only if $j = 1$. □

The *V-torsion order* of a knot, $\mathrm{Ord}_V(K)$ is the smallest integer k with the property that $V^k(Tors(\mathrm{HFK}^-_{\mathbb{F}[V]}(S^3, K))) = 0$. The proofs of Theorem 3.10.1 and 3.10.2, in addition to determining when the satellite knots $Q_n^{i,j}(K)$ are not thin, also gives a lower bound on the torsion order of $Q_n^{i,j}(K)$:

Corollary 3.10.3. *When K is non-trivial, or when $K = U$ and $n \neq -1$ $\mathrm{Ord}_V(Q_n^{i,j}(K)) \geqslant j + 1$. When $K = U$ and $n = -1$ then $\mathrm{Ord}_V(Q_{-1}^{i,j}(U)) \geqslant j$.*

Proof. The proof of theorem 3.10.1 and 3.10.2 shows that the chain omplex $g\mathrm{CFK}^-(Q_n^{i,j}(K))$ has a length $j + 1$ vertical differential in the case K is non-trivial or $K = U$ and $n \neq -1$, or a length j vertical differential in the case $K = U$ and $n = -1$. □

Since the torsion order is a lower bound for the unknotting number of a knot [AE20] the following Corollary is immediate. This verifies a conjecture

of Hom, Lidman and Park in the case that the pattern knot is an n-twisted generalized Mazur pattern [HLP22, Conjecture 1.10].

Corollary 3.10.4. *The satellite knots $Q_n^{i,j}(K)$ with non-trivial companions have unknotting number at least $j+1 = w(Q_n^{i,j})+1$.*

3.11 Heegaard Floer Concordance Invariants and Twisting

In this section we determine the dependence of the invariants τ and ϵ on the parameters i, j and the twisting parameter n. First, we will determine the invariants $\tau(Q_n^{0,j}(K))$ and $\epsilon(Q_n^{0,j}(K))$ in terms of $\tau(K)$, $\epsilon(K)$, j and n, and then we will show that $\tau(Q_n^{i,j}(K))$ and $\epsilon(Q_n^{i,j}(K))$ are independent of $i \in \mathbb{Z}_{\geqslant 0}$.

Recall that by Theorem 3.8.4, the complex $\mathrm{CFK}_{\mathbb{F}[U,V]/UV}(S^3, Q_n^{0,j}(K))$ can be extracted from the pairing diagram by considering disks that cover either the z or w basepoint and do not cover both. Let $\mathrm{CFK}_{\mathbb{F}[V]}(S^3, Q_n^{0,j}(K))$ denote the complex obtained by only counting disks that cross the z-basepoint (so the $U=0$ quotient of $\mathrm{CFK}_{\mathbb{F}[U,V]/UV}(S^3, Q_n^{0,j}(K))$). Theorem 3.8.4 shows that this complex is isomorphic to $g\mathrm{CFK}^-(S^3, Q_n^{0,j}(K))$ and so has homology isomorphic to $\mathrm{HFK}^-(S^3, Q_n^{0,j}(K))$ as an $\mathbb{F}[V]$ module. The structure theorem for HFK^- implies that it has a single free $\mathbb{F}[V]$ summand, and the generator of this summand has Alexander grading $\tau(Q_n^{0,j}(K))$ by [OST08, Appendix A]. Therefore, to determine the value of τ of satellites with arbitrary companions, arbitrary framings and patterns $Q^{0,j}$, we will use Theorem 3.8.4 to identify a collection of intersection points, so generators of the complex $\mathrm{CFK}_{\mathbb{F}[U,V]/UV}(S^3, Q_n^{0,j}(K))$, that form a subcomplex with respect to the vertical z-basepoint differentials (when we set $U=0$) and generate the $\mathbb{F}[V]$ free part of the homology of $\mathrm{HFK}^-(S^3, Q_n^{0,j}(K))$. Setting $V=1$ in this complex gives $\widehat{\mathrm{HF}}(S^3)$ and so, said another way, we identify a cycle in $\widehat{\mathrm{HFK}}(S^3, Q_n^{0,j}(K))$ that, in the V-filtration, survives in $\widehat{\mathrm{HF}}(S^3)$.

We will see in the pairing diagram that the form of this subcomplex is completely determined by the piece of the essential component of $\tilde{\alpha}(K,n)$ in the first column of the lifted pairing diagram corresponding to Lemmas

3.8.2 and 3.8.3. Once we identify the cycle that generates the $\mathbb{F}[V]$-free part of the homology (so survives in the spectral sequence to $\widehat{\mathrm{HF}}(S^3)$), it can be extended to be the distinguished element of some vertically simplified basis, as in [Hom14, Section2.3]. Then it is possible to determine $\epsilon(Q_n^{0,j}(K))$ from the horizontal (w-basepoint crossing) differentials. By [Hom14, Definition 3.4 and Lemma 3.2] $\epsilon(K) = 1, -1$ or 0 depending on whether the distinguished element of the vertically simplified basis has a horizontal differential into it, out of it, or neither respectively.

As in Lemmas 3.8.2 and 3.8.3, we distinguish multiples cases for the essential component of $\tilde{\alpha}(K, n)$ depending on $\tau(K)$, $\epsilon(K)$, and n. In each case the form of the pairing diagram, and thus the subcomplex carrying the $\mathbb{F}[V]$ free part of the homology, changes. Moreover, the Alexander grading labels of the arcs of the β curve relative to the central intersection point of the pairing diagram also change. As in the proof of Theorem 3.7.1, there are also multiple sub-cases depending on whether j and n are even or odd. We mostly draw the pairing diagram in the case j is odd, since the pictures are slightly simpler. We analyze the case j even and n odd in Figure 3.70, and leave the rest of the cases where j is even to the reader.

Proof of Theorem 3.7.6. The proof is divided into many cases, first by the value of $\epsilon(K)$, then into whether $\tau(K)$ is positive or negative, and then into various cases of whether or not $n \geqslant 2\tau(K)$ or $n < 2\tau(K)$. The pictures look slightly different when, for example $\tau(K) \geqslant 0$ and either $n \leqslant 0 \leqslant 2\tau(K)$ or $0 \leqslant n \leqslant 2\tau(K)$, so we separately analyze those cases as well.

Case 0 $\epsilon(K) = 0$: In this case it follows that $\tau(K) = 0$ [Hom14], and the essential component of the immersed curve $\alpha(K, n)$ is the same as the immersed curve for the n-framed unknot complement, and so $\tau(Q_n^{0,j}(K)) = \tau(Q_n^{0,j}(U))$. The case $n = 0$ is clear, since $Q_0^{i,j}(U) \sim U$. We indicate the pairing diagrams for the cases $n < 0$ and $n > 0$ in Figures 3.57 and 3.58. In the case that $n < 0$, the intersection points labelled $\{a_k\}_{k=1}^{2m+1}$ form a subcomplex of $\mathrm{CFK}_{\mathbb{F}[V]}(S^3, Q_n^{0,j}(U))$ with respect to the vertical differentials that contains an $\mathbb{F}[V]$ free part. Setting $V = 1$ in the above subcomplex, we see that the cycle $\sum a_{2i+1}$ generates $\widehat{\mathrm{HF}}(S^3)$. Note that the intersection

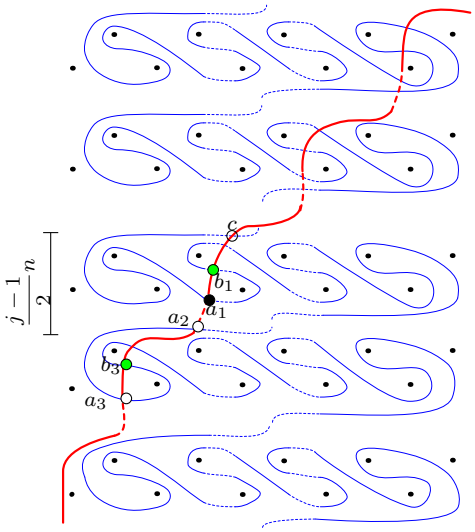

Figure 3.57.
$\epsilon(K) = \tau(K) = 0$ and
$n < 0$

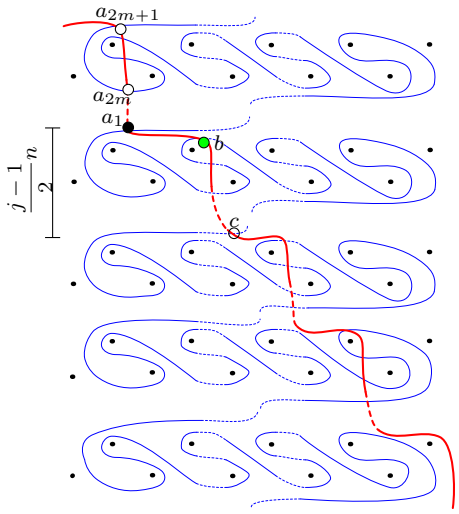

Figure 3.58.
$\epsilon(K) = \tau(K) = 0$ and
$n > 0$

points b_{2i+1} satisfy $\partial^h(\sum b_{2i+1}) = U\sum a_{2i+1}$, so that $\epsilon(Q_n^{0,j}(U)) = 1$ by [Hom14, Section 3]. Recall that $A(\sum a_{2i+1}) = \max\{A(a_{2i+1})\}$, and from this it is easy to see that $\tau(Q_n^{0,j}(U)) = A(a_1)$. Then, $A(a_1) = \ell_{c,a_1} \cdot \delta_{w,z}$, where $\ell_{c,a}$ is the arc of the lifted β curve from c to a by [Che19, Lemma 4.1]. Now as remarked the Alexander grading labels of arcs of the β curve change by $-j$ for each row we go down in the pairing diagram, so we see that $A(a) = \tau(Q_n^{0,j}(U)) = -j\left(\frac{j-1}{2}|n| - 1\right) = \frac{j(j-1)}{2}n + j$

In the case that $n > 0$, The intersection points $\{a_k\}$ form a subcomplex of $\mathrm{CFK}_{\mathbb{F}[V]}(S^3, Q_n^{0,j}(U))$ that contains an $\mathbb{F}[V]$-free part, and we see that the cycle a_1 generates $\widehat{\mathrm{HF}}(S^3)$. Directly from Figure 3.58 we see that the intersection point b satisfies $\partial^h(b) = U^2 a_1$ so $\epsilon(Q_n^{0,j}(U)) = 1$. Furthermore, we have that $A(a_1) = \tau(Q_n^{0,j}(U)) = \frac{j(j-1)}{2}n$.

Case 1 $\epsilon(K) = 1$: In the case $\epsilon(K) = 1$, we first distinguish between the cases $\tau(K)$ positive and negative and then distinguish further between various sub-cases depending on the value of n relative to $\tau(K)$.

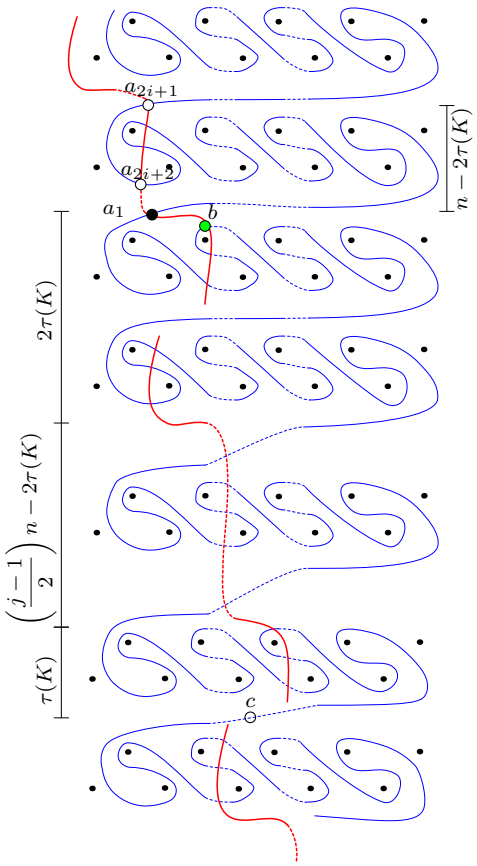

Figure 3.59. The pairing diagram when $\tau(K) \geqslant 0$, $\epsilon(K) = 1$ and $n \geqslant 2\tau(K)$ and j odd

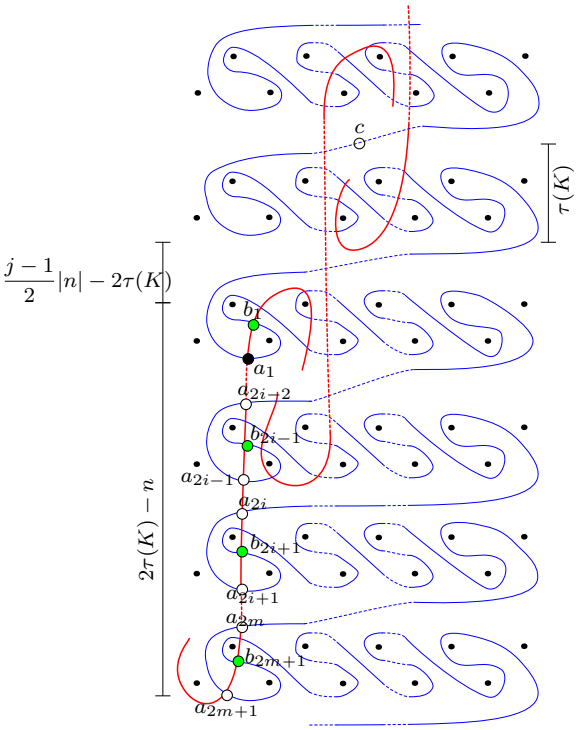

Figure 3.60. The pairing diagram when $\tau(K) > 0$ $\epsilon(K) = 1$ and $n \leqslant 0 < 2\tau(K)$ and j odd

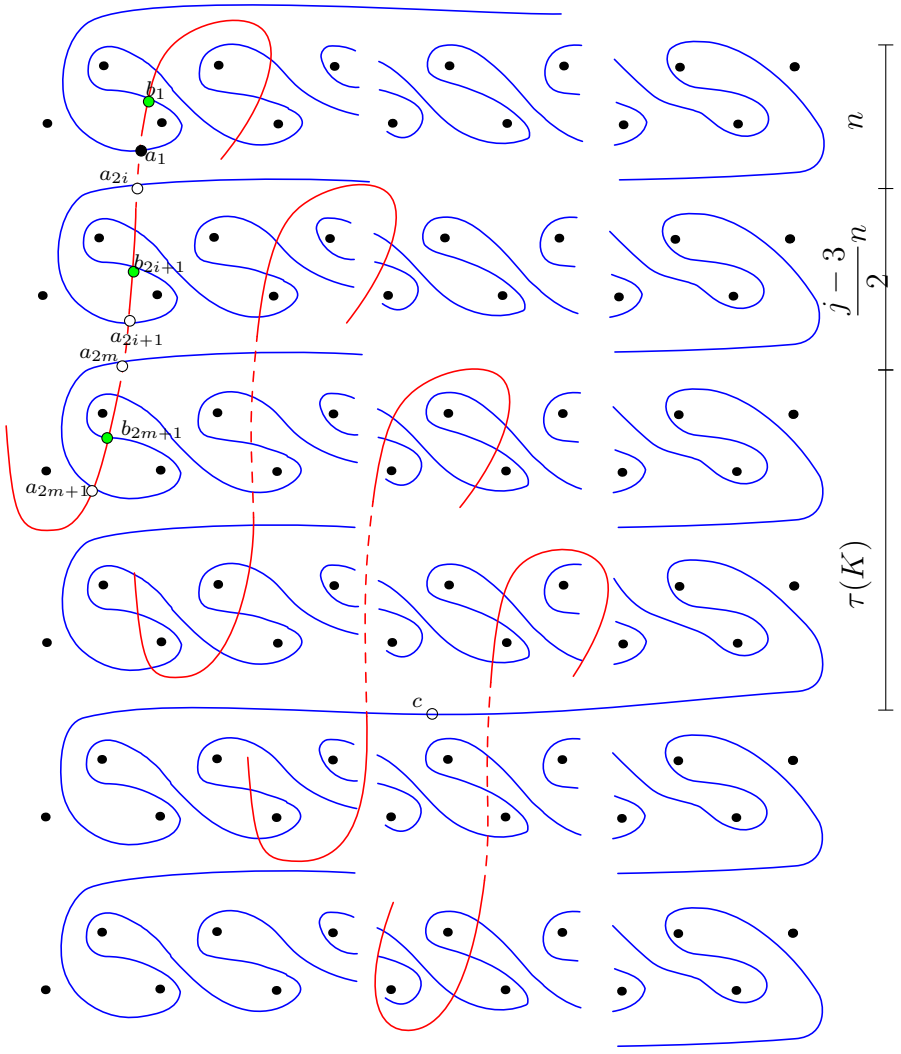

Figure 3.61. Case $\tau(K) > 0$, $\epsilon(K) = 1$ and $0 \leqslant n < 2\tau(K)$ with j odd

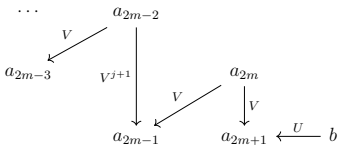

Figure 3.62. Subcomplex carrying the cycle that generates $\widehat{\mathrm{HF}}(S^3)$ together with horizontal differentials from Figures 3.70 and 3.71

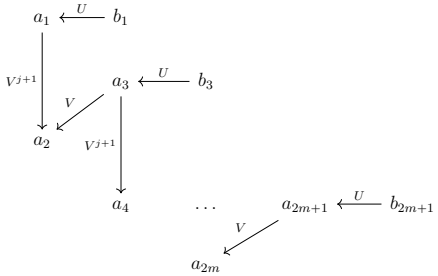

Figure 3.63. Subcomplex carrying cycle that generates $\widehat{\mathrm{HF}}(S^3)$ and horizontal differentials from Figures 3.60, 3.61, and 3.64

Case 1.1a $\tau(K) \geqslant 0$ **and** $n \geqslant 2\tau(K)$: This case is shown in Figure 3.59. In that figure, the intersection points labelled $\{a_k\}_{k=1}^{2m+1}$ form a sub-complex that contains the $\mathbb{F}[V]$-free part of $\mathrm{CFK}_{\mathbb{F}[V]}(S^3, Q_n^{0,j}(K))$ and it is easy to see that the intersection point labelled a_{2m+1} generates $\widehat{\mathrm{HF}}(S^3)$, obtained by setting $V = 1$ in the above sub-complex. Then, the intersection point a_{2m+1} is a distinguished element of some vertically simplified basis of $\mathrm{CFK}^-(K)$. Since the intersection point labelled b satisfies $\partial^h(b) = U^2 a_{2m+1}$, the cycle a_{2m+1} is a boundary with respect to the horizontal differential, so it follows from [Hom14, Section 3] that $\epsilon(Q_n^{0,j}(K)) = 1$. It remains to determine $\tau(Q_n^{0,j}(K)) = A(a_{2m+1})$. By symmetry of the pairing diagram, we see that the intersection point c satisfies $A(c) = 0$, and then by [Che19, Lemma 4.1] $A(a_{2m+1}) = A(a_{2m+1}) - A(c) = \ell_{c,a_{2m+1}} \cdot \delta_{w,z}$. Now, to determine the quantity $\ell_{c,a_{2m+1}} \cdot \delta_{w,z}$ we see in Figure 3.59 that the arc $\ell_{c,a_{2m+1}}$ traverses $\tau(K) + \dfrac{j-1}{2}n$ rows up the pairing diagram, and the Alexander grading changes by j for each row we go up in the pairing diagram. Therefore

$$A(a_{2m+1}) = j\left(\tau(K) + \frac{j-1}{2}n\right) = j\tau(K) + \frac{j(j-1)}{2}n.$$

Case 1.1b $\tau(K) > 0$ **and** $n \leqslant 0 < 2\tau(K)$: This case is shown in Figure

3.60. In the pairing diagram, we can see that the subcomplex generated by the intersection points $\{a_k\}_{k=1}^{2m+1}$ together with the vertical differentials carries the $\mathbb{F}[V]$-free part of the $\mathrm{HFK}^-(S^3, Q_n^{0,j}(K))$. This subcomplex is shown in Figure 3.62 together with the horizontal differentials, and that the cycle $\sum_{k=0}^{m} a_{2k+1}$ survives in $\widehat{\mathrm{HF}}(S^3)$. Then this cycle forms the distinguished element of some vertically simplified basis. Further, we see that for each k, $\partial^h(b_{2k+1}) = Ua_{2k+1}$, so we have $\partial^h(\sum_{k=0}^{m} b_{2k+1}) = U\sum_{k=0}^{m} a_{2k+1}$. Therefore $\epsilon(Q_n^{0,j}(K)) = 1$. Now, it remains to determine $A(a_1) = \tau(Q_n^{0,j}(K))$. By symmetry, $A(c) = 0$ and

$$A(a_1) = A(a_1) - A(c) = \ell_{a_1,c} \cdot \delta_{w,z} = -j\left(\tau(K) + \frac{j-1}{2}|n| - 2\tau(K)\right) + 1,$$

since the Alexander grading changed by $-j$ for each row we go down in the pairing diagram. Simplifying, we see that

$$\tau(Q_n^{0,j}(K)) = j\tau(K) + \frac{j(j-1)}{2}n + 1.$$

Case 1.1c $\tau(K) > 0$ **and** $0 \leqslant n < 2\tau(K)$: This case is shown in Figure 3.61. The analysis here is exactly as in the previous case. The subcomplex $\{a_k\}$ carries the $\mathbb{F}[V]$-free part of the homology $\mathrm{HFK}^-(S^3, Q_n^{0,j}(K))$, and the cycle $\sum_{k=0}^{m} a_{2k+1}$ survives in $\widehat{\mathrm{HF}}(S^3)$, so can be taken to be the distinguished elements of a vertically simplified basis. Further, we have $\partial^h(\sum_{k=0}^{m} b_{2k+1}) = U\sum_{k=0}^{m} a_{2k+1}$, so just like in the previous case it follows that $\epsilon(Q_n^{0,j}(K)) = 1$ It remains to determine $A(a_1)$: Counting the number of rows between a_1 and c in the pairing diagram, we find that

$$\tau(Q_n^{0,j}(K)) = A(a_1) - A(c) = j\left(\tau(K) + \frac{j-1}{2}n\right) + 1 = j\tau(K) + \frac{j(j-1)}{2}n + 1$$

This ends the analysis of the case $\epsilon(K) = 1$ and $\tau(K)$ non-negative. Next, we move on to the case $\epsilon(K) = 1$ and $\tau(K)$ non-positive.

Case 1.2a $\tau(K) \leqslant 0$**,** $\epsilon(K) = 1$ **and** $n < 2\tau(K)$

In this case, the pairing diagram is shown in Figure 3.64. The intersection points labelled $\{a_k\}_{k=1}^{2m+1}$ generate the free part of $\mathrm{CFK}_{\mathbb{F}[V]}(Q_n^{0,j}(K))$, the cycle $\sum_{k=0}^{m} a_{2k+1}$ is the cycle that survives in $\widehat{\mathrm{HF}}(S^3)$, and $\tau(Q_n^{0,j}(K)) =$

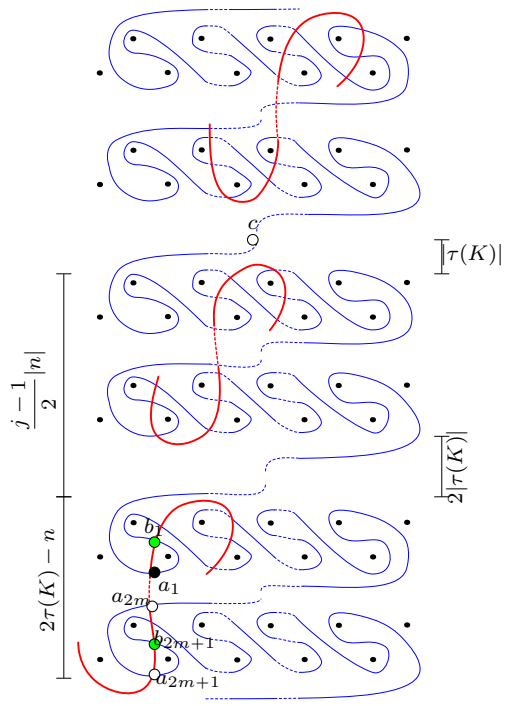

Figure 3.64. $\tau(K) \leqslant 0$ $\epsilon(K) = 1$ and $n \leqslant 2\tau(K)$

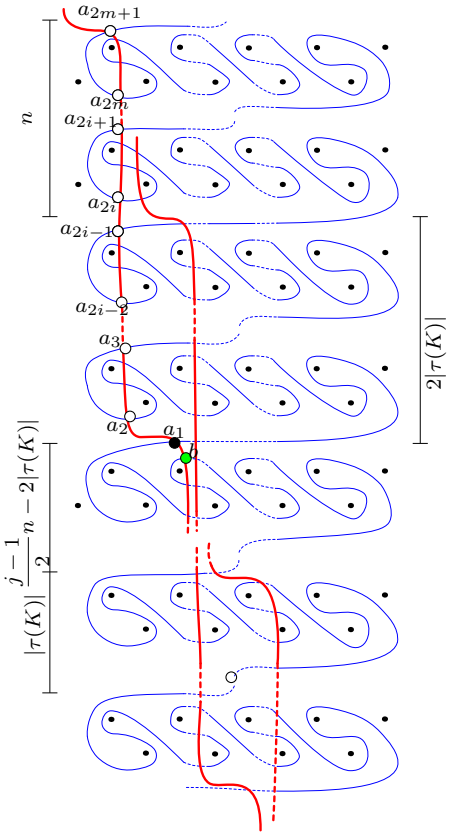

Figure 3.65. $\tau(K) \leqslant 0$ $\epsilon(K) = 1$ and $n \geqslant 0$

$A(a_1)$. The intersection points $\{b_{2k+1}\}_{k=0}^{m}$ satisfy $\partial^h(\sum_{k=0}^{m} b_{2k+1}) = U \sum_{k=0}^{m} a_{2k+1}$, so $\epsilon(Q_n^{0,j}(K)) = 1$. Exactly in the previous cases, we find that

$$\tau(Q_n^{0,j}(K)) = A(a_1) = -j\left(-\tau(K) + \frac{j-1}{2}|n|\right) + 1 = j\tau(K) + \frac{j(j-1)}{2}n + 1$$

Case 1.2b $\tau(K) \leqslant 0$, $\epsilon(K) = 1$ **and** $n \geqslant 0 \geqslant 2\tau(K)$ In this case, the pairing diagram has the form shown in Figure 3.65. In this case the $\mathbb{F}[V]$

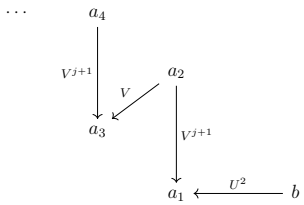

Figure 3.66. Subcomplex carrying the cycle that generates $\widehat{\mathrm{HF}}(S^3)$ corresponding to the cases in Figures 3.59, 3.65, and 3.68

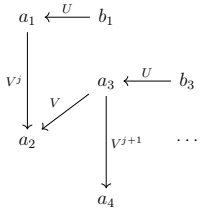

Figure 3.67. Subcomplex carrying cycle that generates $\widehat{\mathrm{HF}}(S^3)$ and horizontal differentials from Figures 3.69 and 3.72

free part of the homology is generated by the intersection points $\{a_k\}_{k=1}^{2m+1}$. Further, the intersection point a_1 generated $\widehat{\mathrm{HF}}(S^3)$. Just as above, the intersection point b satisfies $\partial^h(b) = U^2 a_1$ and hence $\epsilon(Q_n^{0,j}(K)) = 1$. Furthermore $A(a_1) = \tau(Q_n^{0,j}(K))$. Inspecting the pairing diagram we find that

$$A(a_1) - A(c) = j\left(\tau(K) + \frac{j-1}{2}n\right) = j\tau(K) + \frac{j(j-1)}{2}n$$

Case 1.2c $\tau(K) \leqslant 0$**,** $\epsilon(K) = 1$ **and** $0 \geqslant n \geqslant 2\tau(K)$ The pairing diagram for this case is shown in Figure 3.68. The intersection points $\{a_k\}_{k=0}^{2m+1}$ generate the free part of the homology, and the intersection point a_1 generates $\widehat{\mathrm{HF}}(S^3)$. In the pairing diagram, the intersection point labelled b satisfied $\partial^h(b) = U^2 a_1$, so $\epsilon(Q_n^{0,j}(K)) = 1$. Further, we compute

$$\tau(Q_n^{0,j}(K)) = A(a_1) = -j\left(|\tau(K)| + \frac{j-1}{2}|n|\right) = j\tau(K) + \frac{j(j-1)}{2}n$$

That finishes the cases where $\epsilon(K) = 1$.

Case 2 $\epsilon(K) = -1$: As in the case $\epsilon(K) = 1$, we distinguish between various sub-cases depending on the sign of $\tau(K)$ and the value of n relative to $2\tau(K)$

Case 2.1a $\tau(K) \geqslant 0$**,** $\epsilon(K) = -1$ **and** $n \leqslant 0 < 2\tau(K)$

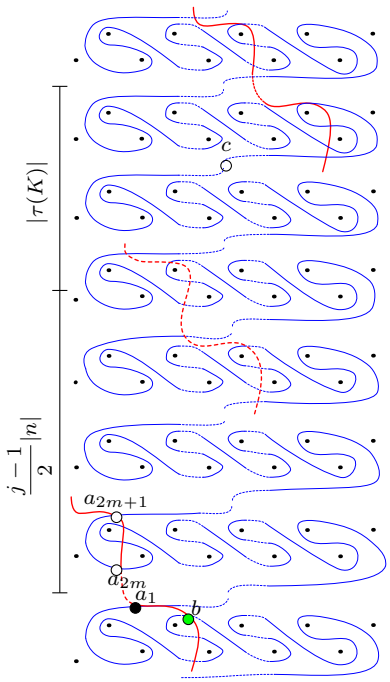

Figure 3.68. The pairing diagram when $\tau(K) < 0$ $\epsilon(K) = 1$ and $0 > n > 2\tau(K)$

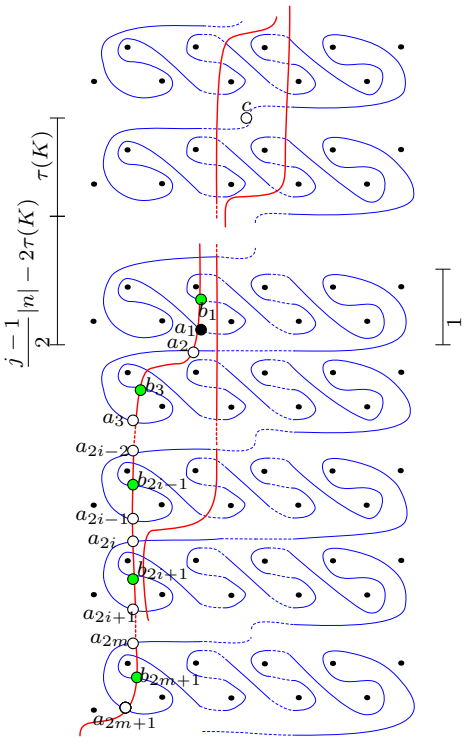

Figure 3.69. The pairing diagram when $\tau(K) > 0$ $\epsilon(K) = -1$ and $n < 0 < 2\tau(K)$ and j odd

This case is shown in Figure 3.69. The intersection points $\{a_k\}_{k=1}^{2m+1}$ generate a subcomplex with respect to the vertical differentials and carries the $\mathbb{F}[V]$-free part of the homology of $\mathrm{CFK}_{\mathbb{F}[V]}(S^3, Q_n^{0,j}(K))$. Setting $V = 1$ we see that the cycle $\sum_{k=0}^{m} a_{2k+1}$ generates $\widehat{\mathrm{HF}}(S^3)$. The intersection points $\{b_{2k+1}\}_{k=0}^{m}$ satisfy $\partial^h(\sum_{k=0}^{m} b_{2k+1}) = U(\sum_{k=0}^{m} a_{2k+1})$, so $\epsilon(Q_n^{0,j}(K)) = 1$. We determine $\tau(Q_n^{0,j}(K)) = A(a_1)$ from the pairing diagram and find

$$A(a_1) = -j\left(\tau(K) + \frac{j-1}{2}|n| - 2\tau(K) - 1\right) = j(\tau(K)+1) + \frac{j(j-1)}{2}n$$

Note: The case $\tau(K) > 0$, $\epsilon(K) = -1$ and $0 < n < 2\tau(K)$ is similar and left to the reader.

Case 2.1b $\tau(K) \geqslant 0$**,** $\epsilon(K) = -1$ **and** $n \geqslant 2\tau(K)$

This case is shown in Figure 3.71. In this case subcomplex generated by the intersection points $\{a_k\}$ generate the $\mathbb{F}[V]$-free part of the homology. We see that the intersection point labelled a_1 generates $\widehat{\mathrm{HF}}(S^3)$ and that $\partial^h(b) = Ua_1$. Therefore $\epsilon(Q_n^{0,j}(K)) = 1$. Now, it is easy to see from the pairing diagram that $A(a_1) = A(a_3)$, and

$$\tau(Q_n^{0,j}(K)) = A(a_1) = j\left(\tau(K) + \frac{j-1}{2}n + 1\right) = j(\tau(K)+1) + \frac{j(j-1)}{2}n$$

Case 2.2a $\tau(K) \leqslant 0$**,** $\epsilon(K) = -1$ **and** $n \geqslant 0 \geqslant 2\tau(K)$ This case is shown in Figure 3.70 where the intersection points $\{a_k\}$ form a subcomplex that carries the $\mathbb{F}[V]$-free part of the homology, and the cycle a_{2m+1} generates $\widehat{\mathrm{HF}}(S^3)$. Considering disks that cross the w-basepoint, we see that $\partial^h(b) = Ua_{2m+1}$ and so $\epsilon(Q_n^{0,j}(K)) = 1$. It remains to determine $\tau(Q_n^{0,j}(K)) = A(a_{2m+1}$. This is similar to the previous cases, but we point out what happens in the case when j is even and n is odd. In this case the central intersection point c with $A(c) = 0$ is shown in Figure 3.70. Since j is even, the central intersection point occurs along the unstable chain, as in the proof of Theorem 3.7.1. Just as in the previous cases, we find that

$$A(a_{2m+1}) - A(c) = j\left(\frac{n-1}{2} - \tau(K) + (\frac{j}{2} - 2\right)n + n + 2\tau(K) + 1) + \frac{j}{2}$$

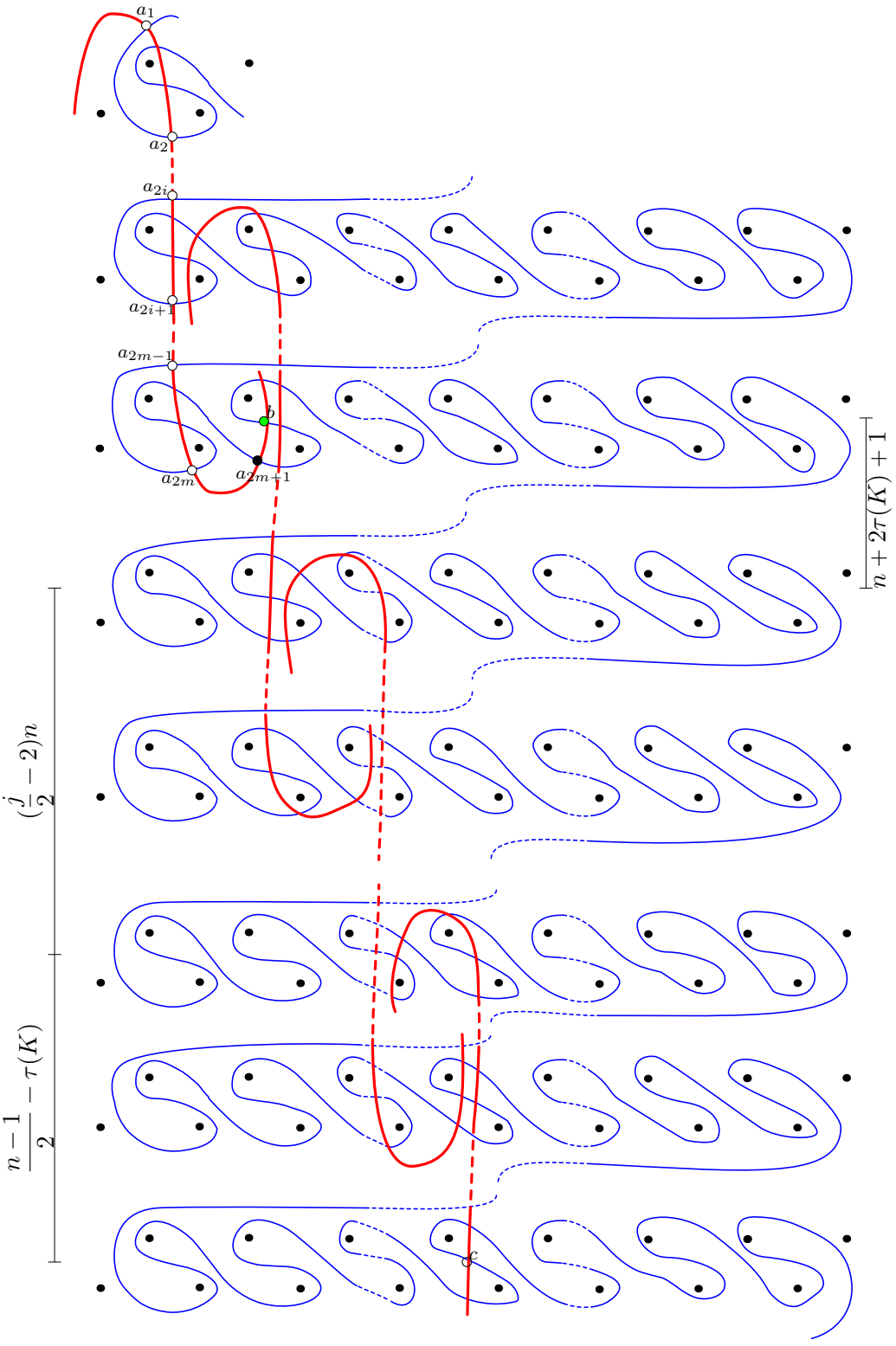

Figure 3.70. Case $\tau(K) < 0$, $\epsilon(K) = -1$ and $n > 0 > 2\tau(K)$ with j even

Simplifying, we see that

$$\tau(Q_n^{0,j}(K)) = A(a_{2m+1}) = j(\tau(K)+1) + \frac{j(j-1)}{2}n.$$

Case $\tau(K) \leqslant 0$ $\epsilon(K) = -1$ **and** $0 > n > 2\tau(K)$
This case is similar to the previous cases and is left to the reader.

Case $\tau(K) \leqslant 0$ $\epsilon(K) = -1$ **and** $n \leqslant 2\tau(K)$ The pairing diagram for this case is shown in Figure 3.72. In that figure we see that the intersection points labelled $\{a_k\}$ generate the free part of the homology of $\widehat{\mathrm{CFK}}_{\mathbb{F}[V]}(S^3, Q_n^{0,j}(K))$ and when we set $V = 1$ the cycle $\sum_{k=0}^{m} a_{2k+1}$ generates $\widehat{\mathrm{HF}}(S^3)$. The intersection points $\{b_{2k+1}\}$ are such that $\partial^h(\sum_k b_{2k+1}) = U\sum_{k=0}^{m} a_{2k+1}$, so $\epsilon(Q_n^{0,j}(K)) = 1$. It remains to determine $\tau(Q_n^{0,j}(K)) = A(a_1)$. Inspecting the pairing diagram, we find that

$$\tau(Q_n^{0,j}(K)) = j(\tau(K)+1) + \frac{j(j-1)}{2}n$$

□

Lemma 3.11.1. *For any $j \in \mathbb{Z}_{>0}$, $n \in \mathbb{Z}$ and $i \in \mathbb{Z}_{\geqslant 0}$,*

$$\tau(Q_n^{i,j}(K)) = \tau(Q_n^{0,j}(K))$$

Proof. Inspection of the pairing diagram shows that the intersection points that form a subcomplex of $\mathrm{CFK}_{\mathbb{F}[V]}(S^3, Q_n^{i,j}(K))$ that generates the $\mathbb{F}[V]$ free part of the homology is independent of i. That is, twisting up the β curve does not change the subcomplex under consideration and as remarked before, does not change the Alexander gradings of the previously existing intersection points. See Figures 3.73 and 3.74. In particular in all cases the cycle that survives to $\widehat{\mathrm{HF}}(S^3)$ and the Alexander grading of that cycle is independent of i. □

Lemma 3.11.2. *For any $j \in \mathbb{Z}_{>0}$, $n \in \mathbb{Z}$ and $i \in \mathbb{Z}_{\geqslant 0}$,*

$$\epsilon(Q_n^{i,j}(K)) = \epsilon(Q_n^{0,j}(K)).$$

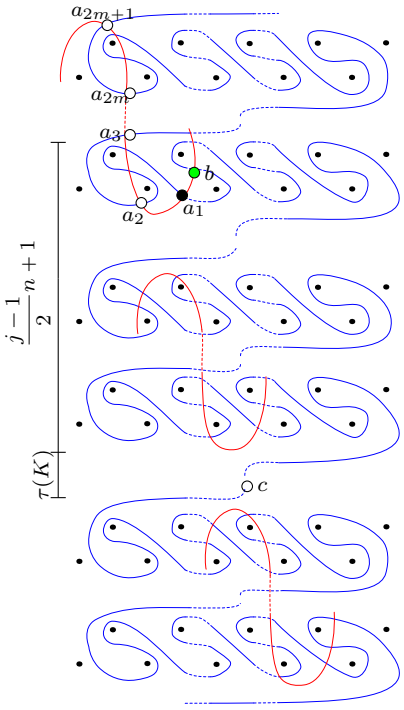

Figure 3.71. The pairing diagram when $\tau(K) > 0$ $\epsilon(K) = -1$ and $n \geqslant 2\tau(K)$ and j odd

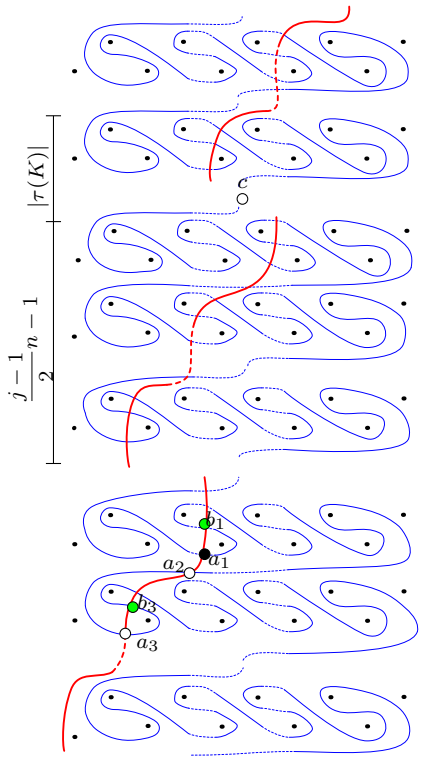

Figure 3.72. $\tau(K) < 0$ $\epsilon(K) = -1$ and $n \leqslant 2\tau(K)$

Proof. There are a few cases depending on the shape of essentail component of the curve $\alpha(K, n)$, but the proof is essentially local in nature so we only indicate the local modification to the complex. Consider the case when the intersection point with Alexander grading $\tau(Q_n^{i,j}(K))$ and the vertical subcomplex nearby this intersection point has the form shown in figures 3.75 and 3.76. For example this covers the cases when $\tau(K) \geqslant 0$ and $\epsilon(K) = 1$ and $n \leqslant 2\tau(K)$ and $\tau(K) \leqslant 0$, $\epsilon = 1$ and $n \leqslant 2\tau(K)$. When we twist the β curve up once, notice that there are now two intersection points b and b' with a horizontal differential to a. However, this does not change the com-

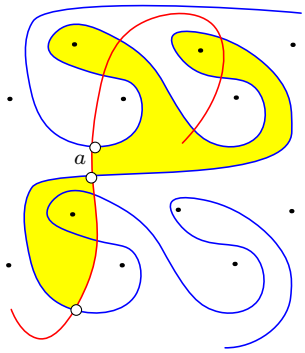

Figure 3.73. The subcomplex that carries the $\mathbb{F}[V]$-free part of the homology before twisting

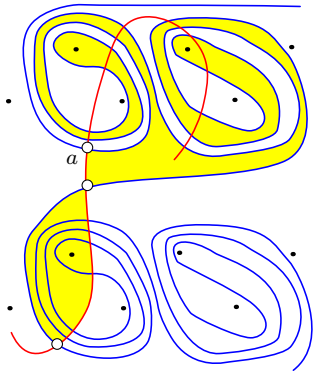

Figure 3.74. The subcomplex that carries the $\mathbb{F}[V]$-free part of the homology after twisting

putation of ϵ, since we can perform a change of basis, letting $b_1 = b$ and $b_2 = b + b'$. Then $\partial^h(b_1) = a$ and $\partial^h(b_2) = 0$. We see from figures 3.77 and 3.78 that this pattern continues for each addition twist we add to the lifted β curve.

□

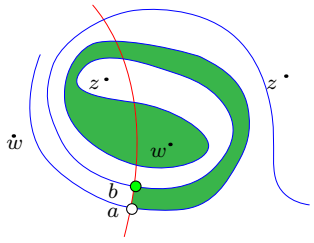

Figure 3.75. A horizontal differential to the intersection point that survives the spectral sequence to $\widehat{\mathrm{HF}}(S^3)$ when $i = 1$

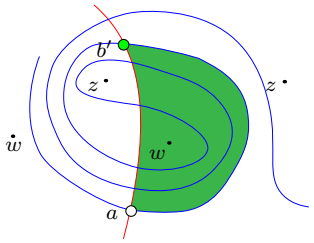

Figure 3.76. Another horizontal differential to the intersection point that survives the spectral sequence to $\widehat{\mathrm{HF}}(S^3)$ when $i = 1$

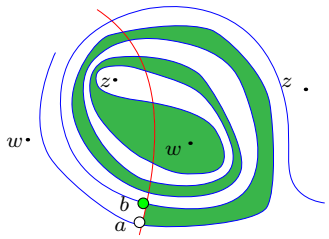

Figure 3.77. A horizontal differential to the intersection point that survives the spectral sequence to $\widehat{\mathrm{HF}}(S^3)$ when $i > 1$

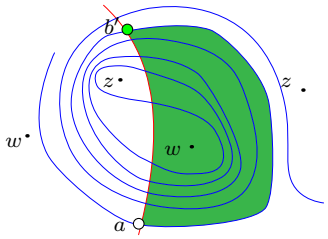

Figure 3.78. Another horizontal differential to the intersection point that survives the spectral sequence to $\widehat{\mathrm{HF}}(S^3)$ when $i > 1$

CHAPTER 4

KHOVANOV STABLE HOMOTOPY TYPE AND RIBBON CONCORDANCE

4.1 Introduction

This chapter contains previously published material. In 2014, Lipshitz and Sarkar introduced a stable homotopy refinement of Khovanov homology [LS14a]. For each fixed j it takes the form of a suspension spectrum $\mathcal{X}^j$. The cohomology $H^*(\mathcal{X}^j)$ of this spectrum is isomorphic to the Khovanov homology $\mathrm{Kh}^{*,j}$. In subsequent work (e.g. [LS14c]) they used this refinement to define stable cohomology operations on Khovanov homology. This lead to a refinement of Rasmussen's s-invariant for each nontrivial cohomology operation, and in particular for the Steenrod squares [LS14c]. In this short note we offer a solution to the following question posed in Lipshitz-Sarkar [LS18, Question 3]: Are there prime knots with arbitrarily high Steenrod squares on their Khovanov homology? Explicitly, we prove the following theorem:

Theorem 4.1.1. *Given any n, there exists a prime knot P_n so that the operation*

$$\mathrm{Sq}^n : \widetilde{\mathrm{Kh}}^{i,j}(P_n) \to \widetilde{\mathrm{Kh}}^{i+n,j}(P_n)$$

is nontrivial for some (i,j). Here $\widetilde{\mathrm{Kh}}$ denotes reduced Khovanov homology.

Corollary 4.1.2. *Given any n, there exists a prime knot P_n so that the operation*

$$\mathrm{Sq}^n : \mathrm{Kh}^{i,j}(P_n) \to \mathrm{Kh}^{i+n,j}(P_n)$$

is nontrivial, on unreduced Khovanov homology, for some (i,j).

In fact a stronger version of Theorem 4.1.1 is true:

Theorem 4.1.3. *Given any n, there exists a hyperbolic knot H_n so that the operation*

$$\mathrm{Sq}^n : \widetilde{\mathrm{Kh}}^{i,j}(H_n) \to \widetilde{\mathrm{Kh}}^{i+n,j}(H_n)$$

is nontrivial for some (i,j). Here $\widetilde{\mathrm{Kh}}$ denotes reduced Khovanov homology.

Theorem 4.1.4. *Given any n, there exists a prime satellite knot S_n so that the operation*

$$\mathrm{Sq}^n : \widetilde{\mathrm{Kh}}^{i,j}(S_n) \to \widetilde{\mathrm{Kh}}^{i+n,j}(S_n)$$

is nontrivial for some (i,j). Here $\widetilde{\mathrm{Kh}}$ denotes reduced Khovanov homology.

Our technique for proving all of the above theorems is to find a ribbon concordance from any given knot K to a prime, hyperbolic or satellite knot, then appeal to the following generalization to reduced Khovanov homology of a theorem of Wilson and Levine-Zemke (for the original statement see [Wil12; LZ19] or Theorem 4.2.2 below).

Theorem 4.1.5. *Suppose C is a ribbon concordance between knots K and K'. Then the induced map $F_C : \widetilde{\mathrm{Kh}}(K) \to \widetilde{\mathrm{Kh}}(K')$ is injective.*

Recall that any prime knot K is either a hyperbolic knot, a satellite knot, or a torus knot. With this in mind, Theorems 4.1.1—4.1.4 suggest the following question:

Question: For any given n, is there a torus knot T_n so that $\mathrm{Sq}^n : \widetilde{\mathrm{Kh}}^{i,j}(T_n) \to \widetilde{\mathrm{Kh}}^{i+n,j}(T_n)$ is nontrivial for some (i,j)?

The organization of the chapter is the following. In Section 4.2, we review the results of Wilson and Levine and Zemke [Wil12; LZ19] showing that ribbon concordances induce split injections on Khovanov homology. In Section 4.3, we prove the analogue of this theorem for reduced Khovanov homology. In Section 4.4, we show that any knot is ribbon concordant to a prime knot, following the arguments in [Lic81; KL79]. In Section 4.5, we collect various results about the naturality of Steenrod squares with respect to births, Reidemeister moves and saddle maps and the behavior of the Khovanov stable homotopy type under connected sums. In Section 4.6 we show that the nontriviality of Steenrod squares on composite knots constructed by Lipshitz-Sarkar [LLS15, Corollary 1.4] and [LS18, Corollary 3.1] propagates to the nontriviality of Steenrod squares on the Khovanov homology of prime knots. In Section 4.7 we prove Theorem 4.1.3 using results of Silver and Whitten [SW05]. In Section 4.8 we prove Theorem 4.1.4 using results of Livingston [Liv81].

Acknowledgements The author would like to thank his advisor Robert Lipshitz, as well as Danny Ruberman for pointing out Theorem 4.1.3, Chuck Livingston for pointing out his construction of ribbon concordances to prime knots that leads to Theorem 4.1.4, and the anonymous referee for their careful reading that improved the exposition.

4.2 Khovanov Homology and Ribbon Concordances

In this section we review the behavior of Khovanov homology under ribbon concordances. Unless explicitly stated otherwise, throughout this paper we write $\mathrm{Kh}(K)$ to mean $\mathrm{Kh}(K;\mathbb{F}_2)$.

Definition 4.2.1. *let K_0 and K_1 be links in S^3. A* concordance *from K_0 to K_1 is a smoothly embedded cylinder in $[0,1]\times S^3$ with boundary $-(\{0\}\times K_0)\cup(\{1\}\times K_1)$. A concordance C is said to be* ribbon *if C has only index 0 and 1 critical points with respect to the projection $[0,1]\times S^3\to[0,1]$.*

Throughout this paper, we will use the notation $\overline{C}$ to denote the ribbon concordance C upside-down.

Theorem 4.2.2. *[Wil12; LZ19] If C is a ribbon concordance from K_0 to K_1, then the induced map*

$$\mathrm{Kh}(C):\mathrm{Kh}(K_0)\to\mathrm{Kh}(K_1)$$

is injective, with left inverse $\mathrm{Kh}(\overline{C})$. In particular, for any bigrading (i,j) the group $\mathrm{Kh}^{i,j}(K_0)$ is a direct summand of the group $\mathrm{Kh}^{i,j}(K_1)$.

The proof of this theorem involves decomposing the cobordism $D:=\overline{C}\circ C$ as the disjoint union of the identity cobordism (a cylinder) and sphere components joined to the cylinder by tubes (formed from the ribbons and their duals). For details, see [LZ19] or [Wil12]. In the next section, we present an analogue of Theorem 4.2.2 for reduced Khovanov homology, after reviewing the necessary definitions.

4.3 The Base-point action and Reduced Khovanov Homology

We begin with the definition of the base-point action on Khovanov homology. For grading conventions, see [Shu14].

Definition 4.3.1. *Fix a diagram of the knot K and pick a base-point $q \in K$ not on any of the crossings. Then we make the Khovanov complex $C_{\mathrm{Kh}}(K)$ of K into a module over $\mathbb{F}_2[X]/X^2$ as follows. Generators of the chain groups are complete resolutions of K and a choice of 1 or X for each component of the complete resolution. Multiplication by X is zero if the generator labels the circle containing q with an X and if the generator labels the circle containing q by 1 it changes the label of the circle to X. With our grading conventions (see [Shu14]), multiplication by X has bidegree $(0,-2)$. That is*

$$X : \mathrm{Kh}^{i,j}(K) \to \mathrm{Kh}^{i,j-2}(K).$$

Definition 4.3.2. *Let $\mathbb{F}$ be the $\mathbb{F}_2[X]/X^2$ module $\mathbb{F}_2$ where X acts trivially. Then define*

$$\widetilde{C}_{\mathrm{Kh}}(K) := C_{\mathrm{Kh}}(K) \otimes_{\mathbb{F}_2[X]/X^2} \mathbb{F}.$$

The homology of the complex $\widetilde{C}_{\mathrm{Kh}}(K)$ is called reduced Khovanov homology *and denoted $\widetilde{\mathrm{Kh}}(K)$.*

Theorem 4.3.3. *[Shu14, Corollaries 3.2.B and 3.2.C] The action of X on $C_{\mathrm{Kh}}(K)$ commutes with the Khovanov differential, so induces a map (also called X) on homology. Further,*

1. *The following sequence is exact:*

$$\cdots \xrightarrow{X} \mathrm{Kh}^{i,j+2}(K) \xrightarrow{X} \mathrm{Kh}^{i,j}(K) \xrightarrow{X} \mathrm{Kh}^{i,j-2}(K) \xrightarrow{X} \cdots$$

2. *The reduced Khovanov homology over $\mathbb{F}_2$ is isomorphic to the kernel of X (which is the image of X by part 1), and we have the direct sum decomposition*

$$\mathrm{Kh}^{i,j}(K) \cong \widetilde{\mathrm{Kh}}^{i,j-1}(K) \oplus \widetilde{\mathrm{Kh}}^{i,j+1}(K).$$

With these preliminaries in mind, we prove Theorem 4.1.5 from the introduction.

Proof of Theorem 4.1.5. By Theorem 4.2.2 we know that the map $F_C : \mathrm{Kh}(K_0) \to \mathrm{Kh}(K_1)$ is a split injection with left inverse $F_{\overline{C}}$. By Theorem 4.3.3, for $a \in \{0, 1\}$,

$$\widetilde{\mathrm{Kh}}(K_a) \cong \mathrm{Ker}(X : \mathrm{Kh}(K_a) \to \mathrm{Kh}(K_a)) \cong \mathrm{Im}(X : \mathrm{Kh}(K_a) \to \mathrm{Kh}(K_a)).$$

Therefore, it is enough to show that the map F_C is a $\mathbb{F}_2[X]/X^2$ module map. Indeed, then $F_C|_{\mathrm{Ker}}$ maps $\mathrm{Ker}(X : \mathrm{Kh}(K_0) \to \mathrm{Kh}(K_0))$ to $\mathrm{Ker}(X : \mathrm{Kh}(K_1) \to \mathrm{Kh}(K_1))$ and $F_{\overline{C}}|_{\mathrm{Ker}}$ maps $\mathrm{Ker}(X : \mathrm{Kh}(K_1) \to \mathrm{Kh}(K_1))$ to $\mathrm{Ker}(X : \mathrm{Kh}(K_0) \to \mathrm{Kh}(K_0))$. Further, $F_{\overline{C}}|_{\mathrm{Ker}} \circ F_C|_{\mathrm{Ker}} = id|_{\mathrm{Ker}}$. Therefore $F_C|_{\mathrm{Ker}}$ is a split injection.
Now, any cobordism can be decomposed into births (0-handles) and saddle moves (1-handle attachments) and deaths (2-handles). So, to show that the maps induced on Khovanov homology by cobordisms respect the X action, it suffices to verify the following.

1. Births and deaths respect the module structure with respect to a base-point not on the circle dying or being born.

2. The isomorphisms of Khovanov homology associated to Reidemeister moves respect the module structure.

3. The maps associated with saddles respect the module structure.

Item 1 is clear from the definition of the X action, provided we chose a base-point on the original knot diagram, away from where the births and deaths occur.
Item 2 follows from Proposition 2.2 of Hedden-Ni [HN13]. Evidently, the homotopy equivalences induced from Reidemeister moves commute with the

X action if the Reidemeister moves does not involve a strand moving across a base-point. Therefore it suffices to show that moving a strand across the base-point does not change the action of X on homology. This follows by writing down an explicit chain homotopy between the different base-point actions associated with choosing two marked points, on the same component, on opposite sides of a crossing. These homotopy equivalences appear in [HN13, Lemma 2.3].

Item 3 reduces to a local calculation in a complete resolution. Either the saddle cobordism merges two components, or splits one component into two. In either case, it is easy to check that the maps involved commute with the X action. □

4.4 Knots and Prime Tangles

The main theorem of this section is the following:

Theorem 4.4.1. *[Lic81; KL79] Any knot is ribbon concordant to a prime knot.*

The proof of this theorem is standard and is well explained elsewhere in the literature. We include a review of the techniques used in the proof for the convenience of the reader and to introduce some notation. We begin with a definition and a convention [Lic81; KL79; Ble82].

Definition 4.4.2. *A (4-ended)* tangle *with no closed components is an embedding of* $[0,1] \sqcup [0,1]$ *into* B^3 *so that* $\{0,1\} \cup \{0,1\}$ *map to* $S^2 = \partial B^3$. *We specify a tangle by a diagram, see Figure 4.3. We denote such a tangle by* (B,T) *or just* T. *A tangle* (B,T) *is* prime *if both of the following conditions hold:*

1. *Any 2-sphere embedded in* B *that intersects the knot transversely at two points bounds on one side a three ball* A *so that* $A \cap T$ *is homeomorphic to the standard ball arc pair* $(D^2 \times [0,1], 0 \times [0,1])$.

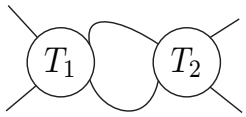

Figure 4.1. $T_1 +_p T_2$

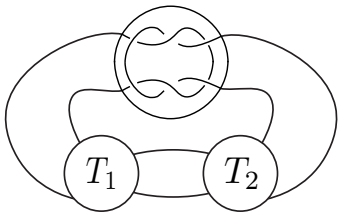

Figure 4.2. $(T_1 +_p T_2) + Cl$

2. *(B, T) is not a rational tangle. Equivalently, (B, T) does not contain any separating disks.*

One motivation for the name prime tangle and illustration of their use is indicated by the following:

Theorem 4.4.3. *[Lic81, Lemmas 1, 2] The sum of two prime tangles is a prime knot. The partial sum of two prime tangles is a prime tangle.*

For the proof, see [Lic81]. In this paper, we use the notation $+_p$ for the partial sum of two tangles and the notation $T_1 + T_2$ for the sum of two tangles. These operations depend on a choice of which endpoints are identified. In the present work, the operations $+_p$ and $+$ mean the operations in Figures 4.1 and 4.2 respectively. For our purposes, we make this explicit as follows. Let NW, NE, SW, SE denote the northwest, northeast, etc corners of the diagram of a tangle T. Then $T_1 +_p T_2$ means the tangle formed by joining the NE and SE corners of T_1 to the NW and SW corners of T_2 respectively by unknotted arcs. Further, $T_1 + T_2$ means the tangle formed from T_1 and T_2 by joining the NE corner of T_1 with the SE corner of T_2, the SE corner of T_1 with the NE corner of T_2, etc. See Figure 4.2, which shows $(T_1 +_p T_2) + Cl$. Note that, even though we use the $+$ sign to denote the tangle sum operation, it is usually not commutative.

Lemma 4.4.4 (See [KL79], [Ble82])**.** *For any nontrivial knot K in S^3 there is an embedded S^2 meeting K transversely in four points separating S^3 into two three balls A and B so that*

1. *$(A, A \cap K)$ is a trivial two-stranded tangle (so homeomorphic, as pairs, to $(D^2 \times I, \{(-1/2, 0)\} \times I \cup \{(1/2, 0)\} \times I))$, and*

2. *$(B, B \cap K)$ is a prime tangle.*

Lemma 4.4.5. *The clasp tangle Cl is a prime tangle.*

Proof. Since each of the individual strings that compose the clasp tangle are unknotted, condition 1 in the definition of a prime tangle is automatically satisfied. We just need to verify that the clasp is not a rational tangle. Suppose for the sake of contradiction that it is. Recall that a knot built out of two rational tangles is a two-bridge knot. It is a classical fact (originally proved by Schubert, see J. Schultens [Sch03] for a modern proof) that the bridge number of a knot, $b(K)$, satisfies $b(K\#K') = b(K) + b(K') - 1$. Further, the only knot with bridge number 1 is the unknot. These two facts together imply that two-bridge knots are prime. However, the numerator closure of the clasp tangle is clearly a connected sum $3_1\#m(3_1)$. □

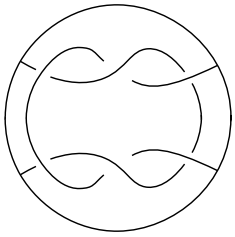

Figure 4.3. The clasp tangle Cl

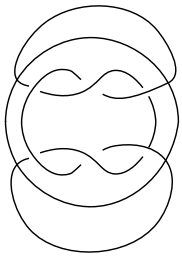

Figure 4.4. The numerator closure of the clasp tangle

Proof of Theorem 4.4.1. Since any knot can be decomposed as a connected sum of prime knots, and connected sum is compatible with concordance, it suffices to prove the result for a knot $K = K_1\#K_2$ where K_i are prime. By Lemma 4.4.4, we can find two disjoint three balls B_1 and B_2 so that $T_i = B_i \cap K_i$ is a prime tangle and $(S^3 \backslash B_i) \cap K_i$ is an untangle. Now, consider $T_1 +_p T_2$. This tangle is prime by Theorem 4.4.3. The denominator closure

of the resulting tangle is $K_1 \# K_2$. The tangle sum $(T_1 +_p T_2) + Cl$ is then a prime knot by Theorem 4.4.3. The ribbon concordance, shown in Figure 4.7—Figure 4.10, between $K_1 \# K_2$ and $(T_1 +_p T_2) + Cl$ establishes the result. □

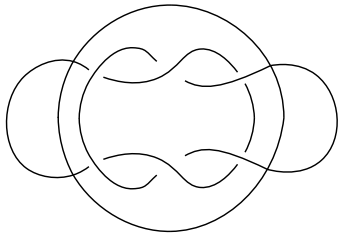

Figure 4.5. Denominator closure of the clasp tangle

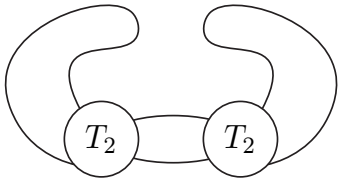

Figure 4.6. Denominator closure of $T_2 +_p T_2$

4.5 Steenrod Operations and Stable Homotopy Type

In this section we review, in bare bones fashion, the necessary facts about Khovanov stable homotopy type needed in establishing Theorem 4.1.1.

We begin with a theorem, which explains how the Khovanov stable homotopy type behaves under the operation of connected sum. Throughout this section, let L denote a link of one or more components.

Theorem 4.5.1. *[LLS15, Theorem 2]*

$$\widetilde{\mathcal{X}}^j_{\mathrm{Kh}}(L_1 \# L_2) \simeq \bigvee_{j_1+j_2=j} \widetilde{\mathcal{X}}^{j_1}(L_1) \wedge \widetilde{\mathcal{X}}^{j_2}(L_2).$$

Next, we recall the precise naturality statement enjoyed by stable cohomology operations.

Theorem 4.5.2. *[LS14b, Theorem 4] Let S be a smooth cobordism in $[0,1] \times S^3$ from L_1 to L_2, and let $F_S : \mathrm{Kh}^{*,*}(L_1) \to \mathrm{Kh}^{*,*+\chi(S)}(L_2)$ be the map associated to S. Let $\alpha : \widetilde{H}^*(\cdot;\mathbb{F}) \to \widetilde{H}^{*+n}(\cdot;\mathbb{F})$ be a stable cohomology operation. Then the following diagram commutes up to sign:*

$$\begin{array}{ccc} \mathrm{Kh}^{i,j}(L_1;\mathbb{F}) & \xrightarrow{\alpha} & \mathrm{Kh}^{i+n,j}(L_1;\mathbb{F}) \\ \downarrow{\scriptstyle F_S} & & \downarrow{\scriptstyle F_S} \\ \mathrm{Kh}^{i,j+\chi(S)}(L_2;\mathbb{F}) & \xrightarrow{\alpha} & \mathrm{Kh}^{i+n,j+\chi(S)}(L_2;\mathbb{F}). \end{array}$$

Then, for α a stable cohomology operation, the following diagram commutes:

$$\begin{array}{ccc} \mathrm{Kh}(U \sqcup K;\mathbb{F}_2) & \xrightarrow{\alpha} & \mathrm{Kh}(U \sqcup K;\mathbb{F}_2) \\ \downarrow{\scriptstyle \cong} & & \downarrow{\scriptstyle \cong} \\ \mathbb{F}_2[X]/X^2 \otimes \mathrm{Kh}(K;\mathbb{F}_2) & \xrightarrow{Id\otimes\alpha} & \mathbb{F}_2[X]/X^2 \otimes \mathrm{Kh}(K;\mathbb{F}_2) \\ \downarrow{\scriptstyle m} & & \downarrow{\scriptstyle m} \\ \mathrm{Kh}(K;\mathbb{F}_2) & \xrightarrow{\alpha} & \mathrm{Kh}(K;\mathbb{F}_2). \end{array}$$

The bottom square commutes by Theorem 9, since the X action on Kh can also be viewed as induced from a merge cobordism $U \sqcup K \to K$ where the unknot is placed near the basepoint. The top square commutes since the Khovanov spectrum of the unknot is homotopy equivalent to a wedge of two S^0's in grading -1 and 1. This homotopy equivalence induces the map in cohomology that identifies $\mathbb{F}_2[X]/X^2 \otimes \mathrm{Kh}(K;\mathbb{F}_2)$ with $\mathrm{Kh}(K;\mathbb{F}_2) \oplus \mathrm{Kh}(K;\mathbb{F}_2)$ with appropriate grading shifts.

Commutativity of the above diagram is the statement that any stable cohomology operation is a map of $\mathbb{F}_2[X]/X^2$ modules. It follows that the analogous diagram to the one in Theorem 4.5.2, with Khovanov homology replaced by reduced Khovanov homology commutes, commutes.

Lemma 4.5.3. *[LLS15, Corollary 1.4] For any n there is a knot K_n so that the operations*

$$\mathrm{Sq}^n : \widetilde{\mathrm{Kh}}^{i,j}(K_n) \to \widetilde{\mathrm{Kh}}^{i+n,j}(K_n)$$

and

$$\mathrm{Sq}^n : \mathrm{Kh}^{i,j}(K_n) \to \mathrm{Kh}^{i+n,j}(K_n)$$

are nontrivial, for some (i, j).

For the proof, see [LLS15, Proof of Corollary 1.4, Page 67]. They find, for the knot $K = 15^n_{41127}$, a class $\alpha \in \widetilde{\mathrm{Kh}}^{-1,0}(K;\mathbb{F}_2)$ so that $\mathrm{Sq}^1(\alpha) \neq 0 \in \widetilde{\mathrm{Kh}}^{0,0}(K;\mathbb{F}_2)$ and $\mathrm{Sq}^i(\alpha) = 0$ for $i > 1$. Then, letting $K_n = K\#K\#\cdots\#K$, the Cartan formula and Theorem 4.5.1 give the result.
Since the knot K_n in the above theorem is the knot K connect summed with itself n times, we can view K_n as the denominator closure of the partial tangle sum $K +_p \cdots +_p K$ (see Figure 4.7).

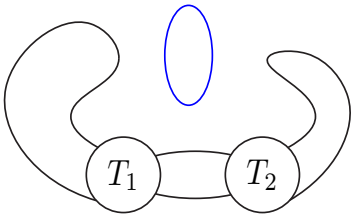

Figure 4.7. $K_1\#K_2 \sqcup$ Unknot

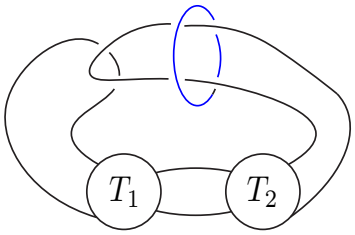

Figure 4.8. $K_1\#K_2 \sqcup$ Unknot after isotopy

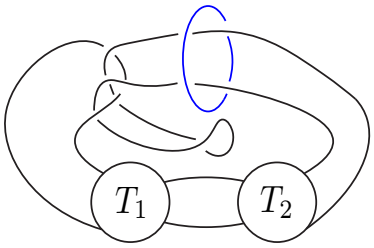

Figure 4.9. Another isotopy.

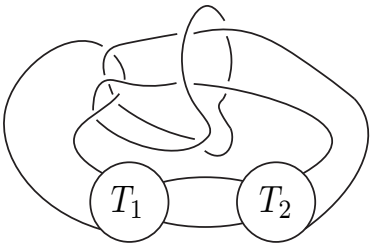

Figure 4.10. The result of adding a band; the final stage of the ribbon concordance between $K_1\#K_2$ and the prime knot $(T_1 +_p T_2) + Cl$.

4.6 Proof of Theorem 1

In this section, we collect the results from the previous sections together to construct a proof of Theorem 4.1.1.

Proof of Theorem 1. By Lemma 4.4.4, the knot K from the proof of Lemma 4.5.3 can be decomposed as a prime tangle T_2 and an untangle T_1, so that the denominator closure of T_2 is K (this is "K with ears"; see [Ble82]). Then, the knot $K_n = K\# \cdots \# K$ is the denominator closure of the (prime) tangle $T_2 +_p T_2 +_p \cdots +_p T_2$, where recall $+_p$ denotes the partial sum of tangles. Consider the ribbon concordance C given in Theorem 4.4.1, from K_n to $P_n := (T_2 +_p T_2 +_p \cdots +_p T_2) + Cl$. This is illustrated, for $n = 2$, in Figure 4.7—Figure 4.10 by replacing T_1 by T_2 in the figures. By Theorem 4.4.3 and Lemma 4.4.5, P_n is a prime knot.

By Theorem 4.1.5, the map

$$F_C : \widetilde{\mathrm{Kh}}(K_n) \to \widetilde{\mathrm{Kh}}(P_n)$$

is injective with left inverse given by $F_{\overline{C}}$ where $\overline{C}$ is the concordance C upside-down. Therefore $\widetilde{\mathrm{Kh}}(P_n) = \widetilde{\mathrm{Kh}}(K_n) \oplus G$ for some complement G. Theorem 4.5.2 implies that the following commutes (note that the Euler characteristic of any concordance is 0):x

$$\begin{array}{ccc} \widetilde{\mathrm{Kh}}^{-n,0}(K_n) & \xrightarrow{\mathrm{Sq}^n} & \widetilde{\mathrm{Kh}}^{0,0}(K_n) \\ \downarrow{\scriptstyle F_C} & & \downarrow{\scriptstyle F_C} \\ \widetilde{\mathrm{Kh}}^{-n,0}(P_n) & \xrightarrow{\mathrm{Sq}^n} & \widetilde{\mathrm{Kh}}^{0,0}(P_n). \end{array}$$

This immediately implies Theorem 4.1.1, since the vertical maps are injective. □

Next, we prove Corollary 4.1.2 from the introduction.

Proof of Corollary 1. This proof follows closely the proof of [LLS15, Corollary 1.4]. There is a long exact sequence in Khovanov homology induced from the cofiber sequence:

$$\widetilde{\mathcal{X}}^{j-1}(P_n) \to \mathcal{X}^j(P_n) \to \widetilde{\mathcal{X}}^{j+1}(P_n).$$

The long exact sequence takes the form:

$$\cdots \to \widetilde{\mathrm{Kh}}^{i,j+1}(P_n) \to \mathrm{Kh}^{i,j}(P_n) \xrightarrow{\pi} \widetilde{\mathrm{Kh}}^{i,j-1}(P_n) \to \widetilde{\mathrm{Kh}}^{i+1,j+1}(P_n) \to \cdots$$

Since over the field $\mathbb{F} := \mathbb{Z}/2\mathbb{Z}$ the Khovanov homology of any knot K is isomorphic to the direct sum $\widetilde{\mathrm{Kh}}^{i,j+1}(K;\mathbb{F}) \oplus \widetilde{\mathrm{Kh}}^{i,j-1}(K;\mathbb{F})$ of the shifted reduced homology, the map π above is surjective. So, there is a class $\gamma \in \mathrm{Kh}^{-n,1}(P_n)$ so that $\pi(\gamma) = \beta$, where the class β is as in the proof of Theorem 4.1.1. Naturality of the Steenrod squares establishes the result. □

Remark 1: The above proof applies to any stable homotopy refinement of Khovanov homology that satisfies the analogue of Theorems 4.5.1 and 4.5.2. The idea of the proof also offers an obstruction to ribbon concordance between two knots. If P and Q are knots with a ribbon concordance between them, the Khovanov homology of P is a summand of the Khovanov homology of Q with the same stable cohomology operations as the Khovanov homology of Q.
As an illustration of the above remark, we have the following lemma. To state it, we recall that in [See12], Seed constructed pairs of links L and L' so that $\mathrm{Kh}(L;\mathbb{Z}) \cong \mathrm{Kh}(L';\mathbb{Z})$ but the invariants $\mathcal{X}_{\mathrm{Kh}}(L)$ and $\mathcal{X}_{\mathrm{Kh}}(L')$ are not stably homotopy equivalent. Then, the following lemma is immediate.

Lemma 4.6.1. *For each of Seed's pairs of knots, there is no ribbon concordance between them.*

4.7 Hyperbolic Knots and Invertible Concordances

In this section we prove that there are hyperbolic knots with arbitrarily high Steenrod operations on their reduced Khovanov homology. The main theorem of this section, Theorem 4.1.3 from the introduction, is a direct consequence of the following that appears in [SW05, Theorem 2.2(iv)]:

Theorem 4.7.1. *Given any knot $K \subset S^3$ there is a hyperbolic knot H and a ribbon concordance from K to H.*

The proof of Theorem 4.1.3 now is the same as the proof of Theorem 4.1.1 in Section 4.6. Following the notation of Section 4.6, and letting C denote the composite ribbon concordance from K_n to H_n, the following commutes:

$$\begin{array}{ccc} \widetilde{\mathrm{Kh}}^{-n,0}(K_n) & \xrightarrow{\mathrm{Sq}^n} & \widetilde{\mathrm{Kh}}^{0,0}(K_n) \\ \downarrow{\scriptstyle F_C} & & \downarrow{\scriptstyle F_C} \\ \widetilde{\mathrm{Kh}}^{-n,0}(H_n) & \xrightarrow{\mathrm{Sq}^n} & \widetilde{\mathrm{Kh}}^{0,0}(H_n). \end{array}$$

Remark 2: It was pointed out to us by Danny Ruberman that there is a stronger result possible. In Kawauchi [Kaw89], it is shown that for any knot K there is an *invertible* concordance from K to a hyperbolic knot. This allows the propagation of Steenrod Squares without the injectivity results of Wilson or Levine-Zemke. See also [Kim00].

4.8 Satellite Knots

In this section, we show how results from [Liv81] imply Theorem 4.1.4.

Proof of Theorem 4.1.4. The reader is referred to [Liv81] for details of Livingston's construction. Glancing at Figure 2 of [Liv81] shows that there is a ribbon concordance from the unknot to a non-trivial knot K' contained in the solid torus $S^1 \times D^2$. Now, consider the knot K_n discussed in section 4.6 and the satellite S_n formed from K' as pattern and K_n as companion. Livingston shows that S_n is prime. The ribbon concordance from the unknot to K' gives a ribbon concordance from K_n to S_n. The remainder of the proof goes through exactly as in the proof of Theorems 4.1.1 and 4.1.3. □

REFERENCES CITED

[AE20] A. Alishahi and E. Eftekhary, *Knot Floer homology and the unknotting number*, Geom. Topol. **24** (2020), no. 5, 2435–2469, DOI: 10.2140/gt.2020.24.2435, MR4194296.

[Auc97] D. Auckly, *Surgery numbers of* 3*-manifolds: a hyperbolic example*, Geometric topology (Athens, GA, 1993), Vol. 2.1, AMS/IP Stud. Adv. Math. Amer. Math. Soc., Providence, RI, 1997, 21–34, DOI: 10.1090/amsip/002.1/02, MR1470719.

[BHL19] J. A. Baldwin, M. Hedden, and A. Lobb, *On the functoriality of Khovanov-Floer theories*, Adv. Math. **345** (2019), 1162–1205, DOI: 10.1016/j.aim.2019.01.026, MR3903915.

[Bin23] F. Binns, *The CFK^∞ Type of Almost L-space Knots*, arXiv: 2303.07249 [math.GT], 2023.

[Ble82] S. A. Bleiler, *Realizing concordant polynomials with prime knots*, Pacific J. Math. **100** (1982), no. 2, 249–257.

[BM19] K. L. Baker and K. Motegi, *Twist families of L-space knots, their genera, and Seifert surgeries*, Comm. Anal. Geom. **27** (2019), no. 4, 743–790, DOI: 10.4310/CAG.2019.v27.n4.a1, MR4025322.

[BNS22] J. A. Baldwin, Y. Ni, and S. Sivek, *Floer homology and right-veering monodromy*, DOI: 10.48550/ARXIV.2204.04093, 2022.

[Boy02] S. Boyer, *Dehn surgery on knots*, Handbook of geometric topology, North-Holland, Amsterdam, 2002, 165–218, MR1886670.

[BS22] J. A. Baldwin and S. Sivek, *Characterizing slopes for* 5_2, arXiv: 2209.09805 [math.GT], 2022.

[BZ96] S. Boyer and X. Zhang, *Reducing Dehn filling and toroidal Dehn filling*, Topology Appl. **68** (1996), no. 3, 285–303, DOI: 10.1016/0166-8641(95)00061-5, MR1377050.

[CH23] W. Chen and J. Hanselman, *Satellite knots and immersed Heegaard Floer homology*, arXiv: 2309.12297 [math.GT], 2023.

[Che19] W. Chen, *Knot Floer Homology of satellite knots with (1,1)-patterns*, DOI: 10.48550/ARXIV.1912.07914, 2019.

[DeY21] R. DeYeso III, *Thin knots and the Cabling Conjecture*, DOI: 10.48550/ARXIV.2112.08074, 2021.

[Eis22] M. M. Eismeier, *Fourier transforms and integer homology cobordism*, DOI: 10.48550/ARXIV.2206.07029, 2022.

[Gab87] D. Gabai, *Foliations and the topology of* 3*-manifolds. III*, J. Differential Geom. **26** (1987), no. 3, 479–536, MR910018.

[Gai17] F. Gainullin, *The mapping cone formula in Heegaard Floer homology and Dehn surgery on knots in* S^3, Algebr. Geom. Topol. **17** (2017), no. 4, 1917–1951, DOI: 10.2140/agt.2017.17.1917, MR3685598.

[GL87] C. M. Gordon and J. Luecke, *Only integral Dehn surgeries can yield reducible manifolds*, Math. Proc. Cambridge Philos. Soc. **102** (1987), no. 1, 97–101, DOI: 10.1017/S0305004100067086, MR886439.

[GL96] ———, *Reducible manifolds and Dehn surgery*, Topology **35** (1996), no. 2, 385–409, DOI: 10.1016/0040-9383(95)00016-X, MR1380506.

[Gre15] J. E. Greene, *L-space surgeries, genus bounds, and the cabling conjecture*, J. Differential Geom. **100** (2015), no. 3, 491–506, MR3352796.

[GS86] F. González-Acuña and H. Short, *Knot surgery and primeness*, Math. Proc. Cambridge Philos. Soc. **99** (1986), no. 1, 89–102, DOI: 10.1017/S0305004100063969, MR809502.

[Hed07] M. Hedden, *Knot Floer homology of Whitehead doubles*, Geom. Topol. **11** (2007), 2277–2338, DOI: 10.2140/gt.2007.11.2277, MR2372849.

[HKL16] J. Hom, Ç. Karakurt, and T. Lidman, *Surgery obstructions and Heegaard Floer homology*, Geom. Topol. **20** (2016), no. 4, 2219–2251, DOI: 10.2140/gt.2016.20.2219, MR3548466.

[HL16] J. Hom and T. Lidman, *A note on surgery obstructions and hyperbolic integer homology spheres*, arXiv: 1604.06047 [math.GT], 2016.

[HLP22] J. Hom, T. Lidman, and J. Park, *Unknotting number and cabling*, arXiv: 2206.04196 [math.GT], 2022.

[HLZ15] J. Hom, T. Lidman, and N. Zufelt, *Reducible surgeries and Heegaard Floer homology*, Math. Res. Lett. **22** (2015), no. 3, 763–788, DOI: 10.4310/MRL.2015.v22.n3.a8, MR3350104.

[HMS08] M. Hirasawa, K. Murasugi, and D. S. Silver, *When does a satellite knot fiber?*, Hiroshima Math. J. **38** (2008), no. 3, 411–423, MR2477750.

[HN13] M. Hedden and Y. Ni, *Khovanov module and the detection of unlinks*, Geom. Topol. **17** (2013), no. 5, 3027–3076, DOI: 10.2140/gt.2013.17.3027, MR3190305.

[Hom14] J. Hom, *Bordered Heegaard Floer homology and the tau-invariant of cable knots*, J. Topol. **7** (2014), no. 2, 287–326, DOI: 10.1112/jtopol/jtt030, MR3217622.

[How02] J. Howie, *A proof of the Scott-Wiegold conjecture on free products of cyclic groups*, J. Pure Appl. Algebra **173** (2002), no. 2, 167–176, DOI: 10.1016/S0022-4049(02)00042-7, MR1915093.

[HRW17] J. Hanselman, J. Rasmussen, and L. Watson, *Bordered Floer homology for manifolds with torus boundary via immersed curves*, arXiv: 1604.03466 [math.GT], 2017.

[HRW22] ———, *Heegaard Floer homology for manifolds with torus boundary: properties and examples*, Proc. Lond. Math. Soc. (3) **125** (2022), no. 4, 879–967, DOI: 10.1112/plms.12473, MR4500201.

[HW16] J. Hom and Z. Wu, *Four-ball genus bounds and a refinement of the Ozváth-Szabó tau invariant*, J. Symplectic Geom. **14** (2016), no. 1, 305–323, DOI: 10.4310/JSG.2016.v14.n1.a12, MR3523259.

[HW18] M. Hedden and L. Watson, *On the geography and botany of knot Floer homology*, Selecta Math. (N.S.) **24** (2018), no. 2, 997–1037, DOI: 10.1007/s00029-017-0351-5, MR3782416.

[HW19] J. Hanselman and L. Watson, *Cabling in terms of immersed curves*, arXiv: 1908.04397 [math.GT], 2019.

[Juh08a] A. Juhasz, *Knot Floer homology and Seifert surfaces*, Algebr. Geom. Topol. **8** (2008), no. 1, 603–608, DOI: 10.2140/agt.2008.8.603, MR2443240.

[Juh08b] A. Juhász, *Floer homology and surface decompositions*, Geom. Topol. **12** (2008), no. 1, 299–350, DOI: 10.2140/gt.2008.12.299, MR2390347.

[Juh08c] ———, *Floer homology and surface decompositions*, Geom. Topol. **12** (2008), no. 1, 299–350, DOI: 10 . 2140 / gt . 2008 . 12 . 299, MR2390347.

[Kaw89] A. Kawauchi, *Almost identical imitations of* $(3,1)$*-dimensional manifold pairs*, Osaka J. Math. **26** (1989), no. 4, 743–758.

[Kho99] M. Khovanov, *A categorification of the Jones polynomial*, arXiv: math/9908171 [math.QA], 1999.

[Kim00] S.-G. Kim, *Invertible knot concordances and prime knots*, arXiv Mathematics e-prints (2000), math/0003034, arXiv: math/0003034 [math.GT].

[KL79] R. C. Kirby and W. B. R. Lickorish, *Prime knots and concordance*, Math. Proc. Cambridge Philos. Soc. **86** (1979), no. 3, 437–441, DOI: 10.1017/S0305004100056280.

[Kro+07] P. Kronheimer et al., *Monopoles and lens space surgeries*, Ann. of Math. (2) **165** (2007), no. 2, 457–546, DOI: 10.4007/annals.2007.165.457, MR2299739.

[Lev16] A. S. Levine, *Nonsurjective satellite operators and piecewise-linear concordance*, Forum Math. Sigma **4** (2016), Paper No. e34, 47, DOI: 10.1017/fms.2016.31, MR3589337.

[Lic62] W. B. R. Lickorish, *A representation of orientable combinatorial 3-manifolds*, Ann. of Math. (2) **76** (1962), 531–540, DOI: 10.2307/1970373, MR151948.

[Lic81] W. B. R. Lickorish, *Prime knots and tangles*, Trans. Amer. Math. Soc. **267** (1981), no. 1, 321–332, DOI: 10.2307/1998587.

[Liv81] C. Livingston, *Homology cobordisms of 3-manifolds, knot concordances, and prime knots*, Pacific J. Math. **94** (1981), no. 1, 193–206, MR625818.

[LL08] D. A. Lee and R. Lipshitz, *Covering spaces and $\mathbb{Q}$-gradings on Heegaard Floer homology*, J. Symplectic Geom. **6** (2008), no. 1, 33–59, MR2417439.

[LLS15] T. Lawson, R. Lipshitz, and S. Sarkar, *Khovanov homotopy type, Burnside category, and products*, arXiv e-prints (2015), arXiv:1505.00213, arXiv: 1505.00213 [math.GT].

[LOT18] R. Lipshitz, P. S. Ozsvath, and D. P. Thurston, *Bordered Heegaard Floer homology*, Mem. Amer. Math. Soc. **254** (2018), no. 1216, viii+279, DOI: 10.1090/memo/1216, MR3827056.

[LS14a] R. Lipshitz and S. Sarkar, *A Khovanov stable homotopy type*, J. Amer. Math. Soc. **27** (2014), no. 4, 983–1042, DOI: 10.1090/S0894-0347-2014-00785-2, MR3230817.

[LS14b] ———, *A refinement of Rasmussen's s-invariant*, Duke Math. J. **163** (2014), no. 5, 923–952, DOI: 10.1215/00127094-2644466.

[LS14c] ———, *A Steenrod square on Khovanov homology*, J. Topol. **7** (2014), no. 3, 817–848, DOI: 10.1112/jtopol/jtu005, MR3252965.

[LS18] ———, *Spatial refinements and Khovanov homology*, Proceedings of the International Congress of Mathematicians—Rio de

Janeiro 2018. Vol. II. Invited lectures, World Sci. Publ., Hackensack, NJ, 2018, 1153–1173.

[LZ19] A. S. Levine and I. Zemke, *Khovanov homology and ribbon concordances*, Bull. Lond. Math. Soc. **51** (2019), no. 6, 1099–1103, DOI: 10.1112/blms.12303.

[Mei17] J. Meier, *A note on cabled slice knots and reducible surgeries*, Michigan Math. J. **66** (2017), no. 2, 269–276, DOI: 10.1307/mmj/1490639817, MR3657218.

[MO08] C. Manolescu and P. Ozsváth, *On the Khovanov and knot Floer homologies of quasi-alternating links*, Proceedings of Gökova Geometry-Topology Conference 2007, Gökova Geometry/Topology Conference (GGT), Gökova, 2008, 60–81, MR2509750.

[Mos71] L. Moser, *Elementary surgery along a torus knot*, Pacific J. Math. **38** (1971), 737–745, MR383406.

[MS03] D. Matignon and N. Sayari, *Longitudinal slope and Dehn fillings*, Hiroshima Math. J. **33** (2003), no. 1, 127–136, MR1966655.

[MT92] W. W. Menasco and M. B. Thistlethwaite, *Surfaces with boundary in alternating knot exteriors*, J. Reine Angew. Math. **426** (1992), 47–65, MR1155746.

[Ni06] Y. Ni, *Sutured Heegaard diagrams for knots*, Algebr. Geom. Topol. **6** (2006), 513–537, DOI: 10.2140/agt.2006.6.513, MR2220687.

[Ni07] ———, *Knot Floer homology detects fibred knots*, Invent. Math. **170** (2007), no. 3, 577–608, DOI: 10.1007/s00222-007-0075-9, MR2357503.

[Ni20] ———, *Exceptional surgeries on hyperbolic fibered knots*, DOI: 10.48550/ARXIV.2007.11774, 2020.

[NW15] Y. Ni and Z. Wu, *Cosmetic surgeries on knots in S^3*, J. Reine Angew. Math. **706** (2015), 1–17, DOI: 10.1515/crelle-2013-0067, MR3393360.

[OS03a] P. Ozsváth and Z. Szabó, *Absolutely graded Floer homologies and intersection forms for four-manifolds with boundary*, Adv. Math. **173** (2003), no. 2, 179–261, DOI: 10.1016/S0001-8708(02)00030-0, MR1957829.

[OS03b] _____, *Knot Floer homology and the four-ball genus*, Geom. Topol. **7** (2003), 615–639, DOI: 10.2140/gt.2003.7.615, MR2026543.

[OS04a] _____, *Holomorphic disks and genus bounds*, Geom. Topol. **8** (2004), 311–334, DOI: 10.2140/gt.2004.8.311, MR2023281.

[OS04b] _____, *Holomorphic disks and knot invariants*, Adv. Math. **186** (2004), no. 1, 58–116, DOI: 10.1016/j.aim.2003.05.001, MR2065507.

[OS04c] _____, *Holomorphic disks and three-manifold invariants: properties and applications*, Ann. of Math. (2) **159** (2004), no. 3, 1159–1245, DOI: 10.4007/annals.2004.159.1159, MR2113020.

[OS04d] _____, *Holomorphic disks and topological invariants for closed three-manifolds*, Ann. of Math. (2) **159** (2004), no. 3, 1027–1158, DOI: 10.4007/annals.2004.159.1027, MR2113019.

[OS11] P. S. Ozsváth and Z. Szabó, *Knot Floer homology and rational surgeries*, Algebr. Geom. Topol. **11** (2011), no. 1, 1–68, DOI: 10.2140/agt.2011.11.1, MR2764036.

[OSS12] P. S. Ozsvath, A. I. Stipsicz, and Z. Szabo, *Combinatorial Heegaard Floer homology and nice Heegaard diagrams*, arXiv: 0912.0830 [math.GT], 2012.

[OSS15] P. S. Ozsváth, A. I. Stipsicz, and Z. Szabó, *Grid homology for knots and links*, *Vol. 208*, Mathematical Surveys and Monographs, American Mathematical Society, Providence, RI, 2015, x+410, DOI: 10.1090/surv/208, MR3381987.

[OST08] P. Ozsváth, Z. Szabó, and D. Thurston, *Legendrian knots, transverse knots and combinatorial Floer homology*, Geom. Topol. **12** (2008), no. 2, 941–980, DOI: 10.2140/gt.2008.12.941, MR2403802.

[Pet13] I. Petkova, *Cables of thin knots and bordered Heegaard Floer homology*, Quantum Topol. **4** (2013), no. 4, 377–409, DOI: 10.4171/QT/43, MR3134023.

[PW21] I. Petkova and B. Wong, *Twisted Mazur pattern satellite knots and bordered Floer theory*, arXiv: 2005.12795 [math.GT], 2021.

[PX24] J. Patwardhan and Z. Xiao, *Generalized Mazur Patterns and Immersed Heegaard Floer Homology*, arXiv: 2404.14578 [math.GT], 2024.

[Ras03a] J. A. Rasmussen, *Floer homology and knot complements*, ProQuest LLC, Ann Arbor, MI, 2003, 126, MR2704683, Thesis (Ph.D.)–Harvard University.

[Ras03b] ———, *Floer homology and knot complements*, ProQuest LLC, Ann Arbor, MI, 2003, 126, MR2704683, Thesis (Ph.D.)–Harvard University.

[Sch03] J. Schultens, *Additivity of bridge numbers of knots*, Math. Proc. Cambridge Philos. Soc. **135** (2003), no. 3, 539–544, DOI: 10.1017/S0305004103006832.

[Sch53] H. Schubert, *Knoten und Vollringe*, Acta Math. **90** (1953), 131–286, DOI: 10.1007/BF02392437, MR72482.

[Sch90] M. Scharlemann, *Producing reducible* 3*-manifolds by surgery on a knot*, Topology **29** (1990), no. 4, 481–500, DOI: 10.1016/0040-9383(90)90017-E, MR1071370.

[See12] C. Seed, *Computations of the Lipshitz-Sarkar Steenrod square on Khovanov homology*, arXiv e-prints (2012), arXiv:1210.1882, arXiv: 1210.1882 [math.GT].

[Shu14] A. N. Shumakovitch, *Torsion of Khovanov homology*, Fund. Math. **225** (2014), no. 1, 343–364, DOI: 10.4064/fm225-1-16, MR3205577.

[SRS14] V. de Silva, J. W. Robbin, and D. A. Salamon, *Combinatorial Floer homology*, Mem. Amer. Math. Soc. **230** (2014), no. 1080, v+114, MR3205426.

[SW05] D. S. Silver and W. Whitten, *Hyperbolic covering knots*, arXiv Mathematics e-prints (2005), math/0503152, arXiv: math/0503152 [math.GT].

[Tru16] L. M. Truong, *Applications of Heegaard Floer Homology to Knot Concordance*, ProQuest LLC, Ann Arbor, MI, 2016, 58, MR3542254, Thesis (Ph.D.)–Princeton University.

[Val99] L. G. Valdez Sánchez, *Dehn fillings of* 3*-manifolds and non-persistent tori*, Vol. 98, **1-3**, 1999, 355–370, DOI: 10.1016/S0166-8641(99)00038-3, MR1720012, II Iberoamerican Conference on Topology and its Applications (Morelia, 1997).

[Wal60] A. H. Wallace, *Modifications and cobounding manifolds*, Canadian J. Math. **12** (1960), 503–528, DOI: 10.4153/CJM-1960-045-7, MR125588.

[Wil12] B. Wilson, *Topics in Khovanov Homology*, ProQuest LLC, Ann Arbor, MI, 2012, 80, MR3122052, Thesis (Ph.D.)–University of California, San Diego.

[Zem19] I. Zemke, *Knot {F}loer homology obstructs ribbon concordance*, Ann. of Math. (2) **190** (2019), no. 3, 931–947, DOI: 10.4007/annals.2019.190.3.5.

[Zha18] M. Zhang, *A rank inequality for the annular Khovanov homology of 2-periodic links*, Algebr. Geom. Topol. **18** (2018), no. 2, 1147–1194, DOI: 10.2140/agt.2018.18.1147, MR3773751.